REPUBLIQUE DU CAMEROUN
Paix-Travail-Patrie

UNIVERSITE DE YAOUNDE I

CENTRE DE RECHERCHE ET DE FORMATION DOCTORALE EN SCIENCES, TECHNOLOGIES ET GEOSCIENCES
UNITE DE RECHERCHE ET DE FORMATION DOCTORALE PHYSIQUE ET APPLICATIONS
B.P 812 Yaoundé
Email: crftstg@uyi.uninet.cm

REPUBLIC OF CAMEROON
Peace-Work-Fatherland

THE UNIVERSITY OF YAOUNDE I

POSTGRADUATES SCHOOL OF SCIENCE, TECHNOLOGY AND GEOSCIENCES
RESEARCH AND POSTGRADUATE TRAINING UNIT FOR PHYSICS AND APPLICATIONS
P.O.BOX 812 Yaoundé
Email: crftstg@uyi.uninet.cm

DEPARTMENT OF PHYSICS

LABORATORY OF NUCLEAR, ATOMIC, MOLECULAR PHYSICS AND BIOPHYSICS

SYNCHRONIZATION OF NONLINEAR INTERCELLULAR Ca^{2+} OSCILLATIONS AND SPIRAL WAVES UNDER IP_3-CYTOSOLIC-Ca^{2+} INTERACTION

THESIS

Submitted and defended in Fulfillment of the Requirements for the award of the Degree of **Doctorate/Ph.D in Physics**

Option: Atomic, Molecular Physics and Biophysics

By:

KENNE TIAYO Thierry

Registration number: 04X407

Master in Physics

Under the supervision of

EKOBENA FOUDA Henri Paul *Professor UY I*

AND

TABI CONRAD Bertrand *Professor BIUST*

YEAR : 2025

UNIVERSITE DE YAOUNDE I
UNIVERSITY OF YAOUNDE I

FACULTE DES SCIENCES
FACULTY OF SCIENCE

DEPARTEMENT DE PHYSIQUE
DEPARTMENT OF PHYSICS

ATTESTATION DE CORRECTION DE LA THESE DE DOCTORAT/Ph.D

Nous, Professeur **MVOGO Alain** et Professeur **NDJAKA Jean-Marie Bienvenu**, respectivement Examinateur et Président du Jury de la thèse de Doctorat/Ph.D de Monsieur **KENNE TIAYO Thierry**, Matricule 04X407, effectuée sous la codirection des Professeurs **EKOBENA FOUDA Henri Paul et TABI Conrad Bertrand,** intitulée « **Synchronization of nonlinear intercellular Ca^{2+} oscillations and spiral waves under IP_3-cytosolic-Ca^{2+} interaction**», soutenue le **mercredi 23 Avril 2025**, en vue de l'obtention du grade de Docteur/Ph.D en Physique, spécialité Physique Nucléaire, Atomique, Moléculaire et Biophysique, option Physique Atomique, Moléculaire et Biophysique, attestons que toutes les corrections demandées par le Jury de soutenance ont été effectuées.

En foi de quoi, la présente attestation lui est délivrée pour servir et valoir ce que de droit.

Fait à Yaoundé le 26 MAI 2025

Examinateur

Pr MVOGO Alain

Le Président du Jury

Pr NDJAKA Jean-Marie Bienvenu

UNIVERSITE DE YAOUNDE I
FACULTE DES SCIENCES
DEPARTEMENT DE PHYSIQUE
Le Chef de Département

Le Chef de Département de Physique

Ndjaka Jean-Marie Bienvenu
Professeur

Dedications

✠ I would like to express my sincere gratitude to **my dear parents** who gave me the life, the opportunity and the knowledge to reach and to end with the PhD study level.

Acknowledgements

In first thanks to almighty God for all he has done for me. At the end of the PhD study, I am deeply grateful for the opportunity to have learned from and worked with so many brilliant teachers, collaborators and students. I am happy to express my sincere gratitude to all those from who near or far have accompanied me during these doctoral years and have directly or indirectly contributed to the completion of this document. Nevertheless, I will do my best to condense my thoughts about this.

★ Furthermore, i thank the Dean of the Faculty of Sciences, and the Coordinator of the School Research and Postgraduate studies training for Physics and Applications who gave the authorisation to go ahead with my thesis.

★ I would like to express my sincere gratitude to my thesis director **Professor TABI Conrad Bertrand** who, despite his multiple academic and family occupations, accepted to guide this work. This thesis would not have been possible without his pernickety vision in nonlinear physics. I thank him for the advices he has provided me and the expertise that he has enabled me to acquire.

★ I would like to express my sincere gratitude to my supervisor **Professor EKOBENA FOUDA Henri Paul**, the Head of laboratory of Atomic, Molecular Physics and Biophysics for his advices and constructive discussions, who despite his multiple academic, administrative and family occupations, accepted to supervise this thesis. I thank him for all his teachings and advices he has provided me.

★ I deeply thank the honorable **members of the Jury**, who agreed to put aside their various occupations so as to evaluate this work. I express to them all my greatest respect.

★ I would like to thank **Professor NDJAKA Jean Marie Bienvenu**, Head of the Department of Physics. I am very grateful for his administrative contribution and encouragement.

★ I would like to thank **Professor KOFANE Timoléon Crépin**, winner of the Kwamer Nkrumah Prize. I am very grateful for the quality of his teaching and for his constructive comments.

★ I am grateful to **Professor OWONO OWONO Jean Calvin**, Chairman of the Cameroon Physical Society for his teaching specially in numerical methods.

★ It would be very pleasing to recognize trade and constructive discussions combined with great moments of sharing with all the teachers of the Department of Physics in general and of the laboratory of Biophysics in particular. I have named; **Professor BEN-Bolie Germain, Professor SAIDOU, Professor MVOGO ALAIN, Professor TCHOMGO Emmanuel, Doctor ETEME Armand, Doctor DANG KOKO Adamou,**

Doctor BELOBO BELOBO Didier; Doctor BANSI KAMDEM Christel, Doctor TEUMA Michel, Doctor Ibrahim MAINA.

★ Special thanks to **Doctor KUIPOU William, Doctor Ndjawa Pavel, Doctor FORWAH Amstrong, Doctor MBIEDA Frank, Doctor ASSEMBE Stephane** for the multitude exchanges and helps.

★ The fulfillment of my thesis is the work of the good atmosphere in my family. I would like to thank:

• My brothers and sisters **TEMGOUA Hilaire, MELACHIO Achille, TSOMENE Ghislain, TEDONGMO Alex, TEMGOUA Ulrich, TEDONGMO Linette**and her husband **NTCHUISSEU Helenos**, **WAKEM Sandrine** and her husband **TAMBO FLorian**, . I thank all of them for their moral and financial supports and for all their prayers for me.

• I thank all my uncles, aunts, cousins, nephews and nieces in particular **Mme MOUAFO Aunorine, la famille feu YONTA Maurice, la famille SONMENE Corentin, la famille Dr MELI Jean, Professeur FOTSING Jean Marie, Me MELY Mariane.** for their encouragements.

• I thank all my best friend **TATCHOU Marius, SIKUBE Celestin, TENE Berlin, NYAMA Roland, DJIENOUASSI Sebastien, NGUESSE Jules, NDOH Moise,**, for all their encouragement.

• Finally, a special thank you to my beloved and sweetheart **MELANG NOUBOSSE Christelle Jorelle** for his unyielding commitment to my side. Together we have done and will continue to make prowess.

- Thanks to all the unmentioned persons who have contributed even a little to this work. I did not forget you...

Contents

List of Figures

List of Abbreviations

Initials	Meaning	**Initials**	Meaning
Ca^{2+}	Calcium ion	IP_3	inositol 1,4,5-trisphosphate
VD	Vitamine D	[Ca^{2+}]	Concentration of Ca^{2+}
PTH	Parathyroid Hormone	IP_3R	inositol 1,4,5-trisphosphate receptor
CICR	Calcium Induce Calcium Release	**IICR**	Inositol 1,4,5-trisphosphate Induce Calcium Release
GJ	Gap-Junction	**CaR**	Calcium sensitive Receptors
PLC	phospholipases C	[IP_3]	Concentration of IP_3
ER	Endoplasmic Reticulum	**SR**	Sarcoplasmic Reticulum
PS	Paracrine Signalling	**HD**	Houart et al model
LF	Low Frequency	**R**	Factor of synchronization
HF	High Frequency	**MI**	Modulational Instability
RK1	First-order Runge-Kutta	**RK2**	Second-order Runge-Kutta
RK3	Third-order Runge-Kutta	**RK4**	Fourth-order Runge-Kutta
WP	Waves Propagation	**CVDs**	Cardiovascular Diseases
PCa	Prostate Cancer	**WHO**	world Health Organization
WP	Waves Propagation	**ATP**	Adenosine triphosphate

Abstract

In this work, we study the interactions between unstable Ca^{2+} waves in networks of coupled cells. Starting from a deterministic model which accounts for complex oscillations of cytosolic Ca^{2+} induced by Ca^{2+} and auto-modulation of the inositol signal 1,4,5- triphosphate (IP_3) by 3-kinase stimulated by Ca^{2+}. We consider the diffusion of Ca^{2+} with paracrine coupling. With the aid of Runge-kutta method of fourth-order, we numerically integrate our generic three-variable models. By means of timing prediction, we studied the intercellular propagation of the Ca^{2+} wave: firstly, in a network of cells with bidirectional paracrine coupling in two dimensions (2D), we note the formation and disappearance of Ca^{2+} spirals waves, as well as the emergence of turbulent modes for a range of parameters. Ca^{2+} spiral waves are maintained robust in case of perpetual balance between IP_3 degradation and degree stimulation under an appropriate paracrine coupling force. Spiral waves are observable for low values (R$\rightarrow$0)of the synchronization factor (R$\rightarrow$0) and tend to disappear for large values (R$\rightarrow$1). Based on these observations, the bifurcation is studied with coupling bidirectional 1D paracrine, with paracrine coupling strength, stimulation degrees and phosphorilation of IP_3 rates as a control parameter. It appears that low values (R$\rightarrow$0) of the coupling paracrine are favorable to the emergence of synchronous modes, the degrees of stimulation for a range phosphorilation rates are favorable to the emergence of quasi-periodic and chaotic behaviors of Ca^{2+} waves in the network. But the passive flow of Ca^{2+} enables frequency modulation unstable Ca^{2+} waves as in the case of muscular stress. In the same vein, it appears that cytosolic IP_3-Ca^{2+} interactions could be used as an important tool to control and control and trigger the formation of Ca^{2+} spiral waves and the creation of other spatio-temporal patterns supported by the cellular cellular network. We argued that robust spiral waves were dependent on the presence of broken cycles and their transition to multi-arm spirals, under the appropriate IP_3 degradation factor. However, the change in topology of the observed patterns bears witness of the dynamic character and the possible key role played by cytosolic IP_3-Ca^{2+} interactions in the recruitment of signaling-inactive cells. In the meantime, this contribution also suggests that the IP_3 cytosolic Ca^{2+} interactions effect, under a pronounced coupling and thus a state of synchronization, is essential for the essential for the control (formation, maintenance transformation and destruction) of Ca^{2+} spiral waves in heart cells and other cellular environments.

Keywords: Coupled cell array;coupling paracrine; Synchronization factors; IP_3 cytosolic Ca^{2+} interactions; calcium wave patterns;spiral calcium wave; cardiac arrhythmia.

Résumé

Dans ce travail, nous étudions les interactions entre les ondes instables de Ca^{2+} dans des réseaux de cellules couplées. Partant d'un modèle déterministe qui rend compte des oscillations complexes de Ca^{2+} cytosolique induitent par le Ca^{2+} et l'auto-modulation du signal de l'inositol 1,4,5-triphosphate (IP_3) par la 3-kinase stimulé par le Ca^{2+}, nous considérons la diffusion du Ca^{2+} avec couplage paracrine. Avec la méthode de Runge-kutta d'ordre quatre, nous intégrons numériquement nos modèles génériques á trois variables. Au moyen de la prédiction de synchronisation, nous avons étudié la propagation intercellulaire de l'onde Ca^{2+}. Tout d'abord, dans un réseau de cellules avec couplage paracrine bidirectionnelle à deux dimensions (2D), on note la formation et disparition d'ondes spirales de Ca^{2+}, ainsi que l'émergence de mode trubulents pour une gamme de paramètres. Les ondes spirales de Ca^{2+} sont maintenues robustes en cas d'équilibre entre la dégradation IP_3 et le degré de stimulation sous une force de couplage paracrine appropriée. Les ondes spirales sont observables pour les faibles valeurs du facteur de synchronisation (R$\rightarrow$0) et tendent à disparaitre pour des grandes valeurs (R$\rightarrow$1). Fort de ces observations, la bifurcation est étudié dans une approche avec couplage paracrine bidirectionnelle à une dimension (1D), avec la force de couplage, le degrés de stimulation et le taux de phosphorilation d'IP_3 comme paramètre de contrôle. Il ressort que les faibles valeurs du couplage paracrine sont favorables à l'émergence des modes synchrones, le degrés de stimulation pour une plage de taux de phosphorilation sont favorables à l'émergence de comportements quasi-périodique et chaotique des ondes Ca^{2+} dans le réseau mais, le flux passif de Ca^{2+} permet une modulation de fréquence des ondes instables de Ca^{2+} comme en situation de strees musculaire. Dans la même lancée, il ressort que les interactions IP_3-Ca^{2+} cytosoliques, peuvent être utilisé comme outil important pour contrôler et déclencher la formation des ondes spirales Ca^{2+} et la création d'autres modèles spatio-temporels soutenus par le réseau cellulaire. Nous avons soutenu que les robustes ondes spirales étaient tributaires de la présence de cycles brisés et leur transition vers des spirales à plusieurs bras, sous facteur de dégradation IP_3 approprié. Cependant, le changement de topologie des modèles observés témoigne du caractère dynamique et du rôle clé éventuel joué par les interactions IP_3-Ca^{2+} cytosoliques dans le recrutement des cellules inactives dans la signalisation. Entre-temps, cette contribution suggère aussi que l'effet des interactions IP_3-Ca^{2+} cytosoliques, sous un couplage paracrine prononcé et donc un état de synchronisation, est essentiel pour le contrôle (formation, maintient, transformation et destruction) des ondes spirales de Ca^{2+} dans les cellules cardiaques et autres milieux cellulaires.

Mots clés: Réseau de cellules couplés; couplage paracrine; interactions IP_3-Ca^{2+} cytosoliques; facteur de synchronisation; motifs d'ondes calcium; arrhythmie cardiaque.

General Introduction

According to the WHO, cardiovascular diseases are the leading cause of death worldwide and cause around 17.9 million deaths each year. They bring together a set of conditions of the heart and blood vessels, including coronary heart disease, cerebrovascular disease and rheumatic heart disease. Moreover, more than 4 out of 5 deaths results from cardiovascular disease are linked to heart attacks and strokes, and a third of these deaths occur prematurely in people under 70 years of age. Recent studies have established a link between these cardiovascular diseases and the dynamics of Ca^{2+} ion. The waves dynamics of calcium (Ca^{2+}) presents a character nonlinear oscillatory system responsible for almost all physiological functions and anomalies, proliferation of coronary infections, as well as apoptosis. This nonlinearity and strong presence in cellular metabolism make this ion the most abundant mineral cellular and messenger in the organism, thus, a marker of choice for a good understanding of the mysteries contained again the cellular metabolism and therefore the organism.

Calcium ions are crucial in several cellular processes, starting from fertilization, and regulate the subsequent cycle of events related to the developmental processes. Upon differentiation, the cell performs specific tasks via Ca^{2+} that control many vital functions such as muscle contraction, energy transduction, secretions, chemotaxis, neuronal and synaptic plasticity in learning and memory, and apoptosis [1, 2, 3, 4]. Additionally, due to the important role that Ca^{2+} signaling plays in cell proliferation, apoptosis, autophagy, migration, and cell cycle, recent studies have reported that tumor initiation, angiogenesis, progression, and metastasis are caused by its dysregulation [5, 6]. Calcium is stored in internal pools such as the endoplasmic reticulum (ER) or sarcoplasmic reticulum (SR), where its concentration is higher than that of cytosol and extracellular medium. The ryanodine receptor (RyR) and the inositol 1,4,5-trisphosphate receptor (IP_3R) are privileged channels that release calcium from the internal stores into the cytosol. The underlying process gives rise to a spatiotemporal encoded signal that transmits information on variations in calcium concentrations [7]. In doing so, Ca^{2+} serves as a second messenger via a mechanism of signaling that relies on changes in Ca^{2+} concentrations and is translated into brief spikes that usually appear as regenerative waves [4, 8, 9]. Calcium waves, at the intracellular level, were initially reported in medaka eggs [10] and then in other cell types such as Xenopus oocytes [11, 12, 13, 14, 15]. For Ca^{2+} response to be initiated, a series of reactions is triggered by an agonist and produces the messenger called inositol 1,4,5-trisphosphate (IP_3) by binding to its receptor [16]. The released IP_3 gets diffused in the cell cytoplasm. It binds to the IP_3 receptors in the ER, which contributes to the release of the Ca^{2+} into the cytosol, via dedicated channels, under the calcium-induced calcium-release (CICR) mechanism. The release is terminated when

the cytoplasmic Ca^{2+} concentration reaches a threshold, therefore inactivating the receptors.

In astrocytes, for example, the above-described sequence of events can propagate to surrounding cells, forming intercellular Ca^{2+} waves. Albeit the fact is well-established for astrocytes, where the signal can be shared with up to thirty cells, the usual open question concerning the intercellular Ca^{2+} waves is the underlying generation and propagation mechanisms. As it is well known, the spreading of extracellular adenosine triphosphate (ATP) messenger and the permeability of intercellular IP_3 of calcium ions are important factors contributing to the propagation of intercellular calcium waves [17, 18, 19, 20, 72, 22, 23]. In multicellular organisms, cell populations experience synchronized bursts of intracellular Ca^{2+} levels, which then propagate among cells as waves. It happens in Dictyostelium discoideum, at the early stages of development, including aggregation, due to synchronous oscillations of the cytosolic calcium level, leading to calcium wave propagation through the cell population [24]. However, the whole process may depend not only on the cell type but also on the physiological conditions engaging either diffusion of IP_3 or calcium through gap-junction or paracrine signaling [25, 26, 27]. Moreover, in embryogenesis, the interplay between mechanical forces and Ca^{2+} signalling has recently been shown to critically impact the healthy development of an embryo [28, 29].

According to some of the available mathematical models, gap-junction diffusion relies on a second messenger such as calcium or IP_3 [30, 31, 32, 33, 34], along with some other factors such as stochastic effects [35, 36] to realistically describe calcium dynamics [37, 38]. On the other hand, paracrine signaling involves the release of a messenger that diffuses in the extracellular space, binds to receptors on adjacent cells, and follows a kinetic that triggers an increase of free calcium in the cytoplasm of the target cells [39]. Moreover, some experimental facts reported calcium-sensing receptors (CaRs) on the membrane of adjacent cells as being activated by the fluctuations of extruded calcium during intracellular Ca^{2+} spiking in one cell, therefore producing secondary spikes in this cells [40]. This may result in cell-to-cell communication in which the target cell is responsible for a new cycle of Ca^{2+} signal communication relayed by the regeneration of the cell calcium signaling events capable of reaching a larger population of cells.

Simplified models to describe intercellular communication via paracrine signaling have been proposed and used to address how information is shared among cells in normal physiological conditions and in the presence of pathologies. For example, Kepseu and Woafo [41] used a discrete Goldbeter-Dupont-Berridge model [42] to characterize the dynamical behaviors of calcium in a one-dimensional chain of cells. They reported some transition zones between possible dynamical modes. The long-range interaction of calcium wave propagation was also studied, where importance was given to intercellular communication in the presence of localized diseases [43]. Along the same line, Tabi and co-workers [44, 45, 46] looked at the emergence of discrete calcium waves in one and two dimensions using the modulational instability mechanism. Further, they pointed out the vital contribution of a well-tuned paracrine signaling coupling. Unfortunately, none of the above discrete models included effects related to the mechanism of CICR, which consists of the calcium-stimulated degradation of IP_3 by a 3-kinase, which constitutes the main ingredient of the present work. In fact, it was shown by begin by Borghan et

al. [47] and next by Houart et *al*. [48], using a continuum model, that the self-modulation of the IP_3 signal by 3-kinase may support various modes of intracellular oscillatory behaviors.

.0.1 Context of the thesis

Studies have established a link between calcium ion dynamics and various diseases, including cardiovascular disease. Calcium ion (Ca^{2+}) dynamics play a crucial role in heart diseases, such as life-threatening ventricular arrhythmia, coronary heart disease, and stroke. Research has shown that disruptions in intracellular calcium homeostasis may contribute to the pathogenesis of these common cardiac conditions. Alterations in intracellular calcium dynamics have also been associated with heart failure. In heart failure, significant changes may occur, such as an increase in end-diastolic cytosolic calcium levels and a lengthening of contraction phases. Mutations affecting calcium channels can also lead to serious dysfunction, including spontaneous death without apparent structural heart disease. These findings highlight the importance of calcium ion dynamics in cardiovascular disease and highlight the need to better understand these interactions for the development of effective treatments and prevention strategies. Therefore it is in this light that we decide to explores the nonlinear dynamics of intercellular calcium Ca^{2+} waves in living cell networks. The study is based on a system of three reaction-diffusion equations which describe the concentration of Ca^{2+} ions, their movement from internal reservoirs to the cytosol and from the cytosol to neighboring cells through paracrine coupling. The dynamics are largely influenced by Ca^{2+}-induced Ca^{2+} release, with a significant role attributed to Ca^{2+}-stimulated degradation of inositol 1,4,5-triphosphate (IP_3) by 3-kinase.

.0.2 Problematic and objectives of the thesis

Information processing by Ca^{2+} networks results to the formation of localized nonlinear waves and appearance of synchronous patterns.From literature, the dynamics of Ca^{2+} ion plays a major role in cardiovascular diseases. Their waves dynamics presents a character nonlinear oscillatory system responsible for almost all physiological functions and anomalies, proliferation of coronary infections, as well as apoptosis. This nonlinearity and strong presence in cellular metabolism make this ion the most abundant mineral cellular and messenger in the organism. Thus, the study of the interactions between unstable Ca^{2+} waves in networks of coupled cells is of great concern. Starting from a deterministic model which accounts for complex oscillations of cytosolic Ca^{2+} induced by Ca^{2+} and auto-modulation of the inositol signal 1,4,5- triphosphate (IP_3) by 3-kinase stimulated by Ca^{2+}. However, numerical research analysis of such structures is less considered. In this thesis, the combination of coupling strength and distributed synchronization methods are used to study waves propagation and Cell Ca^{2+} synchronization phenomena in the context of the transport and transfer of signal in cardiomyocytes networks. Through these, we consider the distribution of Dirac to simulate the networks.

.0.3 Organization of the thesis

This thesis is divided into three main chapters that are outlined as follows:

✠ The first chapter focuses on the organization and properties of Ca^{2+} as a basic unit of cell information processing and cell networks as macroscopic structures for the transport and transfer of ca^{2+} waves. In this chapter mechanism of action of Calcium ions waves, Oscillatory Dynamics of Calcium ions, some of the most prominent Ca^{2+} models are presented.

✠ Chapter 2 presents the different mathematical models developed in this thesis as well as numerical methods used. Some immediate applications are made in order to facilitate the understanding of the methods.

✠ The third chapter is devoted to results and interpretations. We first discuss the coupling effect on cell network communication. Then the effects of distribution of synchronization (R) are studied in a discrete model of two-dimensional cells network. We also address the synchronization of one or bidirection paracrine coupled with cell network. We end with the study of unstable discrete modes in a discrete model.

The thesis ends with a general conclusion including the summary of the main results and future orientations.

CHAPTER I

LITERATURE REVIEW

Discovered in 1808 by Humphry Davy then isolated in its form common in 1892 by Henry Moisson, calcium is one of the elements most present in nature. It belongs to the alkaline-earth family and at atmospheric pressure and room temperature, in ionic solution its known as Ca^{2+}. In the organism, it is at the center of several pathophysiological functions, ranging from fertilization to apoptosis, through genetic transcription, muscle contraction and relaxation, heartbeat, secretion.With this great distribution and versatility of action in a universe as complex as the organism and its cell diversity, the dynamics of the Ca^{2+} presents varied biophysical properties to accommodate almost any cells. This makes the ion an ideal indicator for the understanding of the still poorly known physiological phenomena, where the living is the seat. This justifies the major interest of these decades for this element with applications multidisciplinary.

The heart is an organ whose beats are intimately linked to human life. It is a powerful muscle, responsible for kinetic and thermal properties of blood in the body because it regulates its flow and adapts to internal and external signals to the organism. Its functioning both normal and abnormal in a disease situation requires a good participation of Ca^{2+}, and whose supplementation is often considered as a solution for certain cardiac anomalies, hence our interest.

Human fertilization requires the proper functioning of the prostate. This organ participates in the secretion and propulsion of the seminal fluid, during reproduction. It is therefore an organ with dual function whose good condition is essential for procreation. Like any living organ, it is subject to dysfunction. Various origins, the most serious of which is cancer, one of the causes is supplementation calcium supplementation as solution to heart failure. The presence of Ca^{2+} is again noted both during normal operation and prostate cancer, but considered as a low-risk solution for the treatment of this cancer.

This chapter has three parts. The first part presents the origins of calcium in the body as well as its form, and its distribution. The second part will present the implication of calcium in the functioning of the heart from based of liver model, as well as its mechanism and its dynamics of action in situation pathophysiological. In the third part, we will present some mathematical models accounting for the dynamics of the Ca^{2+} in the living.

The calcium is one of the most common elements in nature which is present in the body. It comes exclusively from diet (food and drink), due to 1 g per day in the body (Truswell 2017). Dairy products and fruits represent the major part of these contributions in the organisms where it is the most abundant mineral (1.5 to 2 percent) of the mass, thus approximately 1 kg for a 70 kg human. It is absorbed at several levels of the device digestive system and divided into four compartments (see Fig.1), the bones where is the main reserve in the body (1 to 1.2 kg), the blood,

interstitial fluid and cells, under the supervision of three hormones, respectively parathyroid hormone (PTH), vitamin D and calcitonin according to the degree of importance. This calcium has a structural, regulatory and messenger function.

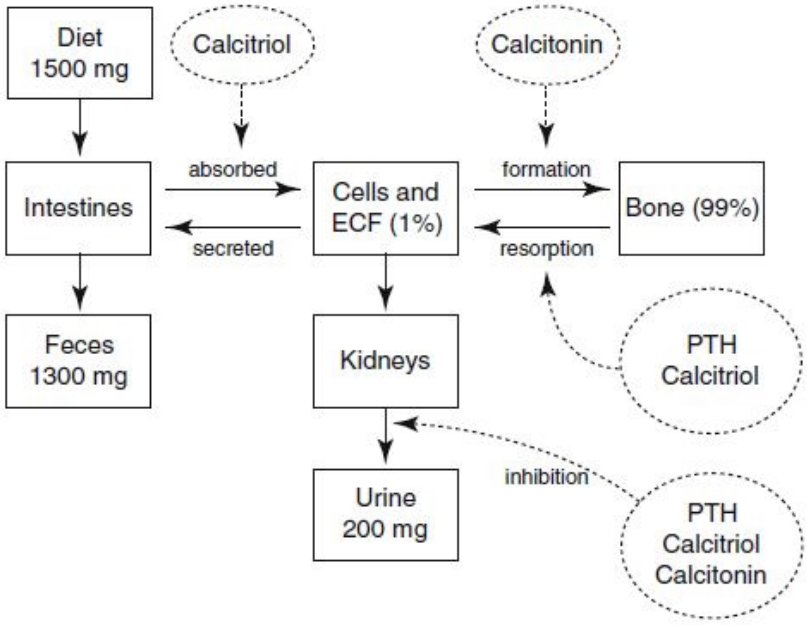

Figure 1: Whole-body Ca^{2+} Homeostasis [53].

I.0.4 In the Blood

The majority of the bone capital (60 to 80 percent) is genetically fixed at birth, the rest evolves with the lifestyle of each individual with perform and complete another think for diet. Calcium is primarily (80) housed in the cortical bone which has a mechanical role and in the spongy bone for the metabolic role of bone remodeling which is on average 10 to 12 years. Calcium is the most plentiful mineral found in the human body. The teeth and bones contain the most calcium. Nerve cells, body tissues, blood, and other body fluids contain the rest of the calcium. Calcium helps your body with: keeping a normal heartbeat, building strong bones and teeth, sending and receiving nerve signals,squeezing and relaxing muscles,clotting blood releasing hormones and other chemicals, expressing gene. The bone have a dynamic evolution before a life. From 30 years when the bone mass begins to decrease and if we can't complete for diet then we speak of osteopenia which is a bone demineralization which results in a loss of bone density and a weakening of the bone. It can evolve to become osteoporosis once the fifties are over. This decrease in bone mass is physiological and increases the risk of fracture. In other words, bone production becomes lower than bone resorption, which weakens the skeleton. Calcium deficiency is one of the main causes. This is how a balanced diet with a sufficient intake of calcium (green vegetables, enriched mineral water, nuts, pulses) and vitamin D (VD) (sun exposure or supplementation). VD is essential for the fixation of calcium and phosphorus on the bone, and therefore for its solidity. In the case of osteoporosis, medication is combined with the previous measures. The most

commonly used are from the bisphosphonate family: alendronate, risedronate and zoledronate. If the recommendation is not controlled the risk of high concentration are observe.

I.0.5 In other part of body

An ionogram is the biological analysis which makes it possible to know the concentration of the various ions (molecules charged positively or negatively) in a liquid. This examination includes the dosage of various ions including Ca^{2+}. An ionogram requires a venipuncture (blood test) to be performed at the bend of the elbow. The normal value for Ca^{2+} concentration ($[Ca^{2+}]$) on the other part of cell body illustrate different concentration from 0.1 μM in cytosol to 100 μM in endoplasmic reticulum [54]. Hypercalcemia is when the level of calcium in the blood is too high. This can have various origins such as hyperparathyroidism, excessive consumption of calcium or vitamin D, cancer, a bone disorder or prolonged immobilization. Generally, hypercalcemia is asymptomatic. The symptoms are non-specific: Constipation; Nausea and vomiting; Abdominal pain; Loss of appetite; dehydration and feeling thirsty. When hypercalcemia is severe, it causes neurological disorders such as: Confusion; Emotional disturbances; Hallucinations; A coma; muscle weakness; Life-threatening heart rhythm disorders. Hypercalcemia is diagnosed through a blood test, usually done for other reasons. Hypercalcemia caused by cancer is difficult to manage. It comes back if the cancer cannot be treated. It is a serious complication of cancer.

In the blood, it is mainly housed in the plasma, for a concentration of between $[2.20; 2.60]$ mmol/L. Serum Ca^{2+} is the average concentration of calcium in the blood plasma. We speak of hypocalcemia if the value is below the lower limit, which occurs when the output of Ca^{2+} is greater than the input (see previous subsection) on one hand and hypercalcemia, if the value above the upper limit, which occurs when the Ca^{2+} input is more than the output on the other. The remaining calcium involved in physiological and pathological functions.

I.1 Physiological function of Calcium

Although calcium is mainly absorbed to provide structural function, with 99 g of total calcium (about 1000 g) in bones, teeth and nails. The remaining percentage (1) is split between blood plasma (where it is bound to proteins), to the interstitial fluid and in the cell under ion form. In this form, it has a greater affinity to bind to a very large number of proteins and thus have a function of interrupting the activity, inactivity or stability of proteins (Kordel, 1994). This reveals the body's preference for the calcium ion, unlike other cations of the same valence.The blood gated Ca^{2+} and lot of other nutriments have pump by heart who need itself to drink their the necessary element from different part of body.

With this in mind, the different organs of the body have a interconnected functioning, reflex movements of respiration of the lungs depends on the supply of complexes proteins into oxygen, heartbeats depend the arrival of blood and its contents, therefore the food of the different organs such as the liver. Some intrahepatic vasvular resistance increased significantly portal

hypertension and contribute to emergency of liver disease like nonalcoholic fatty advance to cirrhosis [55].

After presenting each of these two organs, we present the role of Ca^{2+} ions in their behavior physiological and pathological because Men with high levels of Ca^{2+} in the blood serum have a greater risk of developing fatal disease.

I.1.1 In excitable cells like heart cell

Heart is a powerful muscle that responds to the need of blood absorption and distribute it to the body's anterior compartments by its beats. Heartbeats are among the first vital signals of a living being. These beats result from an overall movement of the three billions of muscle cells that contain the heart. Each beat is a mechanical movement that requires excellent coordination of behavior from all heart cells, which is made possible by the propagation of an electrical signal. This spread is translated by the entry and exit of Ca^{2+} from the cells heart(see Fig.2). The entry leading to the contraction and the exit leading to relaxation and a return to the state of rest for the next heartbeat. Cardiac cell contraction is triggered by an influx of Ca^{2+} and relaxation is due to a release of Ca^{2+} from the cells. The heart is crossed by an electrical signal from one cell to the neighboring cell like a $"Hola"$ in a stadium and this thanks to Ca^{2+}, responsible for the link between electrical activation and mechanical contraction. In the early 1880s, Dr Sydney Ringer have say in experimentally demonstration that Ca^{2+} is essential for the heartbeat so vital.

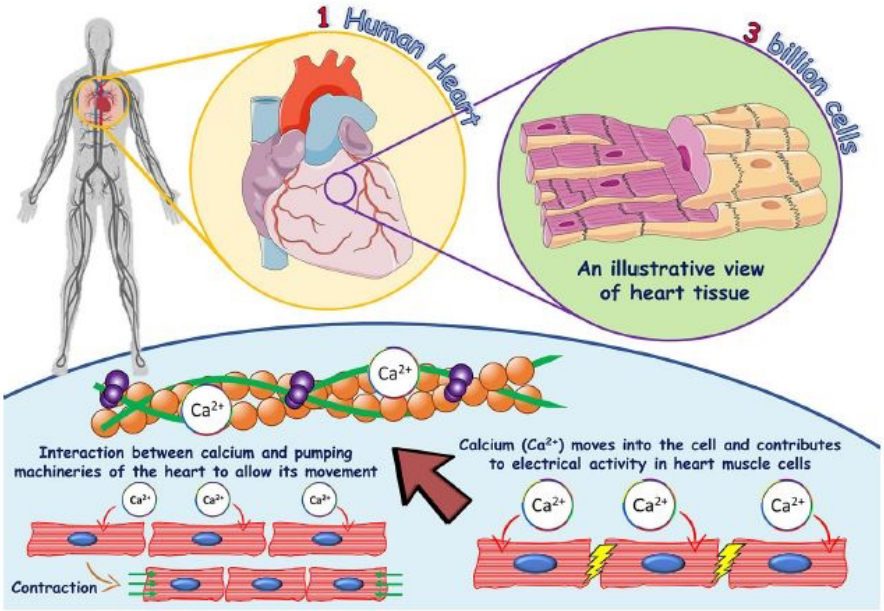

Figure 2: The role of calcium in heart muscle cells.. [56].

In a study of the power and responsibilities of Ca^{2+} in the heart, it is established that the beat of the heart originates at the level of each cell to achieve a movement of the whole organ. Cytosolic Ca^{2+} binds to the complex of troponin and causes the cells to swell and reduce the

space that separates them. Cells shrink corresponds to the contraction of the heart muscle. Concentration of Ca^{2+} having increased, by a specific mechanism, the membrane receptors specific to calcium or not will opened to allow entry of Ca^{2+} into the cellular behaviors such as the RS or an exit from Ca^{2+} of the cell. We observe a return to the initial state of the considered cell which is ready for the next beat and the signal propagation to neighboring cells. This big responsibility of Ca^{2+} is not, however, immune to various malfunctions with risks commensurate with the multitude of functions for which it is responsible. A genetics mutation can lead to receptor malformation membranes and a dysregulation of the movement of Ca^{2+} through the different cell compartments, a variation in function binding protein which leads to the spread of bad electrical signal and therefore heart rhythm disorders simple (fatigue) or heart failure potentially deadly [56]. In some cases, the doors controlling the movement of Ca^{2+} malfunction, causing too much or too little Ca^{2+} to enter the cell. The improved understanding of heart rhythm disorders has helped to predict which patients have a high risk of these problems and has also resulted in better therapies, called electrocardiogram (ECG). In the prevention and treatment of osteoporosis, Ca^{2+} supplementation is commonly prescribed. Thanks to this new study, it now appears that not only Ca^{2+} supplementation is likely to increase the risk of cardiovascular diseases and accidents, but also that it does not provide effective protection against the risk of fracture linked to loss of bone mineralization.

I.1.2 In non-excitable cells like hepatocyte

The liver is the main organ of secretion, synthesis, regulation and control of the body. It ensures the secretion of hormones ensuring the endocrine and exocrine functions of the body, the storage of glycogen, the detoxification of drugs, the control of metabolism, regulation of the synthesis and transport of cholesterol, metabolism of urea, and the secretion of a wide range of plasma proteins. Due to its role as regulator of normal physiological processes, any dysfunction would lead to several anomalies among the top five main causes of death in humans. The liver is made up of a cellular network mainly made up of hepatocytes heavily infiltrated by blood vessels and bile ducts. This structure in many respects shows the participation of the liver, notably of the hepatocytes, in cellular communication which can extend to all levels of the organism by mechanisms that are still little or poorly understood [55, 57] (Fig.3).

Several studies report Ca^{2+} as the first cellular messenger both in terms of its distribution in the body and the number of physiological functions on which it depends. The first observation of Ca^{2+} oscillations induced by hormone are in hepatocyte. Ca^{2+} activates phosphatase enzymes which participate in glycogenolysis. Experimentally, we obtain patterns Ca^{2+} oscillation in respond of agonist like vasopressin and ATP. Other the fact that the activity, proliferation and dead cells are slow and equilibrated to assured slow regenerating hepatocytes and liver tissue, the propagation of a spike Ca^{2+} wave at around 20 μs^{-}, and we have the propagation of complex Ca^{2+} wave in hight frequency. Their mechanism of emergency of this type of Ca^{2+} waves can not well know.

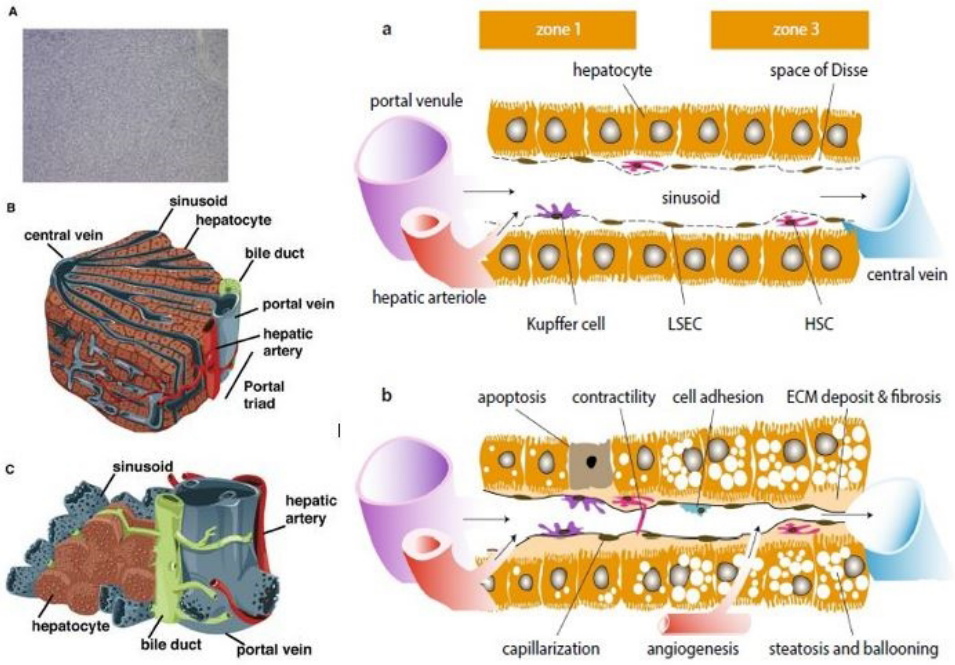

Figure 3: Architecture of the Liver. Different liver scales in left and from right a-normal state b-disease state. [55, 57].

I.2 Mechanism of action of cellular Calcium ions waves

All the four most abundant cations (Na^+; K^+; Mg^{2+} and Ca^{2+}) in the body, Ca^{2+} is divalent, therefore more suitable for forming more stable bonds with proteins and better used as a chemical signal in neurons, its radius is greater and a higher variable coordination number then thermodynamically and kinetically it is more favorable to fix a greater number of substrates. Finally, it has a strong affinity with the carboxylate groups that are abundant in cells. The Ca^{2+} is essential for the fertilization process (movement of sperm flagellates, resumption of the cell cycle at fertilization in oocytes), genetic regulation, process of excitation-contraction of muscle cells, excitation-secretion in synapses neurons Activation of the Ca^{2+} signal The distribution of Ca^{2+} in the different cellular compartments is strictly controlled and any variation has serious consequences. In the cell, the Ca^{2+} is mainly stored in the endoplasmic and sarcoplasmic reticulum, another part in mitochondria, Golgi apparatus and nuclear membrane. A small amount (the order of 1μM) of Ca^{2+} is present in the cytosol (the level in which the organelles are cells), i.e. about 1000 times less than the Ca^{2+} extracellular, which represents a large gradient of concentration between intra and extracellular media. This distribution is very specific to the Ca^{2+} ion unlike other major ions (cations) in the body whose distribution difference is around 10^{-1}, 10^0 and 10^1 respectively for the K^+, Mg^{2+} and Na^+, which further highlights the importance of Ca^{2+} in the body. In blood, the majority of Ca^{2+} is in the plasma and bound to proteins, the rest in the blood cells. To ensure all the needs and guarantee the structural functions and reserves, hormones activate absorption, distribution and storage in specific compartments of the body. When the standard is reached, the signal is still emitted for reduce absorption. It is in case

of need that a dynamic is observed at the level of the cytosol, the study medium of the present work.

I.2.1 In excitable cells like Cardiac cell

Cardiomyocytes are contractile eukaryotic cells measuring 120 μm long and 20 to 30 μm in diameter in adults. In addition to the nucleus, they contain numerous mitochondria (20 to 30 percent of the cell volume) and myofibrils arranged in a linear manner. This structure allows the heart muscle to contract as a unit or not. Depending on physiological conditions, cardiac contraction is a signal corresponding to the release of Ca^{2+} through the membrane receptor (ryanodine) located on the sarcoplasmic reticulum. This release is due to the massive flux of Ca^{2+} through voltage T-type cells. Thus Ca^{2+} dynamics presents patterns ranging from simple oscillations to complex oscillations observable in different physiopathological situations such as arrhythmias and muscular stress.

Electrically excitable cells are those in which one activity is part of an electrical signal can propagate through it. In excitable cells, the Ca^{2+} enters the cell through specific channels that open when the potential transmembrane (-80 to -60 mV) decreases or reverses, that is, when the membrane depolarizes. In the muscles rapid skeletal structures, the plasma membrane maintains the intracellular concentration of free Ca^{2+} around 0.1μM. The increase in the concentration of Ca^{2+} induces the contraction of the muscle cell, while the return to the 0.1μM concentration induces relaxation. This rapid release of Ca^{2+} is ensured by specific receptors located on the membrane of the SR, a specialized organ for which releases Ca^{2+} with the participation of ATP. ATPase-Ca^{2+} pumps Ca^{2+} from the cytoplasm to the organelle (against an unfavorable electrochemical gradient). When the RS is solicited as in heart cells, the entrance gates of the RS are called SERCAs and the exit gates are called ryanodine receptors. The deregulation of blood level of Ca^{2+} could increase the cardiovascular risk and perturb the ECG and induced a lot of cardiac arrythmia like represent in (Fig.4).

Heart beats are among the first vital signs of a living being. These beats result from an overall movement of the billions of muscle cells that contain the heart. Cardiac cell contraction is triggered by an influx of Ca^{2+} and relaxation is due to a release of Ca^{2+} from the cells. A difference in concentration in the cytosol leads to Ca^{2+} dynamics through specific ryanodine receptors type 2 (RYR2), more precisely in the membrane of the sarchoplasmic reticulum. This leads to a release of Ca^{2+} to the cytosol. This Ca^{2+} ion dynamics activated for a return to the state of equilibrium, showed experimentally has been grouped into two classes, a simple elementary oscillation like a spark in cytosol and a global oscillation when the Ca^{2+} overload converts the cytoplasm into an excitable medium such that a Ca^{2+} spark can ignite neighbouring units, thereby setting up a regenerative Ca^{2+} wave [63]. These Ca^{2+} waves in overloaded cardiac cells are somewhat abnormal and can result in cardiac arrhythmias [58], they represent the synchronization mechanism used normally. The spiral patterns and waves observed in cardiac muscle cells under high concentration or arrhythmia were not only quite present but also an emergency regulatory or surviving mechanism activated by the cell for rapid return to normal or recovery. self-defense as

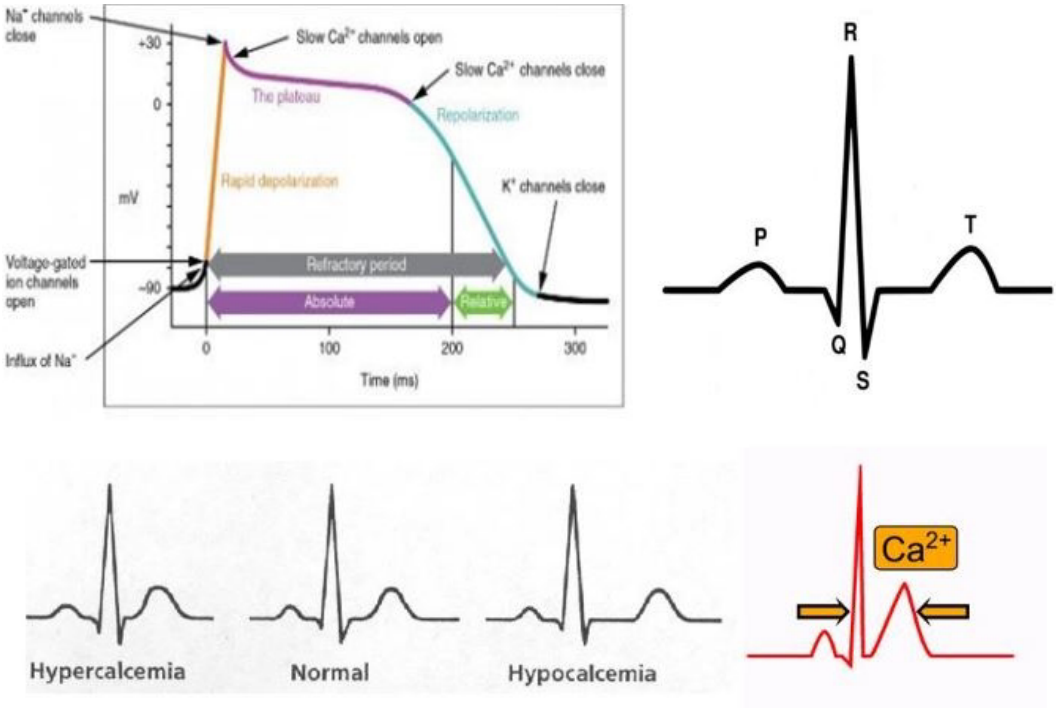

Figure 4: Impact ICC - PA - ECG (top) and Impact ICC with ECG deregulation (bottom) [58]

mentioned by [64].

For example, some targeting Ca^{2+} homeostasis like it a increased blood level (by 0.51 mg/dl or 0.13 mmol/l) not prevent the development or progression of osteoporosis but an increased many disease like coronary artery disease (coronary artery disease) by 25 percent and the risk of myocardial infarction (Fig.7).

Myocardial infarction, commonly called "heart attack" corresponds to the partial necrosis or destruction of the heart muscle. Myocardial infarction is a life-threatening emergency requiring emergency care for immediate hospitalization at the first symptoms. The risk factors for myocardial infarction are the same as those for atherosclerosis.

I.2.2 In non-excitable cells like hepatocytes

These are the cells that are not the seat of activity electric. There are two different types of Ca^{2+} channels. A shape has the same characteristics as the channels of the excitable cells, that is, they open when the plasma membrane is depolarized, inhibited by antagonists calcium. The other channel type Ca^{2+} found is insensitive to calcium channel blockers and activated by the binding of hormones on their receivers. These receptors are present in hepatocytes.

Hepatocytes are the most abundant liver cells (70 percent). are polyhedral cells of 20 to 30 μm, in which spike-type Ca^{2+} waves have been observed during enzymatic synthesis (Fig.3). In relatively large cells such as the hepatocyte, Ca^{2+} signaling is modulated in frequency and amplitude in order to ensure several metabolic functions both at the level of localized cells (contrac-

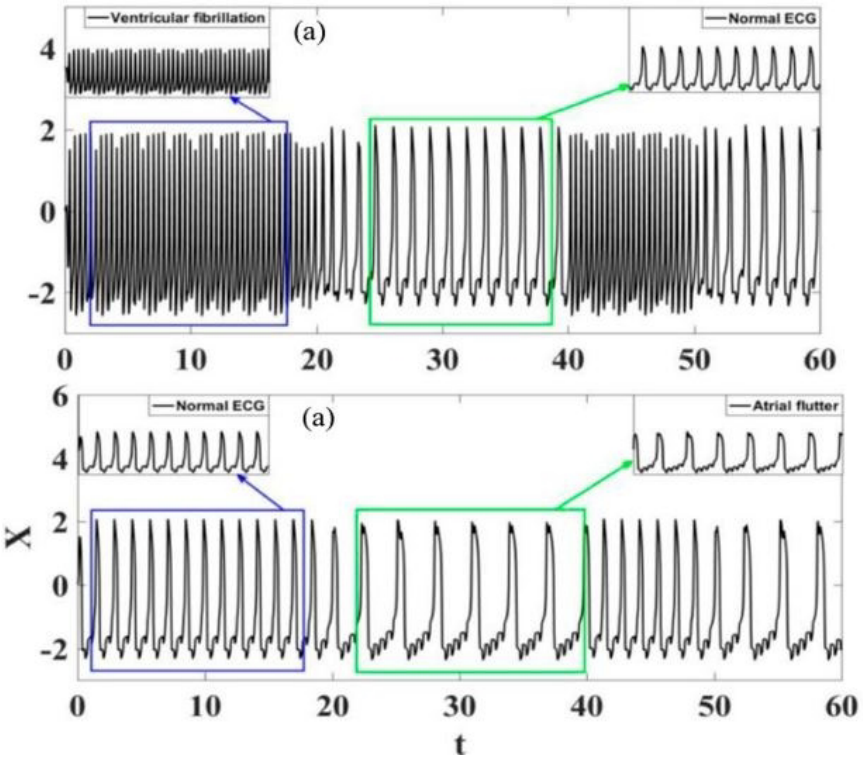

Figure 5: Ventricular fibrillation and Atrial flutter [58].

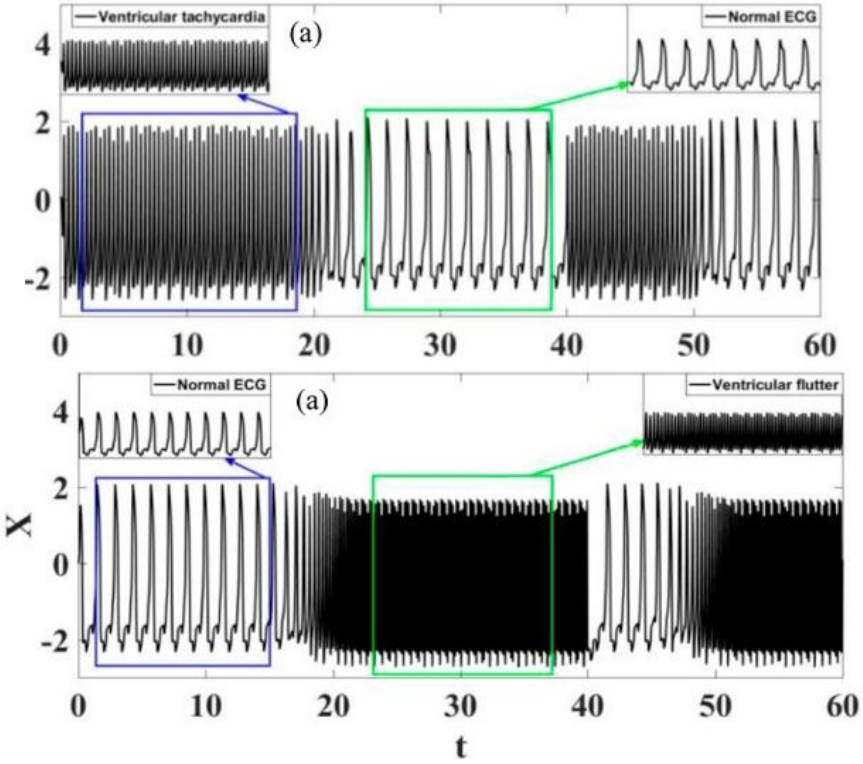

Figure 6: Ventricular Tachycardia and Ventricular flutter [58].

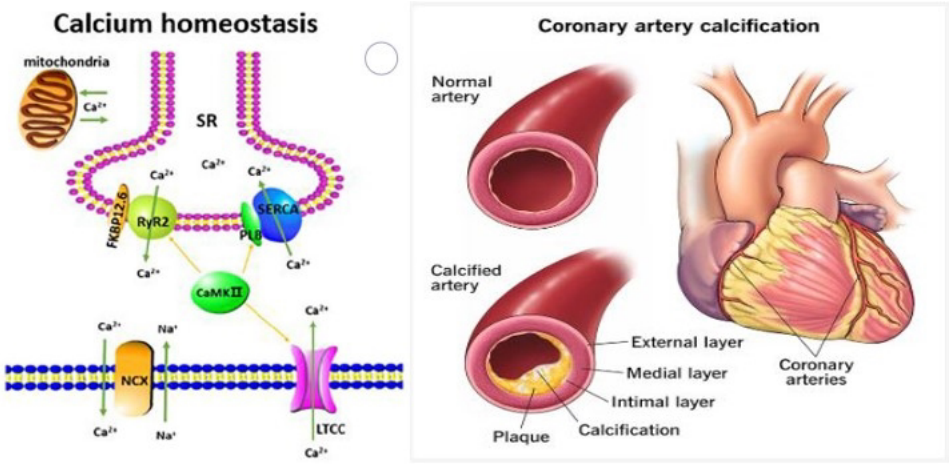

Figure 7: Targeting Ca^{2+} homeostasis (left) and coronary artery calcification (right) [59, 60].

tion of canicular biliary) and cells distributed in different cellular compartments (glycogenolysis and oxidation of the mitochondrial substrate). The transduction of blood hormone signals by specific receptors and G proteins is ensured by Ca^{2+} waves.

In response to hydrogen peroxide stimulation, burst type observations are observed experimentally. Over the years, several hypotheses have been presented, aiming to explain the observed behaviors. First of all, the dynamics of Ca^{2+} is stimulated by an extracellular factor (hormone) is developed by Woods et al, 1986. Subsequently the participation of inositol first at a constant rate then variable in the dynamics of Ca^{2+} is highlighted in different cellular environments. This participation occurs through cytosolic IP_3 and/or these receptors on intracellular reservoirs. Building on this, models based on oscillations of both IP_3 and Ca^{2+} make it possible to account for the complex oscillations of Ca^{2+} observed in hepatocytes, with different frequencies and amplitudes.

Initially intracellular, these waves can propagate at the extracellular level to ensure the collective dynamics of the tissue or even the organ. A poor or interrupted signal could lead to the formation of clusters leading to cell ballooning, even bursting and therefore apoptosis responsible for liver diseases such as cirrhosis [55]. Given the relative size of hepatocytes, such dynamics cannot be ensured by short-term spikes of $[Ca^{2+}]_i$ Fig.9. This is how certain experiments report the emergence of complex hepatocyte $[Ca^{2+}]_i$ waves as indicated [47]. The conditions for the emergence of this type of wave as well as the different oscillatory patterns associated with several anomalies and physiological functions remain poorly understood.

I.3 Oscillatory Dynamics of Calcium Ions and Inositol 1,4,5-triphosphate

Calcium is stored in internal pools, where its concentration is higher than in the cytosol and the extracellular medium. The oscillatory dynamics of Ca^{2+} ions is under the control sensors or

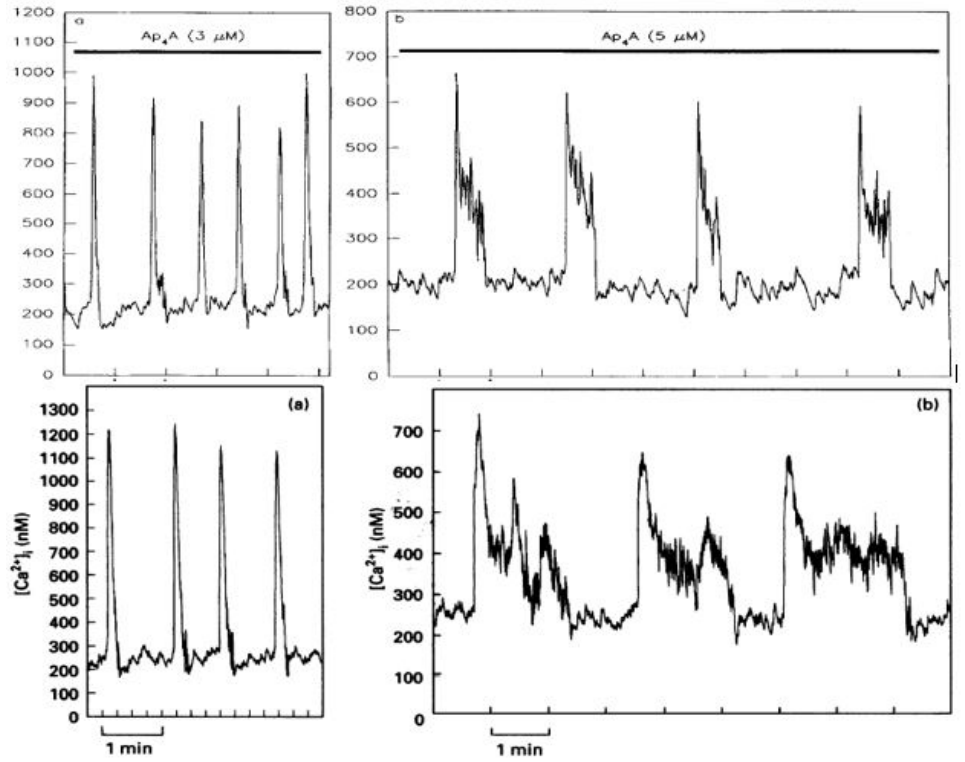

Figure 8: Complex Calcium waves [47].

biological markers present in the intra and extracellular environments, which unfold depending on the situation (low or high) through specific signals. In a situation where the concentration of Ca^{2+} in the body (hypocalcemia), the signal is emitted to solicit the Ca^{2+} of the internal reservoirs and in the long term the structural reserves, which could in the long term weaken the organ and lead to anomalies such as osteoporosis, or a violent and long muscle contraction. In a situation of excess Ca^{2+} (hypercalcemia), which can be following a high Ca^{2+} absorption, a drop in activity physical activity associated with a diet rich in calcium (products dairy). It can lead to malfunctions that can lead to the formation of aggregates at various levels. This formation of Ca^{2+} aggregates in organs such as the parkinson, coronary artery calcification, pancreas cell leading to diabetes, accumulation in the cytosolics cells and prolonged strong concentration of Ca^{2+} causes apoptosis. This shows to sufficiency that the oscillatory dynamics of the Ca^{2+} ions is a very important signaling including regulation, control of knowledge is of paramount importance for the survival of cells, tissues, organs and even organisms.

I.3.1 In the intracellular medium

The Ca^{2+} concentrations in the different cellular compartments are maintained around a well-defined value threshold and any modifying disturbance leads to a dynamic aimed at returning to normal. In the pancreas acinar cells, when the concentration of Ca^{2+} increases, the mitochondria absorb it very quickly to limit the Ca^{2+} response in the cell. Subsequently, a much slower release of Ca^{2+} from the mitochondria serves as a supply of Ca^{2+} in the cytosol which causes calcium

oscillations.

Generally, Fig.9 describe the intracellular dynamics of Ca^{2+}. In equilibrate state $[Ca^{2+}]_i \sim 0.1\mu M$, act like (1), Any stimulus act (2) initiate the liberation of IP_3 in the cytosol. The ryanodine receptor and the inositol 1,4,5-trisphosphate receptor (IP_3R) are privileged channels that release calcium from internal stores into the cytosol. They mechanism is called Inositol triphosphate induced calcium release (IICR). The underlying process gives rise to a spatio-temporal coded signal that conveys information about variations in calcium concentrations [7]. This late activate the channels that release calcium from internal stores into the cytosol (3). In doing so, Ca^{2+} serves as a second messenger via a signaling mechanism that relies on variations in Ca^{2+} concentrations and results in brief spikes that typically appear as regenerative waves [7, 3, 9]. Calcium waves, at the intracellular level, were initially reported in medaka eggs [10] and then in other cell types such as hepatocyte or Xenopus oocytes [65]. For the Ca^{2+} response to be initiated, a series of reactions are triggered by an agonist and produce the messenger called inositol 1,4,5-trisphosphate (IP_3) [16] by binding to the IP_3R. The released IP_3 diffuses into the cell cytoplasm (4). This mean the return of $[Ca^{2+}]_i$ (5) after some high depolarization (4).It binds to IP_3R in the ER, which contributes to the release of Ca^{2+} into the cytosol, via dedicated channels, according to the induced calcium release mechanism by calcium (CICR). Release is complete when the cytoplasmic concentration of Ca^{2+} reaches a threshold, thus inactivating the receptors. In astrocytes, for example, the sequence of events described above can propagate to surrounding cells, forming intercellular Ca^{2+}.

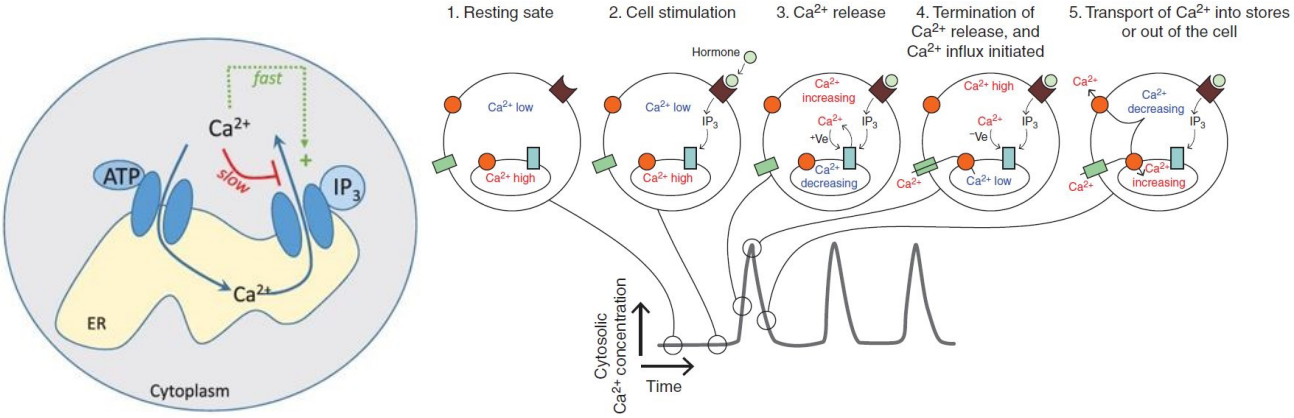

Figure 9: Basic mechanism of cytosolic Ca^{2+} oscillations in non-excitable cells (left) [61]. Generation of Ca^{2+} oscillations via positive and negative feedback on IP_3R (right) [62]

I.3.2 In the intercellular medium

While the fact is well established for hepatocytes, astrocytes or epithelial, where the signal can be shared with up to 2, 3 or 30 cells, the usual open question regarding intercellular Ca^{2+} waves is the mechanism involved (see Fig.1 and Fig.10). Undoubtedly, the propagation of the extracellular messenger adenosine triphosphate (ATP) and the permeability of intercellular IP_3 calcium ions are important factors contributing to the propagation of intercellular calcium waves [17, 23].

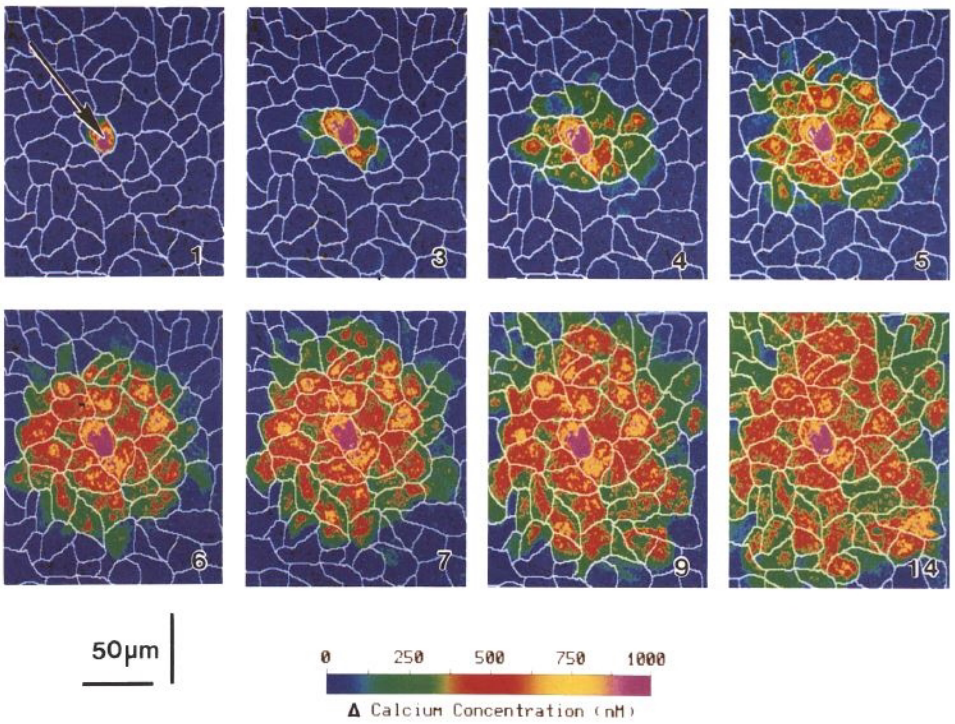

Figure 10: Intercellular Ca^{2+} signalling in non excitable cells.3 hepatocyte cells and 30 epithelial cells [12]

However, this may depend not only on cell type but also on physiological conditions [25, 27], involving either IP_3 or calcium diffusion through gap-junction(GJ) or paracrine signaling. According to some of the available mathematical models, gap junction diffusion relies on a second messenger such as calcium or IP_3 [30, 32], as well as other factors such as stochastic effects [35] to realistically describe calcium dynamics [37, 38]. In contrast, paracrine signaling involves the release of a messenger that diffuses into the extracellular space, binds to receptors on adjacent cells, and follows kinetics that trigger an increase in free calcium in the cytoplasm of target cells [39].

The cell regeneration cycle, is the partial reconstitution of the cells of a damaged organ, leads to a dynamic of all the cells which leads to that of the Ca^{2+} ions. In the case of liver regeneration in rats, the progression of hepatocytes through the cell cycle results from the extracellular dynamics of Ca^{2+}. Michael J. Sanderson et al [12] were able, following a localized infusion on a cell, to observe the propagation of Ca^{2+} through a culture of bound hepatocyte cells. Moreover, some experimental facts reported calcium sensitive receptors (CaR) on the membrane of adjacent cells as being activated by fluctuations of extruded calcium during the intracellular spike of Ca^{2+} in a cell, thus producing spikes secondary in these cells [40]. This may result in cell-to-cell communication in which the target cell is responsible for a new round of Ca^{2+} signal communication relayed by the regeneration of cellular calcium signaling events capable of achieving a higher large population of cells.

I.3.3 Dynamics of Inositol triphosphate (IP_3)

Inositol triphosphate (IP_3) is a messenger resulting from the hydrolysis phosphoinositides by phospholipases C (PLC) membranes. It was discovered by Berridge in 1983 [8]. It discovers that the activation of membrane receptors of salivary glands of flies, causes the rapid formation of a molecule (IP_3) performing the function of second messenger for the exit Ca^{2+} ions organelles intracellular to the cytoplasm. The IP_3 formed in the cytosol is under the influence of two enzymes, 5-phosphatase to form IP_2 or 3-kinase to form IP_4, which subsequently participates in the dynamics of the Ca^{2+} ions (see Fig.11). IP_3 will bind to these receptors (IP_3R) well located on the membrane of internal Ca^{2+} reservoirs, which activates the release of Ca^{2+} ions into the cytosol (IICR). This IP_3 receptor appears to exist normally as a tetramer, with a molecular weight close to 10^6 and ion channel activity. The dissociation rate of IP_3 on its receptor is influenced not only by cations such as Ca^{2+}, but also by ATP The pulsatile, transient aspect of the modulations of [Ca^{2+}]i largely results from retro-controls of the activity of IP_3R in which calcium plays an important role. Some studies show that it is IP_3, among other things, that provides the coupling function between the cytosol depleted in Ca^{2+} and the plasma membrane. In the whole liver, stimulated by hormones, we observe an oscillating release of Ca^{2+} , which implies a coordination in the whole organ of the oscillators present in each cell. Although some models accounting for the oscillations of Ca^{2+} are developed at constant values of the concentration of IP_3 , a more complete model must take into account the dynamics of IP_3 , because all dynamics of Ca^{2+} result from the primary oscillations of the production of IP_3 [1], which thus showed that the complex IP_3 -Ca^{2+} is responsible for many functions and physiological discomfort (see Fig.11.).

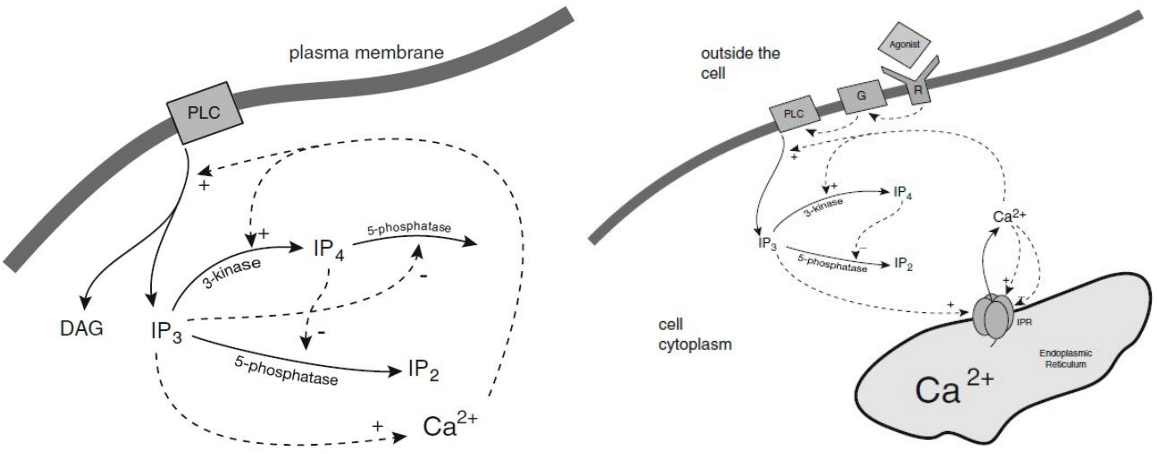

Figure 11: Production and metabolism of IP_3 (left)and [65], Basic mechanism of cytosolic IICR-CICR interactions [61] (right)

Our work will be based on this complex cytosolic interaction (IP_3 -Ca^{2+}) comparable to two coupled oscillators having a non-linear character. This two oscillatory system IICR-CICR are illustrated by Fig.11. The cellular coupling which allows the propagation of the signal in the whole of the network can be done gap-junction, therefore from one cell to another, by seeing

endocrine (through the blood), by voice autocrine (the emitting cell y included) or by paracrine voice which is our chosen mode.

This complex (IP_3 -Ca^{2+}) is responsible of many cells fnction initiate oscillation in cell and propagated in cells network through the gap junction or paracrine signaling with we present in next subsection. Based on these cinematic parameters and spatio-temporal, mathematical models are developed to account for the dynamics of different behaviors observed and thus contributing to an understanding of the dynamics Ca^{2+} waves. We will present some hypotheses and basic mathematical models, depending on the patterns observed oscillations.

I.4 Synchronisation

Synchronization is an adjustment of the time scales of oscillations due to interaction between the oscillating processes. Body is the seat of physiological functions ranging from the sub-cellular scale to the organic scale, and those at orders of equally varied frequencies, which makes him a very complex system. The synchronization between all these phenomena is a very important factor for the coordination of interacting functions in the same system. It allows to the biological clock to control the expression of genes in the time such as the appearance of secondary sexual characteristics, to be in phase with the variations of external factors (temperature, the day and night phenomenon) where we note a good involvement of Ca^{2+}. It is important for the study of collective behavior of neurons during the propagation of nerve impulses [66]. At the level of the signal dynamics Ca^{2+}, it can be activated by entry of extracellular Ca^{2+} in the cell or the release of an internal reservoir following fixing the IP_3 on the IP_3R. The phenomenon of synchronization is essential for the good propagation of this signal, both at the intracellular scale than on the extracellular scale for a network of interconnected cells such as a tissue.

For the study case of Synchronization of Ca^{2+} Oscillations in hepatocyte, individual hepatocyte subjected to the same level of agonist display Ca^{2+} oscillations at different frequencies by [67]. The variation in response is probably a result of differences in the level of hormone receptor or in structural properties of the cell, specifically the ER content. However in preparations of multiple cells [68] and in the intact liver [69] oscillations in connected cells are seen to be synchronized at a common frequency despite the variation of gene expression, hormone uptake and ER level. This synchronization may provide a mechanism by which the body can coordinate the response of a large number of heterogenous cells. The mechanism by which the oscillations are synchronized has not been fully determined but must require some form of intercellular communication. Communication between adjacent cells can occur by the diffusion of messenger molecules through the extracellular medium via gap junctions or paracrine pathways. In hepatocyte, it is commonly agreed that gap junction signaling and not paracrine routes are responsible for the co-ordination of calcium signals [70, 71]. Experimental evidence for this is provided by the work like [68] who observed a loss of synchronization between coupled cells when gap junctions were selectively blocked.

For the study of IP_3 signalling whereby gap junctional communication regulates the coordi-

nated activity of a large number of cells, synchronized calcium signalling has been described in various cellular systems. For example, synchronized calcium oscillations or intercellular calcium waves have been reported after stimulation of epithelial cells [71], hepatocytes and astrocytes [65]. In all these systems, synchronization seems to be dependent primarily on the diffusion of IP_3 through gap junctions [70, 32], although diffusion of calcium may also contribute to synchronization [72, 31]. Moreover, synchronized calcium oscillations in pancreatic -cells in the presence of glucose result from coordinated electrical bursting activity, which is mediated by gap junctions (Santos et al., 1991). Synchronization is important fact in studies of many cells network.

I.5 Spiral waves

A spiral wave is a constant, curved phase line that propagates towards its center or away from the central spiral. It was first observed experimentally in 1971 in an excitable chemical medium subject to reactions (Belousov-Zhabotinsky reaction) but, over the years, it has been observed in several experiments and numerical simulations of reaction-diffusion of organic tissues in various pathophysiological situations where it is the cause of certain pathologies such as epilepsy, cardiac arrhythmia, cirrhosis of the liver [73]. Archimedean spiral waves, illustrated in Fig.12, have also been found in numerical simulations of numerous reaction-diffusion systems. This is a contour plot of a planar Archimedean spiral wave for a fixed time value. The spiral wave rotates rigidly with a time frequency ω around its centre or core and its consecutive spiral arms are approximately equidistant in the radial direction with a period 2 π/k, where k is the spatial wave number. Each spiral arm moves with a velocity approximately equal to ω/k in the radial direction.

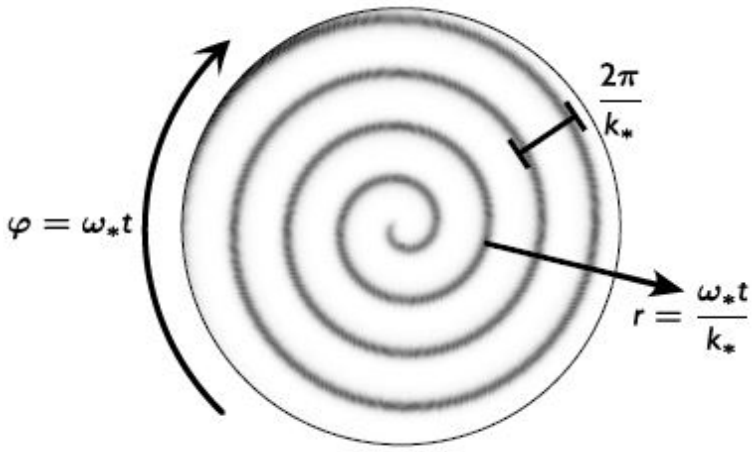

Figure 12: Spiral wave. [74]

In general, spiral waves arise in self-organising coherent structures where the spatio-temporal dynamics of the dissipative systems are spatially extended. Spiral waves are excitation waves

which, unlike plane waves which cause a single excitation (signal propagation), cause several excitations, resulting in prolonged high-frequency dynamics without a return to the steady state.

In cardiac cells, where Ca^{2+} plane waves ensure contraction-relaxation of the muscle, the occurrence of a spiral wave leads to prolonged contraction of the muscle without relaxation, resulting in cardiac arrhythmias. Among the most dangerous cardiac arrhythmias are ventricular tachycardia and fibrillation, in which the rate of cardiac contraction is considerably increased and, in the latter case, becomes completely disorganized. Ventricular fibrillation leads to sudden cardiac death and is the leading cause of natural death in the industrialized world. An excitation generating a spiral wave can be maintained in a spatially reduced medium such as the atrium, but in the face of inhomogeneities due to the presence of obstacles, inexcitable bodies, in short the refractory properties of the excitable medium (nucleus) which, once in the ventricle, gives rise to wavelets or multispiral structure or evolves into turbulent waves Fig.13.

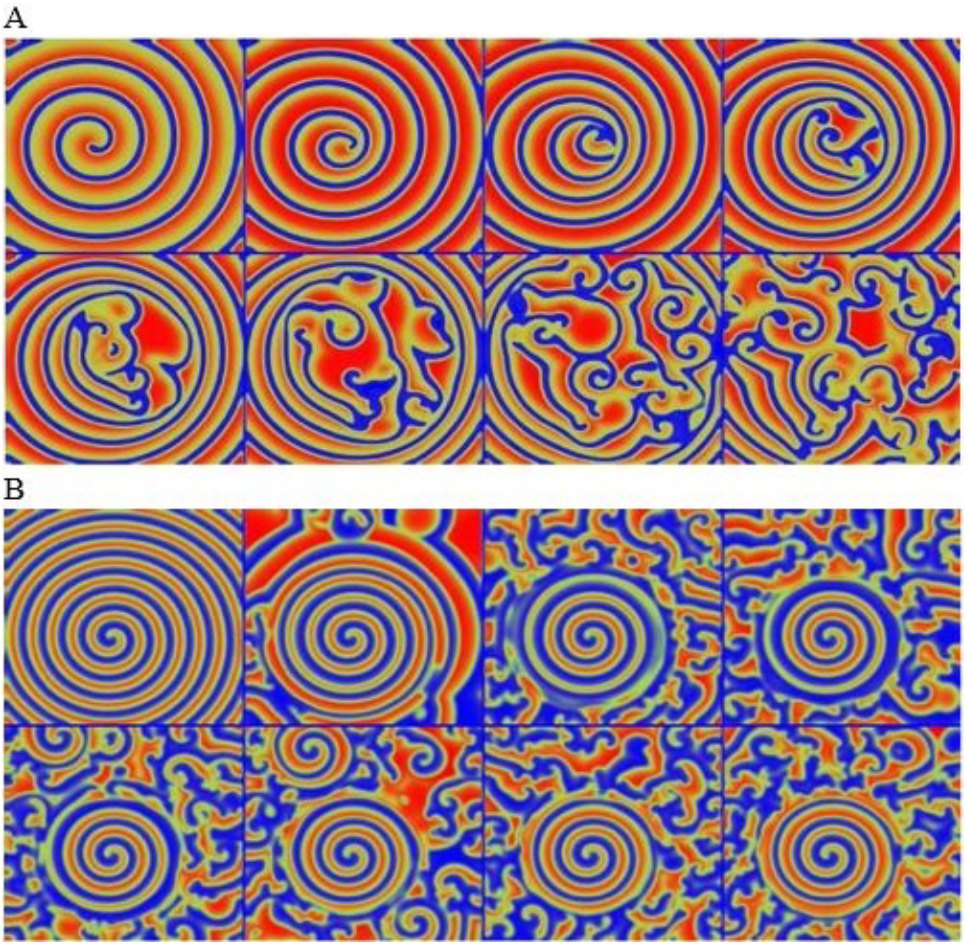

Figure 13: Generation of turbulent state in time after spiral fragmentation [75]

Some experiments report the emergence of spiral waves in cardiomyocytes for [Ca^{2+}]i concentrations of up to 20 to 40 μM at its peak [76] during diastole, which are values close to those of hepatocyte cells [77]. The latter team succeeded, on the basis of a dynamic Ca^{2+} model with two variables and a constant IP_3 level in non-excitable cells, in obtaining the Ca^{2+} spiral waves applicable to cardiomyocytes. This motivated our choice of HD for studying the dynamics of

Ca^{2+} spiral waves in hepatocytes applicable to cardiac arrhythmia conditions. In the following section, we present a few mathematical models to account for the Ca^{2+} dynamics and oscillatory regimes obtained.

I.6 The different oscillatory regimes and mathematical models

Initially in reaction to a stimuli, the dynamics of the Ca^{2+} ion appears in the form of a peak aimed at a return to normal which can be considered as the balance of our system. repeats at a frequency, thus giving rise to an oscillatory movement. This is why simple oscillations are more frequent in the dynamics of Ca^{2+} ions, as well as the models accounting for this state of affairs. The observation of complex waves, not only in excitable cells such as cardiac cells but in non-excitable cells such as hepatocytes, is one of the major concerns of biophysics, in particular their mechanisms of activation and emergences. We will present the evolution of some models and principles, in particular those based on the CICR principle. To the nature of the stimuli and the cell where the oscillations take place, mathematical models are developed to account for experimental observations. We will focus on the dynamics based on the CICR principle with are present in many type of cells, like cardiac and neurons.

CICR is a Ca^{2+} release mechanism where a variation moderate level of Ca^{2+}i sensitizes the Ca^{2+} channel and causes an amplified release of Ca^{2+} from compartments intracellular, with make some potential act like (see Fig.14).

The Ca^{2+} channel is modulated by ryanodine whose receptor has sequence similarities with IP_3R and caffeine. This mechanism was originally described in skeletal muscle and cardiac muscle and later found in the ER of non-muscle cells [11] . The oscillations of Ca^{2+} involve several media, the cytosol, extracellular environment and internal reservoirs such as mitochondria, endoplasmic reticulum and sarcoplasmic. These oscillations observed experimentally and translated by mathematical models such as the CICR (Calcium induced-Calcium libration) where the IP_3 is constant and on the other or IP_3 varies(Fig.14).

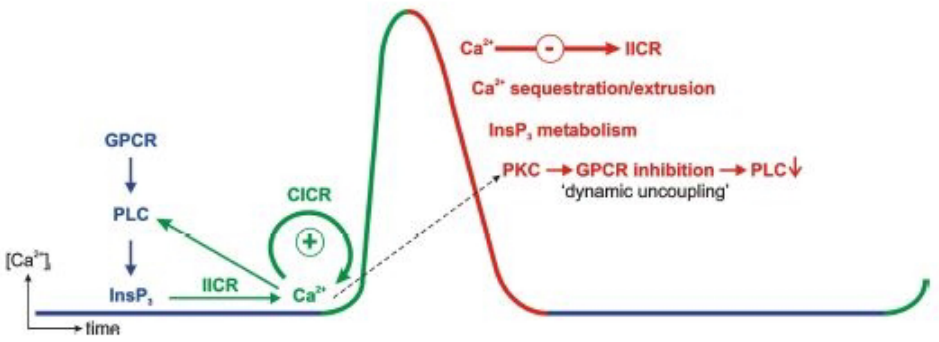

Figure 14: Illustration of potential act of CICR [91]

The complex oscillations of Ca^{2+} are observed in a large number of experimental studies of the Ca^{2+} waves of some cells. Several mathematical models based on laws of chemical kinetics have made it possible to model the oscillations of Ca^{2+}. Some are based on the CICR mechanism (Calcium-induce Calcium-release) or requires involvement of IP_3 or its receivers. Based on the CICR mechanism, Goldberter in 1990 and Dupont in 1993 established models having one or two tanks intracellular Ca^{2+} sensitive or not to IP_3. These models have made it possible to obtain complex oscillations of Ca^{2+}. Based on the minimal model of Goldbeter et al, Kepseu et al en [42, 41] were able to obtain simple oscillations by variation paracrine coupling parameter between neighboring cells. This which has contributed to a better understanding of the dynamics of oscillations simple Ca^{2+}, their formation conditions and their biological implications. In a first solution approach, we will by a discrete approach study the conditions of formation of complex oscillations of Ca^{2+} and their biological implications. The dynamics of Ca^{2+} ions is observed experimentally in the majority of cases using fluorescence markers. These experimental observations report the formation of different oscillatory regimes, ranging from simple oscillations (much more widespread) with complex oscillations namely bursts, chaos, quasi-periodic(less common) see stochastic. These oscillatory regimes are observed both inside the cell (intracellular environment) and outside the cell (extracellular environment), both for excitable cells (which exhibit electrical activity) and non-excitable cells (which do not exhibit electrical activity).

I.6.1 Minimal model of Goldbeter et al 1990

The first model based on CICR mechanism is give by Kuba et Takeshita in 1981 to make a point to Ca^{2+} oscillation in sympathetic neurone. Goldbeter et al in 1990, Extend their results and take into account the external stimulate role of IP_3 to initiate the Ca^{2+} spike waves, illustrated by (Fig.15).

The mathematic model describe by a set of two first-order ordinary differential equations, the concentration of free Ca^{2+} in the cytosol and in the internal spore like RE or SR. In this model, the concentration of IP_3 is constant and the Ca^{2+} wave result is the some like the, muscle cells and neurones.

I.6.2 Minimal model of Dupont et al 1996

The CICR is basic mechanism with control Excitation-contraction coupling in myocyte. The diffusion of Ca^{2+} through cardiac cells is initiate by voltage variation of cell membrane. This Ca^{2+} dynamic in some case induce different patterns waves and induce a lot of pathophysiology behaviors before not clearly mechanism. In basis of minimal models with describe the Ca^{2+} dynamic in astrocytes and epithelial cells, Dupont and *al* [77] address some model to explain the initiation of spiral Ca^{2+} waves in single cardiac cells. To the facts that firstly in last minimal model of Goldbeter the initiation of Ca^{2+} wave is localize from local IP3R on propagated like cardiac simulator and secondly this model is apply in theoretical models to observe the spiral Ca^{2+} wave in Xenopus oocytes [77]. They are apply the CICR mechanism in geometry resembles

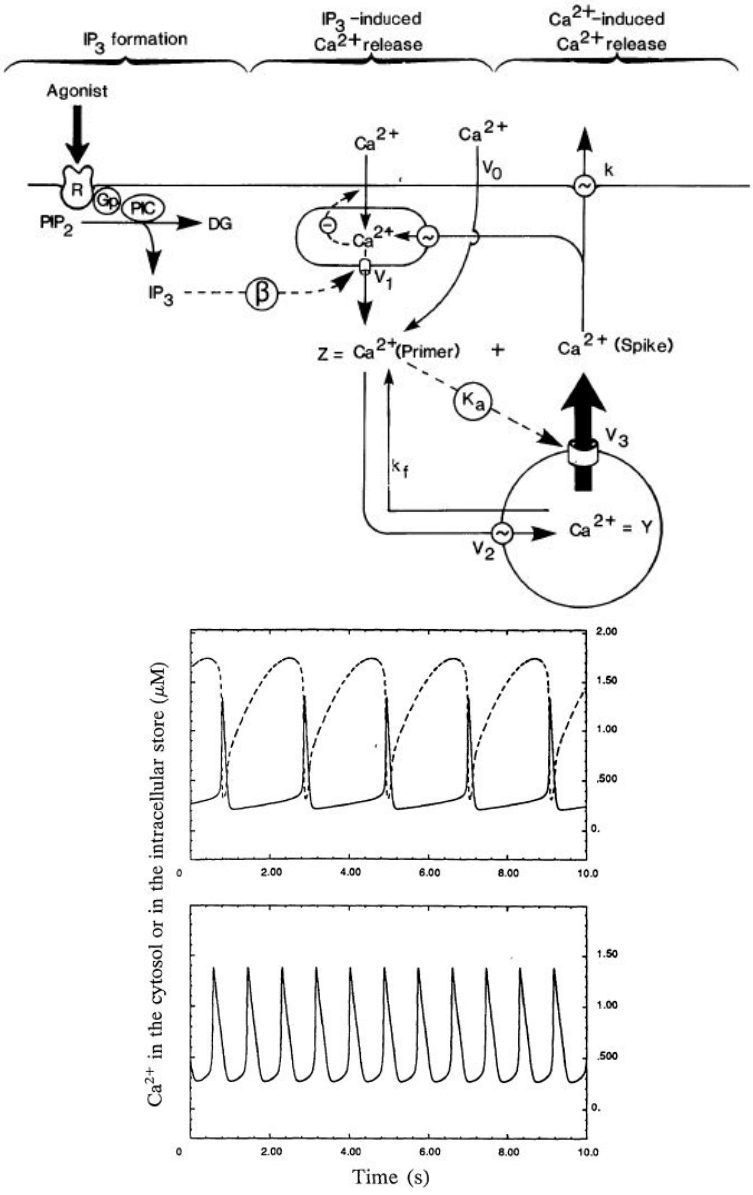

Figure 15: Schematic representation of mechanism (left)and Oscillations in cytosolic Ca^{2+} (right) [42].

of cardiomyocyte and numeric simulation to obtain the spiral Ca^{2+} waves initiated in network why illustrate (Fig.16).

$$\frac{\partial Z}{\partial t} = V_{in} - v_2 + v_3 + k_f Y - kZ + D_L \frac{\partial^2 Z}{\partial x^2} + D_T \frac{\partial^2 Z}{\partial y^2}, \quad (1)$$

$$\frac{\partial Y}{\partial t} = v_2 - v_3 - k_f Y. \quad (2)$$

where

$$\begin{aligned} v_{in} &= v_0 + v_1, \\ v_2 &= V_{M2} \frac{Z^n}{K_2^n + Z^n}, \\ v_3 &= V_{M3} \frac{Y^m}{K_R^m + Y^m} \frac{Z^p}{K_A^p + Z^p}. \end{aligned} \quad (3)$$

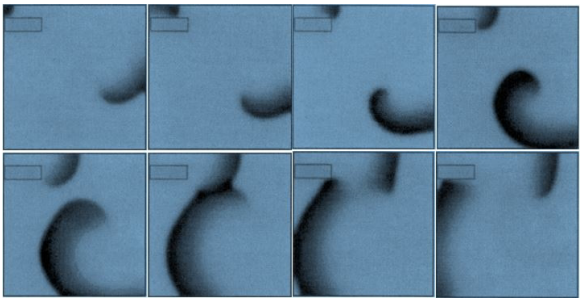

Figure 16: Schematic representation of mechanism (left) and spiral cytosol Ca^{2+} wave (right) [77]

They are suggest to intracellular spiral wave are result of the present of the unexcitable region and the curvature of this wave slows the propagation process. The latter branch is progressively transformed into a planar wave, whereas the first branch of the wave dies out when it returns to the narrow passage between the plasma membrane and the unexcitable region. The are observe (in right part of Fig.16) that, after the onset of stimulation, the Ca^{2+} front spins twice around the obstacle, but when the third front reaches the right end of the unexcitable region, the region beneath it is still refractory. This observation can applies to explain emergence of spiral Ca^{2+} wave oovocyte xenopus.

I.6.3 The discrete Approach of minimal model

Several works have introduced a discrete diffusion term to study the emergence of intercellular Ca^{2+} waves in different cellular environments and those in a physiopathological therapeutic approach. From a realistic apply of minimal model, we can considered the nonlinear property of living cell to study the propagation on intercellular Ca^{2+} wave.

Firstly, the team of WAOFO and Kepseu studied the intercellular dynamics of Ca^{2+} waves,

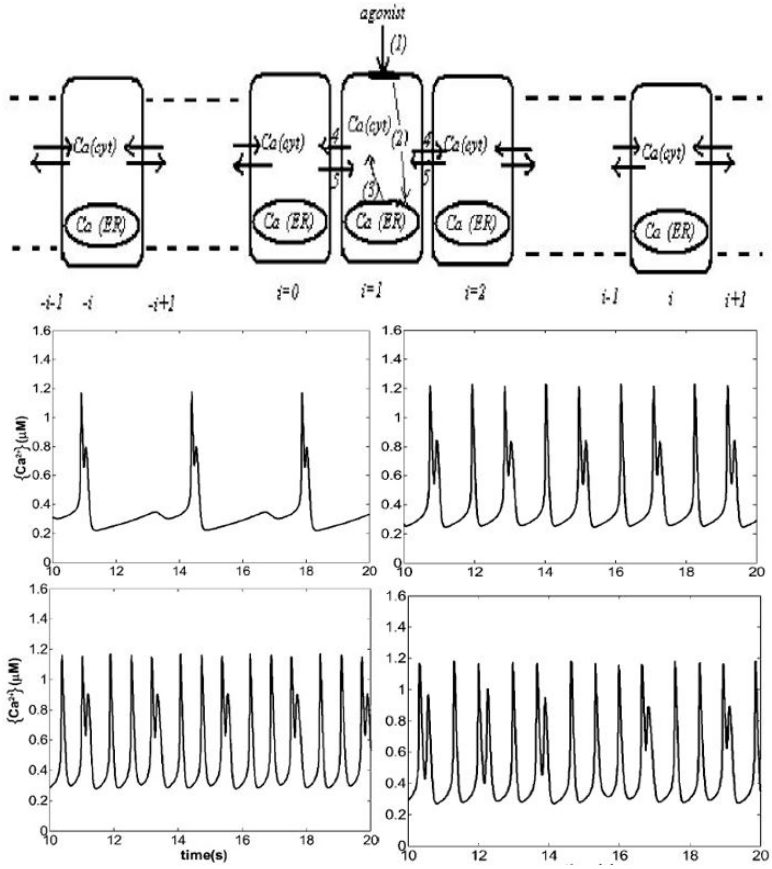

Figure 17: Schematic and model representation of mechanism [41]

with the idea of providing a solution against bacterial invasion in epithelial cells.From minimal model of two parameters cytosolic Ca^{2+} free and internal pool Ca^{2+}, they are use bidirectional linear paracrine coupling chain to study the propagation of Ca^{2+} wave in network in absence of gap-junction [41]. They are propose the schematic representation in (Fig.17). They have shown that the wave propagation in a chain of cells coupled by bidirectional paracrine signal occurs in two zones, the transition zone, where most of the phenomena observed when studying a single cell or a set of cells coupled by the paracrine signal are observed and the regular zone.

$$\dot{Z}_i = a_i - v_{2,i} + v_{3,i} + \beta_1 v_1 (Z_{i+1} + Z_{i-1} - 2Z_i) + k_f Y_i - kZ_i, \quad (4)$$

$$\dot{Y}_i = v_{2,i} - v_{3,i} - k_f Y_i. \quad (5)$$

They have shown that intercellular Ca^{2+} dynamics accompany bacterial invasion and are essential to it, and that, on the strength of this, they offer a possible solution for combating the harmful effects of bacteria on the proper functioning of our digestive cells.

A few years later, teams led by TABI et al worked on the impact of intercellular Ca^{2+} dynamics on the pathophysiological behaviour of neurons. The genesis of this model was based on the experimental observation of Ca^{2+} dynamics in the axon of giant squid (Kuba and Takheshita in 1984). In first time, Tabi et *al* [45] are used Modulational Instability (MI) to explain intercel-

lular communication through paracrine signalling in undirection coupling Ca^{2+} cells. To the analytical study, they are shown that shown that increasing the value of the paracrine coupling parameter considerably modifies the instability features and numerical simulations can be confirms analytical. And to the next, they have used MI both analytically and numerically to show that long-range Interaction (LRI) can be at the basis of a quasi-perfect cell-cell communication (Fig.18). The long-range dispersive coupling have been shown to bring about new features in the emergence of localized Ca^{2+} structures. They have therefore obtained extended breather-like modes for strong coupling while increasing the range parameter has been shown to reduce the wavelength of the formed modulated waves predictions [45].

Their hypothesis was that the onset of neurodegenerative diseases such as epilepsy or Alzheimer's disease is due to disturbances in the propagation of Ca^{2+} waves accompanying the propagation of nerve impulses. They show that the emergence of soliton-type Ca^{2+} waves through the neuron can guarantee the correct propagation of the nerve impulse in a network of neurons, or even the system.

After, nonlinear excitations of Ca^{2+} waves are investigated in a two-dimensional cell network with bidirectional paracrine signaling, both in the longitudinal and transversal directions [46]. The semi-discrete approximation is used to show that the dynamics of the intercellular Ca^{2+} waves can be reduced to complex Ginzburg-Landau equations, depending on the high- or low-frequency (HF and LF) regime. The onset of modulational instability is addressed, where the instability features of the low- and high-frequency modes are compared via the instability growth rate. The (G' /G)-expansion method is employed to find analytically spiral-like wave solutions for the two dynamical regimes. Their response to the effect of paracrine coupling is also addressed. The response of such solutions to parameter change has also been discussed and it has been found that wave spiraling was more robust in the HF mode, which is likely to support important cellular processes.

The EDO system in 2D paracrine coupled are:

$$\begin{aligned} \dot{Z}_{i,j} &= a_{i,j} - v_{2,i,j} + v_{3,i,j} + \beta_1 v_1 (Z_{i+1,j} + Z_{i-1,j} - 2Z_{i,j}) \qquad (6) \\ &+ \beta_2 v_1 (Z_{i,j+1} + Z_{i,j-1} - 2Z_{i,j}) + k_f Y_{i,j} - k Z_{i,j}, \\ \dot{Y}_{i,j} &= v_{2,ij} - v_{3,i,j} - k_f Y_{i,j}. \qquad (7) \end{aligned}$$

There are just many modified model which contributed for the knowledge of dynamic of Ca^{2+} waves in the bodies, the some many case of situation.

They show, in the case of the Ca wave frequency mode, the properties of the medium allowing adaptive propagation of a soliton-type wave in the intercellular medium of neurons and therefore a possible solution to the search for solutions in response to neurodegenerative diseases.

These different models are based on a constant [IP_3], and do not take account of IP_3 dynamics in the intra- and intercellular Ca^{2+} dynamics.

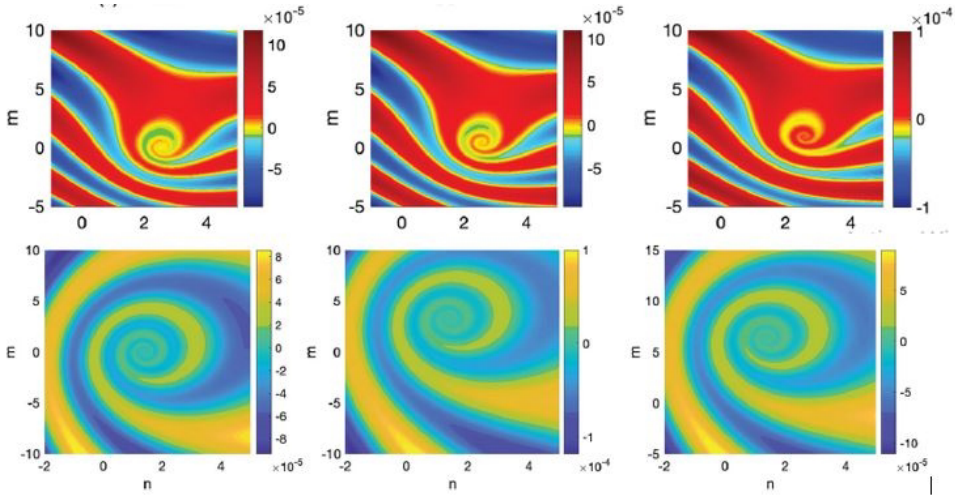

Figure 18: CICR and frequence mode of Ca^{2+} wave [46].

I.6.4 Minimal model of Houart and al 1999

.

Ca^{2+} oscillations are observed in almost all cells and are initiated by an extracellular electromechanical stimulus. Although most of these oscillations are spike oscillations, some cells exhibit complex oscillations, such as bursts, quasi-periodic oscillations or chaotic oscillations. On the basis of models based on Ca^{2+}-induced Ca^{2+} release (CICR), several theoretical models have been developed to account for the experimental observations of the different types of Ca^{2+} oscillations observed. Thus, on the basis of the work of Goldbeter and Dupont (1990) [42] based on the CICR mechanism as presented in the previous section, several theoretical models have been proposed as plausible explanations of the complex dynamics of intracellular Ca^{2+}, firstly by Borghan et *al* (1997) [47] based on the presence of one or two cell pools, with receptors that may or may not be sensitive to Ca^{2+} or to Ca^{2+} and IP_3. Subsequently, Houart et *al* (1999) presented a model based on the CICR mechanism in which Ca^{2+} induces degradation of IP_3 by 3-kinase [48].

And the associate differential equation are:

$$\dot{Z}_i = a_i - v_{2,i} + v_{3,i} + k_f Y_i - kZ_i, \tag{8}$$

$$\dot{Y}_i = v_{2,i} - v_{3,i} - k_f Y_i, \tag{9}$$

$$\dot{X}_i = \gamma v_{4,i} - v_{5,i} - \epsilon X_i. \tag{10}$$

In this model(Fig.19), which consists of three equations, cytosolic Ca^{2+} dynamics is governed by three kinematic parameters, Ca_i^{2+} (Z), Ca_r^{2+} (Y) and $IP_{3,i}$ (X). This deterministic model states that Ca^{2+} dynamics are governed by birhythmicity, IICR and CICR. They establish the conditions for the emergence of the different complex regimes observed experimentally following any variation in the steady state of cytosolic Ca^{2+} estimated to be around 1 μM. This variation acts as

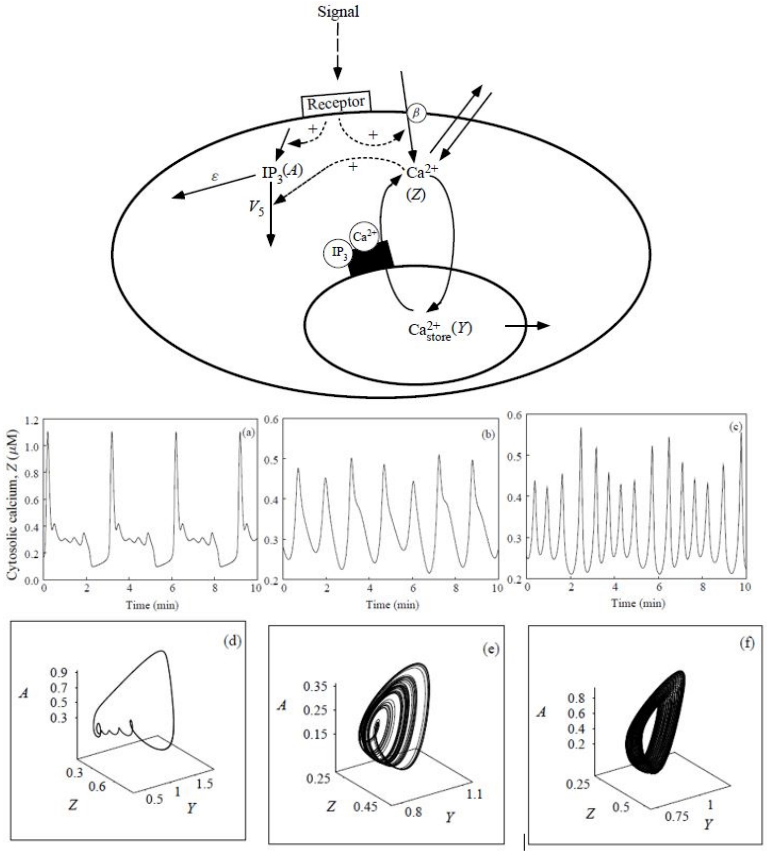

Figure 19: CICR - IICR interactions and complex waves [48].

a stimulus on the cell membrane, releasing phospholipase C (PLC) which synthesises cytosolic IP_3. This IP_3 can either be converted to IP_4 by 3-kinase or to IP_2 by 5-phosphatase, as shown above. According to the IICR mechanism, this IP_3 will initiate the release of Ca^{2+} which, by positive feedback, will keep these channels open and facilitate other Ca^{2+} releases according to the CICR mechanism and also allow the release of 3-kinase which will act on the IP_3 and control its dynamics.

Although based on the dynamics of Ca^{2+} waves observable in non-excitable hepatocyte, this model accounts for the complex Ca^{2+} (Fig.19) waves observable in excitable cells such as neurons and muscles, particularly cardiac muscles. This diversity of applications makes this model of great interest as a possible explanation of the mechanism of emergence of the Ca^{2+} spiral waves observed during several cardiac arrhythmias and thus offer a possible therapeutic solution.

I.7 Conclusion

In this Chapter, we can present the review of literature of Ca^{2+} waves dynamics in many type of cell from physiopathology aspect, digestion, cardiac cell, neuron and pancreas, and some type disease like arrythmia or cancer which are the many serious public health. We elaborated on their importance and why we are interest of patterns Ca^{2+} wave, like one of the possible solution to prevent or healing of these diseases. Because any of these disease begin with a local dysfunctioning or infection that spread to the rest of the tissues, organs or body. This proliferation takes place with the interaction or coordinating motion of the same cells organs, and the global coordination of the body operation. Moreover, we consider in the next chapter, the synchronization property to study the dynamic of Ca^{2+} in a particular organs and disease, with two coupling situations or approach.

CHAPTER II

IMPROVED MODELS OF HOUART AND METHODOLOGIES

Introduction

To explain the experimental observation of complex Ca^{2+} waves in many types of cells such as hepatocytes, and in basic of lasted work of Borghan in 1997, Hoaurt et al [48] in the same institution propose some mechanism to account for the global dynamic of complex Ca^{2+} waves obsrvable in several cells types. They thus establish the Houart madel (HD).

The HD is based on the complex wave dynamics of Ca^{2+} ions observed in the cytosol, based on the CICR and IICR mechanisms. This model takes account of IP_3-Ca^{2+} interactions, where IP_3 stimulates Ca^{2+} release, and subsequently, Ca^{2+} sustains its own release with also the degradation of IP_3 by 3-kinase. Based on the environment of the hepatocyte cytosol, the simple periodic behaviours observed in almost all cytosols and even more so in non-excitable cells (epithelia), but also complex behaviours of the rupture, chaos or quasi-periodic type observable in excitable cells (myocytes), are taken into account. Since its implementation, several modifications or applications have been proposed [78, 79, 80, 81] to better understand the mechanisms of production and propagation of the second cellular messenger most present in cellular communication. For example, A. Rozi [78], based on HD, studied the impact of simple and complex oscillations on the regulation of a cycle of phosphorylation-dephosphorylation processes involved in the degradation of glycogen by the alpha form of glycogen phosphorylase. Depending on the oscillatory regime (simple or complex), the action of glycogen phosphorylase depends on the value of the maximum rate of IP_3 degradation by 3-kinase. They show that cytosolic Ca^{2+} oscillations, both simple and complex, could help to increase the efficiency and specificity of cell signalling. M Lavrentovich [79] manages, on the basis of cytosolic IP_3-Ca^{2+} interactions, reservoirs and the extracellular environment, to generate spontaneous Ca^{2+} oscillations in the astrocyte. Thus, they show that the oscillatory regime has trigger points both internal and external to the cell, is therefore potentially capable of processing a variety of signal types and significantly influencing its neighbouring cells, including neurons. Hongkun. Z [80] In a theoretical study of the stability and bifurcation of spontaneous Ca^{2+} oscillations in astrocytes, with passive Ca^{2+} flux from extracellular vesicles across the membrane and into the cytosol as the controlling parameter. They conclude, in agreement with the numerical data, that two subcritical bifurcation points play an important role in the appearance of Ca^{2+} oscillations. They thus offer an avenue for understand-

ing the role of the emergence of spontaneous Ca^{2+} oscillations in astrocytes, but a concern for synchronization in the appearance of these different oscillatory regimes has an impact on good communication in the cellular network. Quanbao Ji1 and Min Ye, [81] based on HD where they integrate a Brusselator chemical reaction-diffusion system with a biological cellular system via a gap junction to control and visualize the frequency and magnitude of chaotic intracellular calcium oscillations in two cell types, non-excitable cells and glial cells. They were thus able to obtain a wide variety of oscillatory behaviors similar to those reported in numerous biological experiments. In particular, they show that, in the majority of chaos cases, reactor-cell coupling can induce the generation of regular calcium oscillations when the coupling force varies.

In the dynamics of extracellular communication, the notions of coupling and synchronization are crucial, as in the functioning of the heart, where the heartbeat corresponds to the collective behavior of the cardiomyocytes. A number of studies have been carried out in this area [82]. By means of the synchronization distribution, it has been shown that the synchronization of Ca^{2+} spiral waves is optimised in the presence of significant white Gaussian noise and even reaches complete synchronization, thus exhibiting behavior similar to resonance due to noise [83]. Based on a study of the impact of the diffusion of complex Ca^{2+} waves in a cellular network of the Houart model, they established that the size of the network, the diffusion of cytosolic Ca^{2+} and the coupling mode are determining factors giving rise to coordinated behavior of the cells and thus to synchronize cells. This is consistent with the behavior observed in cells such as acinar cells and muscle cells. However, the calcium flux terms present in the model, the connectivity of the variables and the non-linear nature of the receptor channels are favorable criteria for heterogeneity in the architecture of the network, which can certainly have an impact on signal processing and intercellular synchronization in a biological network such as cardiomyocytes.

The CICR mechanism present in excitable cells such as cardiomyocytes is the basis of the models developed to study the dynamics of Ca^{2+} waves in these cells. The choice of Ca^{2+} in the study of the intercellular dynamics of a cardiomyocyte network is all the more motivated since, in excitable cells, the propagation of extracellular Ca^{2+} waves is much stronger than electrical coupling for intercellular synchronization [84]. The self-regulatory properties observed in excitable systems may also be advantageous for crucial insights into spatiotemporal dynamics, synchronization and chaos.

Spiral waves are one of the most important and typical spatiotemporal patterns in excitable media and can be self-sustaining in autonomous systems. Such heterogeneous waves are supported by two-dimensional dynamical models. In refs [77, 85], the authors searched for good parameters for which Ca^{2+} spiral waves take shape in a cellular environment and found that inhomogeneity acting as a random perturbation at the boundary could induce coherence resonance-like behavior, so that a spiral wave could be developed in the lattice. In addition, the spiral wave is more easily broken by multiplicative noise in the presence of channel noise.

One of the major challenges in handling the mathematical models developed is the numerical resolution, which gives a good long-term view of the time or space-time dynamics of the systems studied. Consequently, given their complexity, these generic models are sometimes reduced to

partial differential equations with numerical resolutions via well-known numerical methods that lead to stable solutions. These generally laborious methods require a certain skill in the choice of boundary conditions in order to provide more reliable information on results consistent with physical reality. It is well known that the HD can support the propagation of intracellular Ca^{2+} waves and drive possible extracellular dynamics where the problem of synchronization between cell units is crucial. However, numerical methods such as fourth-order Runge-Kutta and an integration method are generally exploited, not only to give validity to the linear stability of the solutions, but also to reveal different models of the model.

In this chapter, we will present the two important cellular communication approaches that we have developed in this thesis, with a particular focus on extracellular communication morphology networks, coupling modes and signal transmission. This is known as the extracellular communication drive belt.

II.1 Improved Houart models

The complex cytosolic Ca^{2+} oscillations observed in a wide variety of cellular environments, including muscle, cardiac cells and hepatocytes, are observed following stimulation by specific agonists. Based on experimental observations of complex cytosolic Ca^{2+} oscillations in excitable and non-excitable cells, several hypotheses have been put forward, notably that these oscillations are based on the interaction of two intracellular mechanisms capable of destabilising the stationary state of the medium. On this basis, several theoretical models have been developed to account for these cytosolic Ca^{2+} dynamics, which can be summarised as a combined Ca^{2+}-IP_3 action. The model by Houart et al is unique in that it is based on the interaction between CICR at IP_3R and the degradation of this IP_3 stimulated by cytosolic Ca^{2+}, which releases 3-kinase, an enzyme that metabolises IP_3. This mechanism generates a wide variety of dynamic behaviour, ranging from simple oscillations to complex waves. It is a deterministic model that accounts for the conditions that produce most of the oscillatory regimes observable in cellular environments. This deterministic model states that Ca^{2+} dynamics are governed by birhythmicity. They establish the conditions for the emergence of the different complex regimes observed experimentally following any variation in the steady state of cytosolic Ca^{2+} estimated to be around 1 μM. This variation acts as a stimulus on the cell membrane, releasing phospholipase C (PLC) which synthesises cytosolic IP_3. This IP_3 can either be converted to IP_4 by 3-kinase or to IP_2 by 5-phosphatase, as shown above. According to the IICR mechanism, this IP_3 will initiate the release of Ca^{2+} which, by positive feedback, will keep these channels open and facilitate other Ca^{2+} releases according to the CICR mechanism and also allow the release of 3-kinase which will act on the IP_3 and control its dynamics. This model follows on from that of Borghan et al in 1997, who developed a series of models, one in which Ca^{2+} dynamics is a result of high cytosolic Ca^{2+} concentrations due to their release from reservoirs being uniquely sensitive or not to constant IP_3 and another in which IP_3 metabolism with the activation of the 3-kinase enzyme by Ca^{2+}. These hypotheses give rise to simple Ca^{2+} waves and simple and complex chaotic waves.

Based on this model by Houart et al, possible diffusive coupling mechanisms among a group of coupled cells arranged according to a certain topology to see if there are synchronization behaviors in local [Ca^{2+}]i oscillations and search for long-distance communication between them. To this end, they considered a network of N identical cells that are coupled by the exchange of free cytosolic Ca^{2+} and IP_3 ions, allowing these molecules to diffuse through ion channels on the surface of each cell. The numerical results obtained show that when the number of information-carrying molecules and/or molecular species increases, the rate of information processed by the cells also increases accordingly, as does the correlation rate of the cells. They succeeded in obtaining oscillatory behaviors no longer visible in hepatocytes, but in excitable astrocyte cells, by cytosolic Ca^{2+} release via the CICR mechanism and pumping of Ca^{2+} into internal reservoirs via PLC are important building blocks occurring in astrocytes in particular. In addition, Ca^{2+} propagation in astrocytes can reach a few hundred micrometers, which will play an important role in intercellular communication, as confirmed by our simulation results. Cell-to-cell diffusion of IP_3 and cytosolic Ca^{2+} through ion channels on the surface of coupled cells results in coordinated cell behavior. Furthermore, as the number of molecules diffusing between cells increases, the amount of information transferred between cells also increases, and cells synchronize more rapidly. If the number of diffusion channels increases due to an increase in the number of neighboring cells, more cells will be coupled and the transfer of information will be faster. They argue that the role of chemical coupling contributed significantly to the synchronization of astrocytes and the long-distance transfer of information between them. Diffusion of IP_3 between coupled cells may increase the rate of synchronization of calcium oscillations. However, if IP_3 diffusion is allowed alone, it can act as a synchronizing agent to synchronize calcium oscillations at a high coupling rate constant. This shows that diffusion of IP_3 alone among oscillators is very low to allow coupled oscillators to synchronize in a manner similar to the reported role of IP_3 in other cell types such as acinar cells and smooth muscle cells. However, this problem still raises a number of questions, including the impact of network structure in modulating calcium signalling and synchronization. There may be an important role for the variable nature of gap junction connectivity in the network, in the mechanism of intercellular calcium signalling. This broad connectivity and variability of global connections, the non-linear nature of the gap junction coupling function and the emergent heterogeneity of network architecture can certainly affect signal processing and intercellular synchronization in such a biological network.

II.1.1 The two-dimensional coupling Houart model

The model used in our work is inspired by the minimal model from Ref. [42] that has been extended to its discrete version and studied on many occasions to study various dynamical properties of intercellular calcium waves under paracrine signaling [41, 44, 45, 46]. Except for the two initial variables building the initial model, i.e., the cytosolic Ca^{2+} concentration and the concentration of calcium in the internal store (ER), a third variable was added to account for the self-modulation of the IP_3 signal by 3-kinase [48]. In the discrete model proposed in this paper, for simplicity, we assume the paracrine coupling is established between cells due to the excita-

tion of neighboring cells by the Ca^{2+} extruded from one cell. To avoid modeling the complex kinetic brought by the CaR dynamics [40], the coupling assumes the stimulus of the target cell to be proportional to the cytosolic Ca^{2+} content of its adjacent cells. In doing so, each cell is coupled to four other cells through paracrine signaling. The network, therefore, that forms a large grid on which spherical cells are fixed can be used to shed more light on how Ca^{2+} is shared in multicellular systems like hepatocyte cells, liver cells, astrocytes, and epithelial cells. Mathematically, the system of equations to be solved numerically in our context contains the following three variables related to the node (i, j) of the network: $Z_{i,j}$ is the concentration of Ca^{2+} in the cytosol, $Y_{i,j}$ is the concentration of Ca^{2+} in the internal pool or ER, and $X_{i,j}$ represents the concentration of the IP_3. The cell at the node (i, j) is then described by the set of differential-difference equations given by:

$$\begin{aligned}
\dot{Z}_{i,j} &= a_{i,j} - v_{2,i,j} + v_{3,i,j} + \beta_1 v_1(Z_{i+1,j} + Z_{i-1,j} - 2Z_{i,j}) \qquad (11)\\
&+ \beta_2 v_1(Z_{i,j+1} + Z_{i,j-1} - 2Z_{i,j}) + k_f Y_{i,j} - kZ_{i,j},\\
\dot{Y}_{i,j} &= v_{2,ij} - v_{3,i,j} - k_f Y_{i,j}, \qquad (12)\\
\dot{X}_{i,j} &= \gamma v_{4,i,j} - v_{5,i,j} - \epsilon X_{i,j}, \qquad (13)
\end{aligned}$$

where

$$a_{i,j} = \begin{cases} v_0 + \gamma v_1 \;\; if \;\; excited, \\ \\ v_0 \qquad\quad if \;\; not \;\; excited, \end{cases} \qquad (14)$$

$$\begin{aligned}
v_{2,i,j} &= V_{M2,i,j}\frac{Z_{i,j}^2}{K_2^2 + Z_{i,j}^2},\\
v_{3,i,j} &= V_{M3,i,j}\frac{Z_{i,j}^m}{K_Z^m + Z_{i,j}^m}\frac{Y_{i,j}^2}{K_Y^2 + Y_{i,j}^2}\frac{X_{i,j}^4}{K_X^4 + X_{i,j}^4},\\
v_{5,i,j} &= V_{M5,i,j}\frac{X_{i,j}^p}{K_5^p + X_{i,j}^p}\frac{Z_{i,j}^n}{K_d^n + Z_{i,j}^n}. \qquad (15)
\end{aligned}$$

The parameter $a_{i,j}$ characterizes the excitation state of the cell while v_0 refers to a constant input of Ca^{2+} from the extracellular medium. γv_1 is a constant hormonal stimulus localized on the first cell of the array, with γ being the degree of stimulation of the cell by the agonist. Longitudinal and transverse cell-to-cell paracrine interaction strengths are materialized by the parameters β_1 and β_2. The rates $v_{2,i,j}$ and $v_{3,i,j}$ translate, respectively, the pumping of cytosolic Ca^{2+} into the internal stores and the release of Ca^{2+} from these stores into the cytosol mediated by a process known as CICR, with $V_{M2,i,j}$ and $V_{M3,i,j}$ being their respective maximum values. K_2, K_Y, K_Z and K_X are threshold constants for pumping, release, and activation of release by Ca^{2+} and by IP_3, while k_f represent a rate constant measuring the passive, linear leak of $Y_{i,j}$ into $Z_{i,j}$. The parameter k relates to the assumed linear transport of cytosolic Ca^{2+} into the extracellular medium, and v_4 is the maximum rate of stimulus-induced synthesis of IP_3. $v_{5,i,j}$ is the rate of phosphorylation of IP_3 by the 3-kinase, which is characterized by a maximum value $V_{M5,i,j}$ and a

half-saturation constant K_5. In general, the 3-kinase is stimulated by Ca^{2+}, and this is taken into account in the mathematical model by including a term of the Hill form, with a threshold Ca^{2+} level corresponding to K_d. The term -$\epsilon X_{i,j}$ is related to the fact that IP_3 can also be metabolized in a Ca^{2+} -independent by the 5-phosphatase, where ϵ is the degradation factor of IP_3. The effect of that term becomes significant when the level of cytosolic Ca^{2+} drops, therefore reducing the effect of the term $v_{5,ij}$ in Eq.(11). Indeed, cooperative effects are included in the set of Eqs. (11)-(13), which, in the kinetics of Ca^{2+} release, Ca^{2+} pumping, and IP_3 phosphorylation by the 3-kinase, are characterized by the Hill coefficients m, n and p. It should be noted that different values of such parameters support a broad range of complex oscillations and may exhibit more interesting behaviors when diffusive effects are included, especially in two dimensions. In this paper, we consider $m = 2$, $p = 1$, and $n = 4$, values that are supposed to support chaotic oscillations [48].

When it comes in studying the dynamics of the complex systems that abound in nature, chaotic systems are of major interest. The entry leading to the contraction and the exit leading to relaxation and a return to the state of rest for the next heartbeat. Cardiac cell contraction is triggered by an influx of Ca^{2+} and relaxation is due to a release of Ca^{2+} from the cells. The heart is crossed by an electrical signal from one cell to the neighboring cell like a $''Hola''$ in a stadium and this thanks to Ca^{2+}, responsible for the link between electrical activation and mechanical contraction. They are as close as possible to the behaviour of biological systems. They are seen as a reservoir of periodic behaviour that can be activated in response to changing stimuli or external conditions. This consideration highlights the advantages of chaotic systems which, through appropriate coupling, become the seat of propagation of a synchronisation wave.

We are analysing synchronisation between two populations of interacting oscillators of different phase, such as in neighbouring columns of the visual cortex, cortical areas and communication between different brain areas. These different macroscopic environments are made up of interacting microscopic environments whose synchronisation is of vital interest. In its original sense, synchronisation describes the mutual adjustment of frequencies between two interacting oscillators. The study of synchronisation properties is important in understanding the architectures of complex networks.

The increase in cytosolic calcium due to the release of Ca^{2+} by the IP_3-(IP_3R) receptor opens Ca^{2+}-dependent Cl^- channels in the membrane, causing a depolarisation that can lead to an action potential that can propagate to neighbouring cells via gap junctions and L-type Ca^{2+} channels causing intercellular calcium-induced calcium release (CICR). This type of electrical coupling is sufficient to synchronise Ca^{2+} oscillations in neighbouring cells and is much faster than synchronisation by IP_3 diffusion, which has a much longer time scale than electrical coupling. Synchronisation of a group of cells leads to depolarisation in neighbouring cells, creating an influx of Ca^{2+} and activation of the CICR mechanism via IP3R channels, resulting in a wave of intracellular calcium. Under specific conditions (coupling between the action potential and the intracellular calcium oscillator and thanks to gap-junctional coupling), cells whose intracellular calcium oscillations have different frequencies synchronise, creating a group powerful enough

to act as a pacemaker group in the layer of the two-dimensional network.

II.1.2 The one-dimensional coupling Houart model

Generally, within cells in their physiological environment, Ca^{2+} signal can travel from one cell to its neighbours, which promotes intercellular communication. The global dynamics of calcium involves Ca^{2+} oscillations inside the cell, in the cytosol, and outside the cell, where the Ca^{2+} signal is received via other cells via gap junctions or paracrine signalling. Moreover, several studies have highlighted the significance of IP_3 receptors (IP_3R) and IP3 production and degradation in calcium signaling. One of these studies proposed a three-dimensional mathematical model to explain the mechanism in cardiomyocytes [49]. Another recent study developed a novel model to investigate the interactions between the spatiotemporal systems of calcium, IP_3, and $\beta-$amyloid in neurons [50]. Additionally, to understand the impact of disturbances in the processes of calcium and IP_3 dynamics on $\beta-$amyloid production and degradation, a model was proposed based on a system of two reaction-diffusion equations for Ca^{2+} and IP_3 in the nerve cell under an initial boundary value problem [51]. In recent years, the minimal model by Dupont et al. [52], also adopted by Gracheva [35], has been extensively used in unlocking several experimental aspects of cell-cell communication without gap junctions. An extension of such a model was also considered to include the self-modulation effect of IP_3 by the $3-kinase$, leading to three variables in the description of Ca^{2+} dynamics [48]. It comprises the cytosolic Ca^{2+} concentration $(z(t))$, the Ca^{2+} concentration in the internal store $(y(t))$, and the IP_3 concentration $(x(t))$. The proposed discrete model implies intercellular communication via paracrine signalling, whereby neighbouring cells excite each other due to the Ca^{2+} extruded from one cell. In the process, the model ignores the complex kinetics brought by the calcium-sensing receptor (CaR) dynamics under the assumption that the coupling considers the stimulus of the target cell to be proportional to the cytosolic Ca^{2+} content of its adjacent cells. Therefore, the i^{th} cell is coupled to its neighbouring cells, i.e., the $(i-1)^{th}$ cell and the $(i+1)^{th}$ cell. In such a context, the time evolution of these three variables is described by the set of coupled equations:

$$\dot{Z}_i = v_{in} - v_{2,i} + v_{3,i} + \beta_1 v_1 (Z_{i+1} + Z_{i-1} - 2Z_i) + k_f Y_i - kZ_i \tag{16}$$

$$\dot{Y}_i = v_{2,ij} - v_{3,i,j} - k_f Y_{i,j}, \tag{17}$$

$$\dot{X}_i = \gamma v_{4,i} - v_{5,i} - \epsilon X_i, \tag{18}$$

where

$$v_{in} = \begin{cases} v_0 + \gamma v_1 \quad if \quad excited, \\ \\ v_0 \qquad\quad if \quad not \quad excited, \end{cases} \tag{19}$$

$$
\begin{aligned}
v_{2,i} &= V_{M2,i}\frac{Z_i^2}{K_2^2+Z_i^2},\\
v_{3,i} &= V_{M3,i}\frac{Z_i^4}{K_Z^4+Z_i^4}\frac{Y_i^2}{K_Y^2+Y_i^2}\frac{X_i^4}{K_X^4+X_i^4},\\
v_{5,i} &= V_{M5,i}\frac{X_i^1}{K_5^1+X_i^1}\frac{Z_i^2}{K_d^2+Z_i^2}.
\end{aligned}
\tag{20}
$$

The parameters are the same values to the previous approach, v_{in} represents the excitation state of the cell, with v_0 referring to a constant input of Ca^{2+} from the extracellular medium. γv_1 is a constant hormonal stimulus, which comes into play when a cell gets excited, with γ being the degree of stimulation of the cell by the agonist. β is the paracrine coupling strength. $v_{2,i}$ and $v_{3,i}$ represent, respectively, the rates for pumping of cytosolic Ca^{2+} into the internal stores and to the release of Ca^{2+} from these stores into the cytosol in a process activated by cytosolic calcium, also known as the CICR, where the quantities V_{m2} and V_{m3} are the maximum values of these rates threshold constants associated with these processes. The parameters k_2, k_y, k_z and k_x are threshold constants for pumping, release, and activation of release by Ca^{2+} and by IP_3. k_f is a rate constant measuring the passive, linear leak of $y(t)$ into $z(t)$. k relates to the assumed linear transport of cytosolic Ca^{2+} into the extracellular medium. $v_{4,i}$ is the maximum rate of stimulus-induced synthesis of IP_3 and $v_{5,i}$ is the rate of phosphorylation of IP_3 by the $3-kinase$. The latter is characterized by a maximum value V_{m5} and a half-saturation constant k_5. The model does not explicitly consider the formation of a Ca^{2+}/calmodulin complex, which stimulates the $3-kinase$ through binding with Ca^{2+}. However, the model considers this through a Hill-form term, which has a threshold Ca^{2+} level of k_d. The term -ϵx_n is related to the fact that IP_3 can also be metabolized in a Ca^{2+} -independent by the 5-phosphatase, where ϵ is the degradation factor of IP_3. The effect of that term becomes significant when the level of cytosolic Ca^{2+} drops, therefore reducing the effect of the term v_{5n} in Eq.(18). Indeed, cooperative effects are included in the set of Eqs. (16), which, in the kinetics of Ca^{2+} release, Ca^{2+} pumping, and IP_3 phosphorylation by the 3-kinase, are characterized by the Hill coefficients that are supposed to support chaotic oscillations [48]. It should be noted that different values of such parameters support a broad range of complex oscillations and may exhibit more interesting behaviors when diffusive effects are included, especially in two dimensions. The set of Eqs.(16)-(20) is solved numerically using the fourth-order Runge-Kutta computational scheme.

II.2 The Numerical methods

To study the dynamics of systems modeled by complicated sets of equations, various studies have been developed recently, mainly dedicated to numerical integration methods. Namely, neural investigations using the artificial neural networks have been successfully used, emphasizing global and local search approaches based on genetic algorithm and interior-point algorithm scheme applied to three-dimensional nonlinear food chain system [86]. Interesting extensions of the method include the particle swarm optimization for the singular two-point boundary value

problems [87], the Gudermannian neural networks optimized by the mutual strength of global and local search abilities of genetic algorithms and sequential quadratic programming [88] and its application to a three-species food chain nonlinear model is dependent upon the prey populations, top-predator, and specialist predator [89]. The numerical investigation of the infectious disease based on the nonlinear fractional-order prey-predator model, using the Levenberg-Marquardt backpropagation based on the artificial neuron networks, was also recently addressed along the same line, where the fractional prey-predator model was classified into three categories, the densities of the susceptible, infected prey, and predator populations [90].

II.2.1 The algorithm

In most scientific fields, the phenomenon studied is reduced to equations or systems of differential equations with partial or ordinary derivatives, with complex calculations whose resolution requires the use of appropriate function representation techniques and calculation algorithms. Numerical methods have the advantage, through the ideal choice and optimization of numerical algorithms, of executing reference calculations in a short time, the only limit to which is the patience of the person performing them. A carefully thought-out and optimized approach saves a considerable amount of calculation time, enabling us to move from unreasonable to trivial calculations. Numerical methods are used in the development of calculation codes, simulation problems and mathematical experiments. They rely on numerical calculations based on the stability and convergence of the method, its optimization, the error and precision of the result. Although it relies heavily on mathematics in its theoretical part, its practical execution generally results in the implementation of algorithms on the computer. Its methods are based both on the search for exact solutions, as in the case of matrix analysis or symbolic calculation, and on approximate solutions, which are most often the result of discretization processes, as in the treatment of differential equations. Recently, numerical study methods have been enriched by probabilistic techniques such as synchronization distribution.

Understanding the dynamics of a system in physic or other fields of research and development can lead to equations whose resolution is complex. This resolution by numerical calculation methods using computer software are fairly effective contribution requiring the development of code specific to the situation studied. This development involves a procedural approach in which the algorithm and a stable method are decisive.The solution search of our EDO system in 1D is broken down into several steps constituting the following algorithm (Fig.20):

In the same vein, the logarithmic diagram of our 2D ODE study is derived from the 1D one but the solve ODE can give by specific numerical integration like RK4.

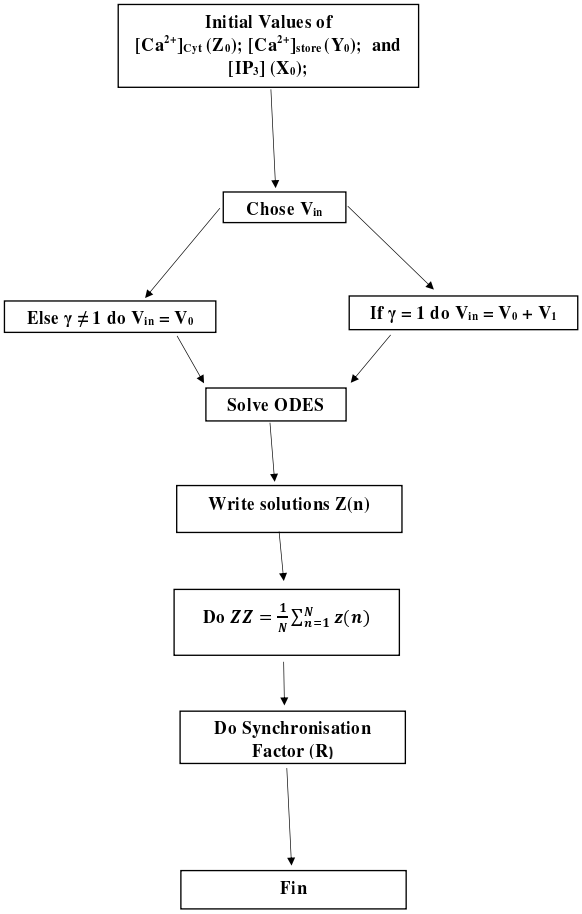

Figure 20: Algorithm of distribution of synchronization R in 1D.

II.2.2 The RK4 numerical integration method

The EULER numerical integration method

In the procedure of solving our ODE system at initial values, the choice of an efficient and stable method is important. We will present three main Euler's methods (L. Euler 1707-1783 Fig.21) following the increasing order of stability. The method of Leonhard Euler, or simply Euler's method, is one of the simplest methods in use for solving ordinary differential equations, as it is a first-order split-step method with a beautiful geometric interpretation.

Euler method, also called the first derivative method, its iterative formula is as follows:

$$\dot{y} = f(t, y), \quad y(t_0) = y(0). \tag{21}$$

where y is an unknown function (scalar or vector) of time t, which we would like to approximate; we are told that $\dot{y}$, the rate at which y changes, is a function of t and of y itself. At the initial time t_0 the corresponding y-value is y_0. The function f and the data t_0, y_0 are given. Therefore the formulas of Euler method are given by:

Figure 21: Leonhard Euler 1707-1783 [91].

Carle Runge 1856-1927
German mathematician and physicist

Martin Wilhelm Kutta 1867-1944
German mathematician

Figure 22: C. Runge and M.W. Kutta [91].

$$\begin{aligned} y(n+1) &= y(n) + h * f(t_n, y_n), \\ t(n+1) &= t(n) + h. \end{aligned} \tag{22}$$

Euler's method perfectly well if y_0 is a vector and f returns a vector. The integrand is evaluated only once and it is exact if f(t,y) is constant, but not if f(t,y) is linear. So the error is proportional to h and we obtain the better solution from the slow values of h. The biggest defect of Euler's method is that it does not provide an error estimate. If Euler's method is followed by a second function evaluation, we begin to get a viable algorithm. Nevertheless, it gives low precision, which makes its use relatively limited.

The Runge-Kutta numerical integration method

Runge-Kutta methods are one-step numerical schemes for solving ordinary differential equations. They are among the most popular methods on the part their ease of implementation and their precision. It was Carle Runge and Martin W Kutta (see Fig.22) who, at the start of the 20^{th} century, invented these methods. In 1894 C. Runge are and improved by M. W. Kutta towards

1901. the Runge-Kutta methods are a family of implicit and explicit iterative methods, which include the well-known routine called the Euler Method, used in temporal discretization for the approximate solutions of ordinary differential equations. These methods are the most used because they are very stable. The Runge-Kutta method it is based on the integral trapezium formula. Given the initial value problem specified as follows:

$$\dot{y} = f(t, y), \quad y(t_0) = y(0). \tag{23}$$

where y is an unknown function (scalar or vector) of time t, which we would like to approximate; we are told that $\dot{y}$, the rate at which y changes, is a function of t and of y itself. At the initial time t_0 the corresponding y-value is y_0. The function f and the data t_0, y_0 are given.

The first-order Runge-Kutta method (RK1) give:

$$\begin{aligned} y(n+1) &= y(n) + h * f(t_n, y_n), \\ t(n+1) &= t(n) + h. \end{aligned} \tag{24}$$

The RK1 is identical to the Euler method.

The Second-order Runge-Kutta method (RK2) it is based on the integral trapezium formula. Given the initial value problem specified as follows: Therefore the formulas of RK2 method are given by:

$$\begin{aligned} y(n+1) &= y(n) + h * (L_2), \\ t(n+1) &= t(n) + h, \end{aligned} \tag{25}$$

for $n = 0, 1, 2, 3, ...$, using

$$\begin{aligned} S_1 &= f\bigg(t(n), y(n)\bigg), \\ S_2 &= f\bigg(t(n) + \frac{h}{2}, y(n) + \frac{h}{2} * L_1\bigg). \end{aligned} \tag{26}$$

where $h > 0$ represents the step-size and n stands for the iteration number. The RK2 method is a second-order method, meaning that the local truncation error is on the order of $O(h^2)$.

Thirt-order Runge-Kutta method (RK3) are given by:

$$\begin{aligned} y(n+1) &= y(n) + \frac{1}{6}(L_1 + 4L_2 + L_3), \\ t(n+1) &= t(n) + h. \end{aligned} \tag{27}$$

for $n = 0, 1, 2, 3, ...$, using

$$\begin{aligned} L_1 &= hf\bigg(t(n), y(n)\bigg), \\ L_2 &= hf\bigg(t(n) + \frac{h}{2}, y(n) + \frac{L_1}{2}\bigg), \\ L_3 &= hf\bigg(t(n) + \frac{h}{2}, y(n) + 2L_2 - L_1\bigg). \end{aligned} \tag{28}$$

The RK3 method is a second-order method, meaning that the local truncation error is on the order of $O(h^3)$. In practice, the fourth-order Runge-Kutta method is the most used.

Therefore the formulas of fourth-order Runge-Kutta method (RK4) are given by:

$$\begin{aligned} y(n+1) &= y(n) + \frac{1}{6}(L_1 + 2L_2 + 2L_3 + L_4), \\ t(n+1) &= t(n) + h. \end{aligned} \tag{29}$$

for $n = 0, 1, 2, 3, ...$, using

$$\begin{aligned} L_1 &= hf\bigg(t(n), y(n)\bigg), \\ L_2 &= hf\bigg(t(n) + \frac{h}{2}, y(n) + \frac{L_1}{2}\bigg), \\ L_3 &= hf\bigg(t(n) + \frac{h}{2}, y(n) + \frac{L_2}{2}\bigg), \\ L_4 &= hf\bigg(t(n) + h, y(n) + L_3\bigg). \end{aligned} \tag{30}$$

where $h > 0$ represents the step-size and n stands for the iteration number. $y(n+1)$ is the RK4 approximation of $y(t_{n+1})$, and the next value $(y(n+1))$ is determined by the present value $(y(n))$ plus the weighted average of four increments, where each increment is the product of the size of the interval, h, and an estimated slope specified by function f on the right-hand side of the differential equation. The RK4 method is a fourth-order method, meaning that the local truncation error is on the order of $O(h^5)$, while the total accumulated error is on the order of $O(h^4)$. It is defined by the formula with presents an error of order five and is the most used. For further calculations, we use direct numerical simulations to characterize such dynamical behaviors.

However, considering a discrete model, one needs moreover to these results, additional conditions called boundary conditions whose choice depends on the studied problem. Throughout our experiments, we have adopted periodic boundary conditions since the different models explored are assumed to be cyclic. For example, a network of N cells with nearest neighbors interactions obeys the following boundary conditions

$$x(0) = x(N) \;\; and \;\; x(N+1) = x(1). \tag{31}$$

The reader can easily deduce such conditions for two-dimensional models. The Runge-Kutta method is a method which, when it presents instabilities in the form of oscillations which cause the algorithm to diverge, a choice for the smallest time scale of the system ensures the stability of the method, even when the calculated variables evolve slowly. This illustrates the value of the concept of uniform convergence.

II.2.3 For two-dimension coupled network

For further calculations, we use direct numerical simulations to characterize such dynamical behaviors. In doing so, the set of Eqs. (11) including conditions (14) to (15) has been integrated via the fourth-order Runge-Kutta computational scheme on a grid of 200×200 cells, with a time-step $\Delta t = 10^{-3}$, with periodic boundary condition. Here we use the initial conditions $Z_{i,j} = 0.4$, $Y_{i,j} = 1.5$, and $X_{i,j} = 0.1$. Also, for our numerical simulations, we use the parameter values [48]in the following table.

Initials	Values
v_0	2.0 μMmin^{-1}
v_1	2.0 μMmin^{-1}
$V_{M2,i,j}$	6.0μMmin^{-1}
$V_{M3,i,j}$	20.0μMmin^{-1}
$V_{M5,i,j}$	2.0μMmin^{-1}
v_4	2.0μM
K_2	0.1μM
K_Y	0.2μM
K_Z	0.5μM
K_X	0.2μM
K_5	1.0μM
K_d	0.4 μM
K	10.0μM
k_f	1.6 min^{-1}

Additionally, a circular region with radius $r_0 = 10$ cells is assumed to be stimulated at the center. This stimulated domain is defined as

$$(i - i_0)^2 + (j - j_0)^2 = 10^2, \tag{32}$$

where (i_0, j_0) is the coordinate of cell. Thus the stimulation process is implemented as: if

$$(i - i_0)^2 + (j - j_0)^2 < r_0^2, \tag{33}$$

then

$$a_{i,j} = \begin{cases} v_0 + \gamma v_1 \quad if \quad excited, \\ \\ v_0 \qquad\quad if \quad not \quad excited, \end{cases} \tag{34}$$

The various wave patterns are studied using the statistical distribution based on field theory. The results and their interpretations are presented in the next chapter. For a complete study, a bidirectional approach is envisaged

II.2.4 For intercellular coupled network

In a paracrine coupling approach with bidirectional propagation, numerical integration is performed and dynamic regimes are studied on the basis of bifurcation diagrams and synchronization theory. Cytosolic Ca^{2+} binds to the complex of troponin and causes the cells to swell and reduce the space that separates them. Cells shrink corresponds to the contraction of the heart muscle. Concentration of Ca^{2+} having increased, by a specific mechanism, the membrane receptors specific to calcium or not will opened to allow entry of Ca^{2+} into the cellular behaviors such as the RS or an exit from Ca^{2+} of the cell. We observe a return to the initial state of the considered cell which is ready for the next beat and the signal propagation to neighboring cells. This big responsibility of Ca^{2+} is not, however, immune to various malfunctions with risks commensurate with the multitude of functions for which it is responsible. A genetics mutation can lead to receptor malformation membranes and a dysregulation of the movement of Ca^{2+} through the different cell compartments, a variation in function binding protein which leads to the spread of bad electrical signal and therefore heart rhythm disorders simple (fatigue) or heart failure potentially deadly. For further calculations, we use direct numerical simulations to characterize such dynamical behaviors. In doing so, the set of Eqs. (16) including conditions (35) to (20) has been integrated via the RK4 computational scheme on a grid of 100×100 cells, with a time-step $\Delta t = 10^{-3}$, with periodic boundary condition. Here we use the initial conditions $Z_i = 0.04$, $Y_i = 1.5$, and $X_i = 0.1$. Also, for our numerical simulations, we use the parameter values [48] in the following table and the stimulation process is implemented as:

$$v_{in} = \begin{cases} v_0 + \gamma v_1 \; else, \\ \\ v_0, \end{cases} \tag{35}$$

Initials	Values
v_0	2.0 μMmin^{-1}
v_1	2.0 μMmin^{-1}
$V_{M2,i}$	6.0μMmin^{-1}
$V_{M3,i}$	20.0μMmin^{-1}
$V_{M5,i}$	30.0μMmin^{-1}
v_4	2.5μM
K_2	0.1μM
K_Y	0.2μM
K_Z	0.3μM
K_X	0.1μM
K_5	1.0μM
K_d	0.6 μM
K	10.0μM
k_f	1.0 min^{-1}

The considerations made in our two IP_3-Ca^{2+} interactions hypotheses are highly nonlinear, due to the random distribution of the membrane receptors on which this cellular mechanism depends. Thus, a study of linear stability and synchronization is necessary to guarantee the quality of the results.

II.2.5 Linear stability analysis and synchronizability

The study of the dynamics of biologics or physics systems has led to the development of several models that translate plausible mechanisms. We can cite, among others, intracellular and extracellular couplings, gap-junction couplings, couplings between identical and different cells, the influence of magnetic flux or magnetic radiation, phase delay, electrical activity of the cytoplasmic membran and the noise phenomenon. In the cell, the Ca^{2+} is mainly stored in the endoplasmic and sarcoplasmic reticulum, another part in mitochondria, Golgi apparatus and nuclear membrane. A small amount (the order of 1μM) of Ca^{2+} is present in the cytosol (the level in which the organelles are cells), i.e. about 1000 times less than the Ca^{2+} extracellular, which represents a large gradient of concentration between intra and extracellular media. These different mechanisms contribute to the emergence of dynamics, to their transformations and modifications, or simply to their evolutions towards a state of equilibrium. This is how single-cell and multi-cell network models have been developed, with unidirectional and bidirectional propagations in one or two dimensions to account for them. Given that network nodes are interacting and frequently experiencing chaotic conditions, a realistic study of the individual or collective dynamics of network nodes must take into account the phenomenon of synchronization. Thus, different types of synchronization (phase synchronization, oscillatory amplitude synchronization, error and delay synchronization, in excitable and non-excitable cells, in the dynamics of pathogens, the impact of internal and external noise on intracellular and extracellular Ca^{2+}

dynamics, synchronization of cells under gap-junction coupling, as well as stabilities or multistability. Although these different works are highly significant contributions, none is based on the Houart model whose implications have been presented previously, with two-dimensional or two-directional paracrine coupling has not yet been realized, hence the objective and specificity of the present work.

Importance is particularly given to the synchronization phenomenon and its impact on the emergence of intracellular Ca^{2+} spiral waves when paracrine signaling is involved. In excitable cells, the Ca^{2+} enters the cell through specific channels that open when the potential transmembrane (-80 to -60 mV) decreases or reverses, that is, when the membrane depolarizes. In the muscles rapid skeletal structures, the plasma membrane maintains the intracellular concentration of free Ca^{2+} around 0.1μM. The increase in the concentration of Ca^{2+} induces the contraction of the muscle cell, while the return to the 0.1μM concentration induces relaxation. In hepatocyte, the dynamics of Ca^{2+} is stimulated by an extracellular factor (hormone) is developed by Woods et al, 1986. Subsequently the participation of inositol first at a constant rate then variable in the dynamics of Ca^{2+} is highlighted in different cellular environments. This participation occurs through cytosolic IP_3 and/or these receptors on intracellular reservoirs. Building on this, models based on oscillations of both IP_3 and Ca^{2+} make it possible to account for the complex oscillations of Ca^{2+} observed in cells type, with different frequencies and amplitudes.The dissociation rate of IP_3 on its receptor is influenced not only by cations such as Ca^{2+}, but also by ATP The pulsatile, transient aspect of the modulations of [Ca^{2+}]i largely results from retro-controls of the activity of IP_3R in which calcium plays an important role. Some studies show that it is IP_3, among other things, that provides the coupling function between the cytosol depleted in Ca^{2+} and the plasma membrane. In the whole liver, stimulated by hormones, we observe an oscillating release of Ca^{2+} , which implies a coordination in the whole organ of the oscillators present in each cell.

To study the dynamics of systems modeled by complicated sets of equations, various studies have been developed recently, mainly dedicated to numerical integration methods. Namely, neural investigations using the artificial neural networks have been successfully used, emphasizing global and local search approaches based on genetic algorithm and interior-point algorithm scheme applied to three-dimensional nonlinear food chain system. Interesting extensions of the method include the particle swarm optimization for the singular two-point boundary value problems, the Gudermannian neural networks optimized by the mutual strength of global and local search abilities of genetic algorithms and sequential quadratic programming and its application to a three-species food chain nonlinear model is dependent upon the prey populations, top-predator, and specialist predator. The numerical investigation of the infectious disease based on the nonlinear fractional-order prey-predator model, using the Levenberg-Marquardt backpropagation based on the artificial neuron networks, was also recently addressed along the same line, where the fractional prey-predator model was classified into three categories, the densities of the susceptible, infected prey, and predator populations. Therefore, the calculations performed in the present paper are fully numerical, using direct numerical simulations to char-

acterize such dynamical behaviors. In doing so, the set of Eqs. (11) has been integrated via the fourth-order Runge-Kutta computational scheme on a grid of 200×200 cells, with a time-step $\Delta t = 10^{-3}$, with periodic boundary conditions. Importance is particularly given to the synchronization phenomenon and its impact on the emergence of intracellular Ca^{2+} spiral waves when paracrine signaling is involved. In that direction, it is well-established nowadays that synchronicity and pattern formation are uncorrelated phenomena [92, 93], which sometimes calls for the use of some bifurcation functions, such as the synchronization factor R [94] to differentiate both phenomena and predict the stability of the subsequent oscillatory behaviors that include spiral waves, in general. Beyond the commonly known cooperative behaviors, the emergence of chimera states on bifurcation points [95] has been demonstrated to strongly rely on strong inputs from the synchronization factor R, under different coupling topologies as well as different types of coupling functions, such as long-range and global couplings [95, 96, 97]. A value close to zero of this function implies the absence of synchronization, which suggests the emergence of spiral waves in the medium. Otherwise, a value of R close to 1 supposes the appearance of synchronous patterns in the studied cell network [95]. The spatial statistical factor of synchronization R [98] to be used from one-dimension in the first study is written as:

$$R = \frac{< F^2 > - < F >^2}{\frac{1}{N}\sum_{n=1}^{N}[< z(n)^2 > - < z(n) >^2]}, \tag{36a}$$

$$F = \frac{1}{N}\sum_{n=1}^{N} z(n). \tag{36b}$$

In the above, N is constant, and $N^2 = 10000$ site in one-dimensional space are used in this study.

From the second approach, the spatial statistical factor of synchronization R [98] to be used from two-dimension in the second study is written as:

$$R = \frac{\left\langle F^2 \right\rangle - \langle F \rangle^2}{\frac{1}{N^2}\sum_{i=1}^{N}\sum_{j=1}^{N}\left[\left\langle Z_{i,j}^2 \right\rangle - \langle Z_{i,j} \rangle^2\right]}, \tag{37}$$

with

$$F = \frac{1}{N^2}\sum_{i=1}^{N}\sum_{j=1}^{N} Z_{i,j}. \tag{38}$$

In the above, N is constant, and $N^2 = 40000$ sites in two-dimensional space are used in this study. To consired the LR interaction, G = 10. This synchronization distribution has been used to account for the synchronization stability and wave pattern formation in a memristor neural network, the synchronous behavior of a neural network under fractional order coupling, under the effect of electromagnetic radiation, for the synchronization of Ca^{2+} spirals in an excitable medium. It is based on the mean field theory which is used in neuroscience to analyze the collective behavior of a dynamic system composed of many interacting particles such as a neural network, in nuclear physics to describe the motion of a nucleon in terms of a self-consistent single-particle potential well that approximates the interactions of a nucleon with all other nucleons. This theory effectively reduces the behavior of the system to the properties of a handful of parameters.

The regulation of synchronisation in a system of identical oscillators with specific properties gives rise to interesting collective dynamic phenomena. Synchronisation, as the adjustment of the rhythms of oscillating objects due to their interactions, is a widespread phenomenon that plays an important role in natural, social and technological systems. A study of the synchronisation of neural networks with dynamic heterogeneity, showing that network structures with the same propensity for synchronisation (quantified by analysis of the master stability function) can develop radically different synchronisation properties when heterogeneity is introduced with respect to the type of neuronal excitability. This shows that the spatial distribution and type of coupling between the different sites in a neuronal network are important factors in the emergence of synchronous behaviour in the network, which is a source of cells system dysfunction, which in the hippocampus contributes to epileptic seizures. Spiral waves, also known as vortices, which can be observed in a variety of environments and scientific fields, can encounter inhomogeneities, large obstacles, a reduction in the dimension of the propagation medium and spin around, causing very important physiological phenomena such as cardiac arrhythmias. A matching and dimension reduction rule is a theoretical method for analysing instability that can shed light on other non-linear problems. Our theoretical results correspond quantitatively to the numerical simulation under all circumstances. In order to provide useful guidance for the practical applicability of in real cardiac tissue, further research is needed taking into account more realistic cardiac activities.

Spiral Ca^{2+} waves are probably the most intriguing patterns in inspired extended systems. They have been observed in a variety of systems. Spiral waves have been actively studied for several reasons, one of which is their potential clinical importance for cardiac arrhythmias, in particular ventricular fibrillation, which can cause clinical death in as little as one minute and is the leading cause of sudden cardiac death in industrialised countries. In general, most studies in these fields focus on the mechanisms of formation, stability, rupture and disappearance of spiral waves, with the main motivation being the possible applications and control of spiral waves. A specific example is spiral wave drift induced by wave train stimulation, which has recently been proposed as a possible alternative approach for the treatment of myocardial infarction.

Conclusion

This chapter has been organized around two main themes. The presentation of the improved minimal models including the one-dimensional coupled model with the consideration of the intercellular paracrine coupling cells, the two-dimensional coupled model of paracrine and phosphorylation effects. In addition, the statistical synchronization are use to study the behavior of complex system in physiopathologic context where many Ca^{2+} patterns wave are formed and the RK4 numerical integration method furnished the second part of the chapter.

CHAPTER III

RESULTS AND DISCUSSIONS

III.1 Ca^{2+} Patterns in two-dimensional cell networks

Patterns formation could be observed in lot spatiotemporal systems like physics, chemistry, biology and economics. Spiral wave is a class of spatiotemporal pattern it could be found in the oscillatory and excitable media such as cardiac tissue [99]. It has been confirmed that there are involvements of spiral waves in both atrial and ventricular [100]. The sudden cardiac death resulting from ventricular fibrillation is due to the fragment or breakup of the spiral wave and the potential mechanism for breakup of spiral wave has been detected [101]. We study the nonlinear dynamics of two coupled oscillators (Ca^{2+} and IP_3) from effect of coupling strength, stimulate degree and phosphorylation degree.

III.1.1 Effect of the paracrine coupling

As indicated earlier, the transition between different states highly depends on the initial conditions and can also be predicted through the distribution of the synchronization factor. Its dependence on the coupling features of the cell network is commented in Figs. 23 and 24, where emphases is given to the paracrine coupling strength. Additionally, one of the main factors in the studied system is the rate k related to calcium ion transport into the extracellular area. Its value is, therefore, important in establishing intercellular communication via synchronized and other modes of oscillations. Under different values of the constant stimulus, Fig. 23 shows how its affects the synchronization factor. It is of course, important to indicate that from Fig. 23(a), its small values are likely to trigger synchronized patterns when the paracrine signal is weak. In Fig. 23(a), we have fixed $\gamma = 0.4$, with k taking the increasing values 8, 10, and 12. For $k = 8$, the synchronization factor decreases with β increasing, which may favor the formation of target or spiral waves. However, another synchronization window appears for values of $\beta_1 = \beta_2 \to 1$. Increasing k does not support such a second window but expands paracrine couplings' regions where synchronized states are favorable. The same features are shared by Fig. 24(b), where $\gamma = 0.8$, except that for $k = 2$, there is a sudden drop in the synchronization factor followed by a hump of synchronization. In contrast, the distribution of R follows the same dynamics as previously for the rest of the cases. Interestingly, for $\beta_1 = \beta_2 = 0.4$, the synchronization factor being not zero but small indicates the existence of another state that can be strictly related to target waves. That was already discussed by Wang et al. [102], who showed that very small synchronization factor values probably would not support homogeneous states in a neural network.

However, from a global view, our results suggest that stronger values of the paracrine coupling may enhance not only intercellular communication but also the emergence and propagation of spiral and target waves under the right choice of other system parameters, such as the rates k and k_f and the constant stimulus strength γ.

Results from direct numerical simulations corresponding to the predictions of Fig. 23 are displayed in Figs. 24-26. In Fig. 24, patterns are displayed for $\beta = 0.4$, where the initial state shows a target wave that expands with time increasing. In fact, as predicted from the synchronization factor R of Fig. 23, the value $\beta = 0.4$ of the paracrine coupling strength was expected to lead to mixed modes or to target waves. Here, the initial target wave gives rise to additional layers as time increases, while there is no evidence of spiraling. Moreover, the features of Fig. 25 are also obtained where one clearly sees the formation of an initial target wave that evolves with time and gives rise to secondary target waves. Taking $\beta = 0.8$ and keeping the other parameters intact, there is still a target wave formation that serves as a seed and disintegrates into a set of two spiral waves that delocalize with time increasing. At the time $t = 90$, another set of spirals appears that progressively evolves towards the lower boundary of the $i-$axis, pushing the initial one, which completely disappears. Although surrounded by target waves, the chosen values of paracrine coupling strengths confirm themselves to support the spiraling of Ca^{2+} waves in the system. The results also agree with predictions from Fig. 23, from which the selected values of β_1 and β_2 are likely to support the observed behaviors. Although it was shown by Ma et al. [103] that synchronization of Ca^{2+} waves between two cells were possible in a continuum model, at the intracellular level through gap junctions, it was already confirmed by Tabi et al. [44], then by Kepseu and Woafo [41], that paracrine signaling in discrete lattices may enhance intercellular communication by triggering Ca^{2+} oscillations in neighboring cells, even in pathological situations. In such a context, the system under study, in the dynamical frame, shows spirals with longer arms that progressively grow. In a hybrid mode model, it was demonstrated that stronger coupling does not always guarantee the appearance of spiral waves, which, if other conditions are not satisfied, will die. An illustrative case is given in Fig. 26, where the initial target wave grows, leading to turbulent spiraling events.

Paracrine coupling undeniably plays a vital role in generating spiral waves. In neural networks, for example, it was shown that spiral waves dissipate under strong diffusive coupling [98], which seems to be expected in most reaction-diffusion systems. This can lead to many other states like turbulent and target waves, among others. In the studied case, Fig. 26 displays the spontaneous disintegration of the initial state into turbulent patterns for $\beta_1 = \beta_2 = 0.98$. According to the features from Fig. 26, the coupling strength may affect the concentration of IP_3, which also offers the possibility for intercellular Ca^{2+} wave generation through, for example, the iontophoresis of IP_3 into a single cell of cultured epithelial cells [104]. More precisely, since the release of Ca^{2+} from IP_3RS is stimulated by IP_3, it should be indicated that a local increase in Ca^{2+} concentration actually characterizes IP_3 diffusion, which does not always relate to a bulk dynamics of Ca^{2+}. Therefore, a suitable regulation of the IP_3 concentration and paracrine coupling may trigger, from an adjacent cell, via CICR, a Ca^{2+} response with specific characteristics

capable of stimulating adjacent but quiescent cells.

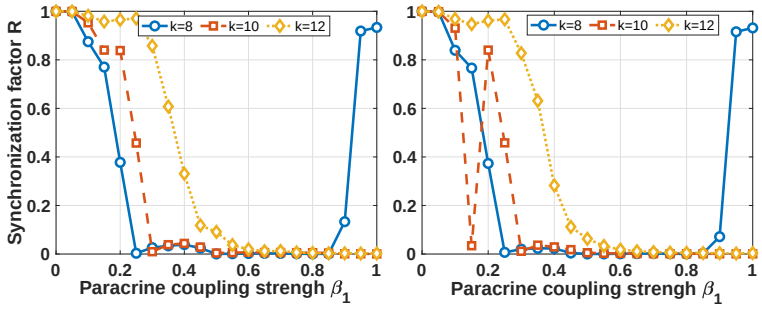

Figure 23: The panels show the distribution of synchronization factor R versus the longitudinal paracrine coupling strength β_1, with $\beta_2 = \beta_1$, $\epsilon = 0.1$ and the degree of simulation taking the respective values $\gamma = 0.4$ [panel (a)] and $\gamma = 0.8$ [panel (b)]. Each of the panels compares results due to the changes in the calcium ion transport rate into the extracellular area k.

III.1.2 Effect of the degradation factor of IP_3

For this particular case, where the effect of the degradation factor of IP_3, ϵ, is studied, the synchronization factor is shown in Figs. 27, where the paracrine coupling is supposed to be asymmetric in the longitudinal and transverse directions. Therefore, Fig. 27(a) has been recorded for $\beta_2 = 0.4$, while β_1 takes different values, where decreasing values give rise to wide regions of desynchronization for ϵ. It is observed that for weak values of β_1, it is possible to get target or spiral waves when $0.05 < \epsilon < \epsilon_{th}$, where ϵ_{th} increases with β_1. In Fig. 27(b), where $\beta_2 = 0.8$, the same spectrum of behaviors is ostensible, where the window of desynchronization is preserved. Obviously, synchronization is more likely to happen for $\beta_1 = 0.8$ than for its smaller values. The numerical patterns corresponding to this case are given in Figs. 28-30, where ϵ takes increasing values. Fig. 28, for example, Fig. 28-29 gives the patterns for $\epsilon = 0.1$. The initial state disintegrates, with the early stage being the generation of spiral seed at time $t = 50$. However, due to the weak input of the IP_3, the spirals are dissolved with time increasing lading to band patterns. When ϵ is increased to 0.18, the patterns of Fig. 29 are obtained, where the Ca^{2+} wave dynamics is governed by spiral seeds, which shows the strong input from the IP_3, metabolized by the 3-kinase resulting from the activation of Ca^{2+}. The persistence of spiral waves in the system and their repetitive occurrence relies on the Ca^{2+}-releasing via CICR. However, a strong and prolonged input of IP_3 will contribute to disintegrating the spiral waves as depicted in Fig. 30. Nevertheless, the persistence and presence of a few spiral seeds show their robustness in this particular mode, where the paracrine coupling is tuned to support coherent states. Also, this shows the interdependence between the degradation of IP_3 and the degree of stimulation of the cells that may contribute to sustaining the occurrence of spiral waves. Their complementarity is addressed in the next section.

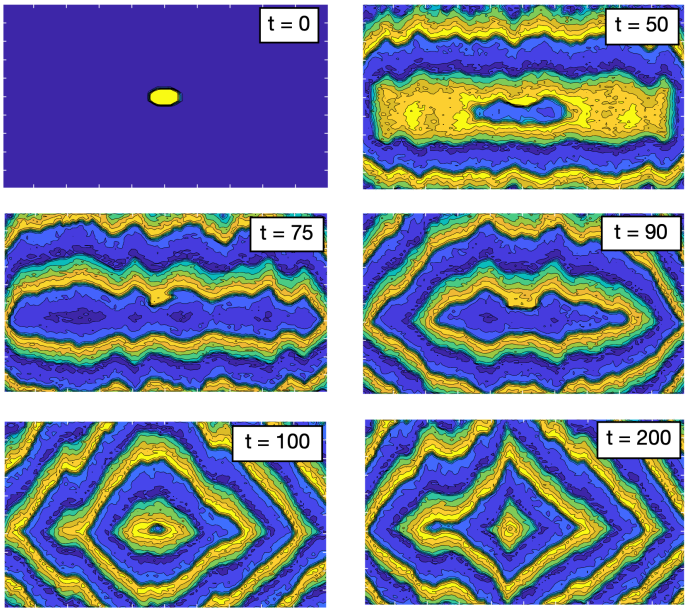

Figure 24: The panels show the development of wave pattern of Ca^{2+} at different instants induced by IP_3, with the paracrine coupling strength $\beta_1 = \beta_2 = 0.4$, $\epsilon = 0.1$, and $\gamma = 0.5$.

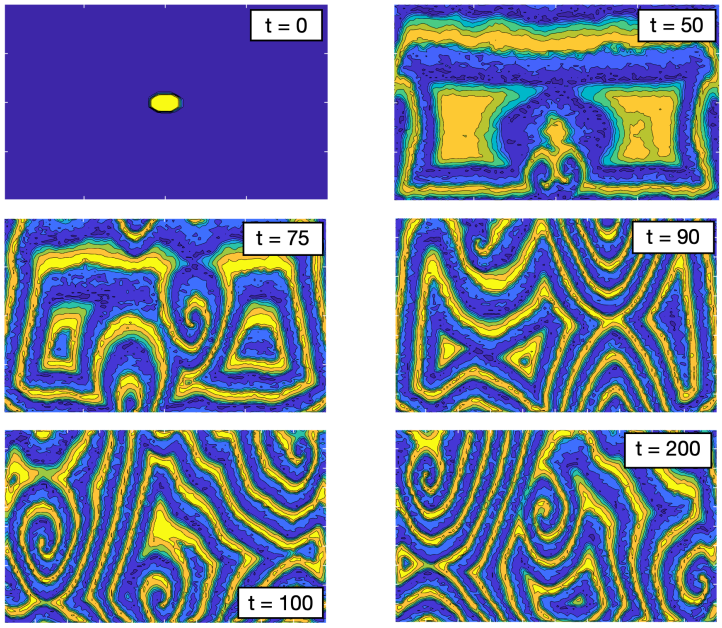

Figure 25: The panels show the development of wave pattern of Ca^{2+} at different instants induced by IP_3, with the paracrine coupling strength $\beta_1 = \beta_2 = 0.8$, $\epsilon = 0.1$, and $\gamma = 0.5$.

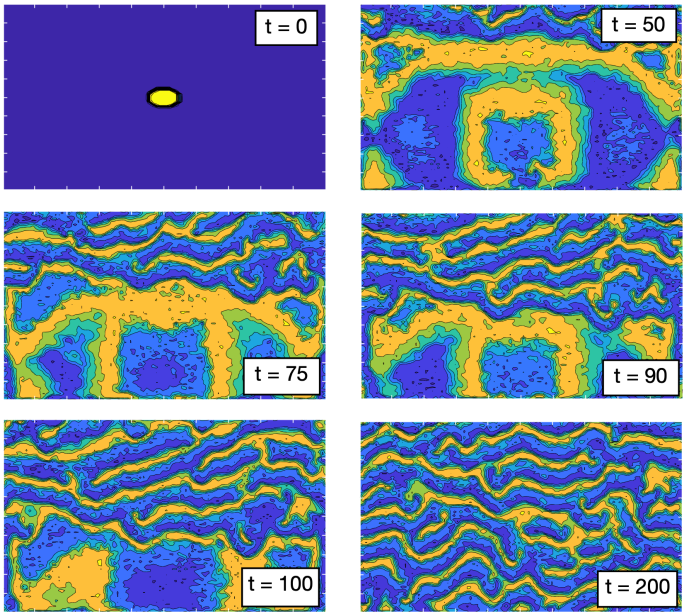

Figure 26: The panels show the development of wave pattern of Ca^{2+} at different instants induced by IP_3, with the paracrine coupling strength $\beta_1 = \beta_2 = 0.98$, $\epsilon = 0.1$, and $\gamma = 0.5$.

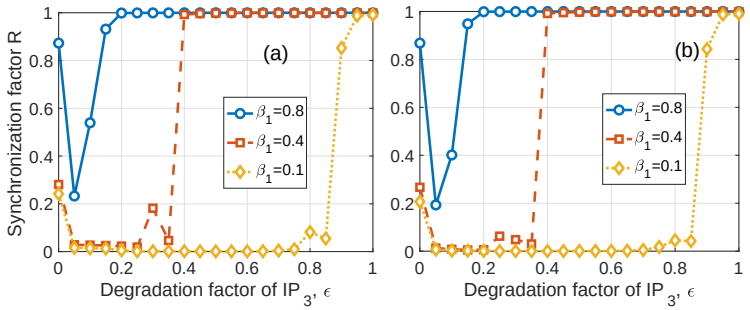

Figure 27: The panels show the distribution of synchronization factor R versus the degradation factor of IP_3, with the longitudinal paracrine coupling strength taking the respective values γ =0.8, 0.4, and 0.1. Panel (a) corresponds to $\beta_1 = \beta_2 = \beta = 0.4$, while panel (b) is plotted for $\beta_1 = \beta_2 = 0.8$.

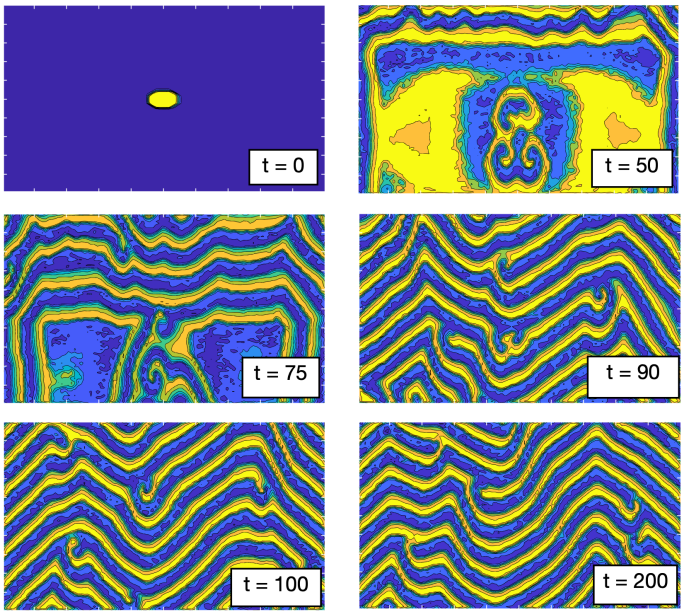

Figure 28: The panels show the development of spiral wave pattern of Ca^{2+} at different instants induced by IP_3, with the IP_3 degradation factor $\epsilon = 0.1$, $\gamma = 0.5$, and $\beta_1 = \beta_2 = 0.4$.

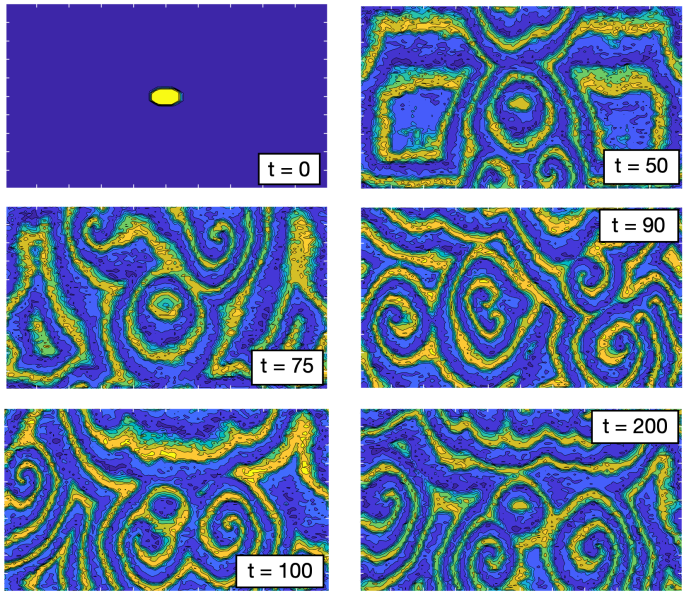

Figure 29: The panels show the development of spiral wave pattern of Ca^{2+} at different instants induced by IP_3, with the IP_3 degradation factor $\epsilon = 0.18$, $\gamma = 0.5$, and $\beta_1 = \beta_2 = 0.4$.

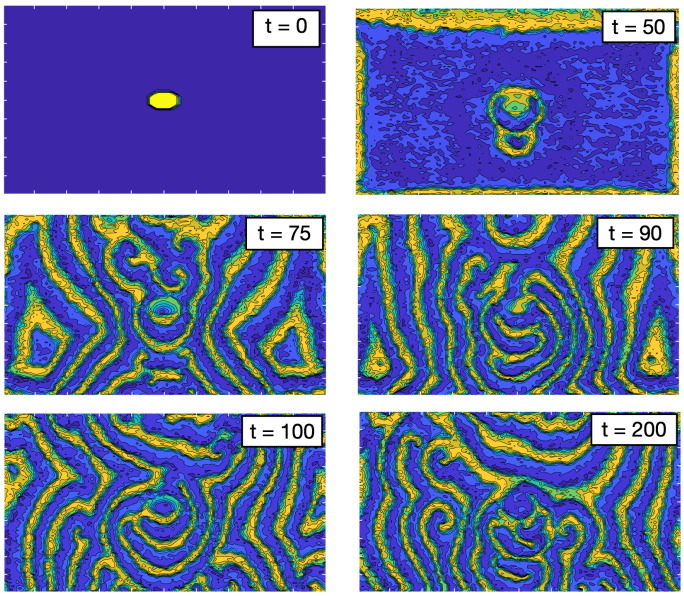

Figure 30: The panels show the development of spiral wave pattern of Ca^{2+} at different instants induced by IP_3, with the IP_3 degradation factor $\epsilon = 0.2$, $\gamma = 0.5$, and $\beta_1 = \beta_2 = 0.4$.

III.1.3 Effect of the degree of cell stimulation γ

To start, the interdependence between IP_3 degradation and external stimuli of cells for nonlinear patterns to occur is regarded in Fig. 31, where the synchronization factor is recorded versus ϵ, with γ taking increasing values and $\beta_1 = \beta_2 = 0.4$. For strong stimulus, the synchronization factor shows a marginal synchronization region of ϵ, which means an eventual absence of spiral waves for any value of the IP_3 degradation. However, with decreasing γ to 0.4, R suddenly drops from $\epsilon = 0$ and increases when $\epsilon = 0.1$, also leading to a saturated synchronization factor. In Fig. 31(b), where $\beta_1 = \beta_2 = 0.8$, the synchronization factor drops for strong stimuli while decreasing γ supports regions of IP_3 degradation, where synchronous states may appear, which is more pronounced for $\gamma = 0.1$. This further implies the dependence on coupling intensity and external stimuli of the distribution for synchronization factors. The curves, for high γ, show monotonicity by changing the stimulation degree, and the IP_3 input is helpful to support spiral waves on the condition that a smaller synchronization factor is approached.

According to the numerical results of Fig. 32, where we have picked $\gamma = 0.79$ and $\epsilon = 0.2$, with $\beta_1 = \beta_2 = 0.8$, the initial condition progressively disintegrates into spiral waves that grow and tend to fill the entire extracellular space with time increasing. One also notices some transitory states showing double spiral seeds that grow as time advances. Under the same condition for the paracrine couplings and the IP_3 degradation, the stimulation strength is increased to

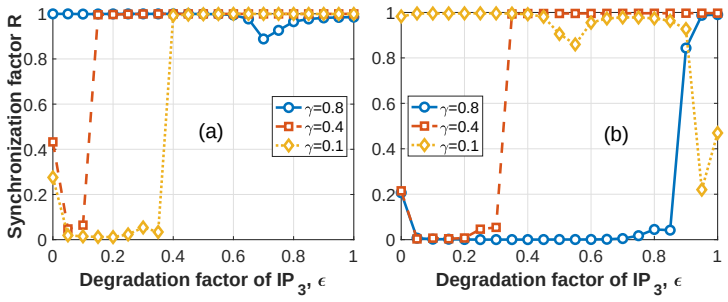

Figure 31: The panels show the distribution of synchronization factor R versus the degradation factor of IP_3, with the longitudinal paracrine coupling strength taking the respective values γ =0.8, 0.4, and 0.1. Panel (a) corresponds to $\beta_1 = \beta_2 = 0.4$, while panel (b) is plotted for $\beta_1 = \beta_2 = 0.8$.

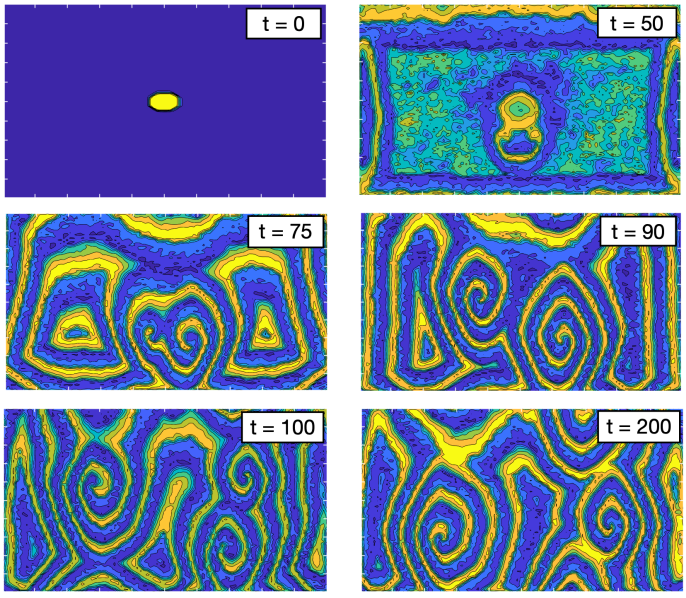

Figure 32: The panels show the development of spiral wave pattern of Ca^{2+} at different instants induced by IP_3 under the effect of the degree of cell stimulation γ, with $\epsilon = 0.2$, $\beta_1 = \beta_2 = 0.8$ and $\gamma = 0.79$.

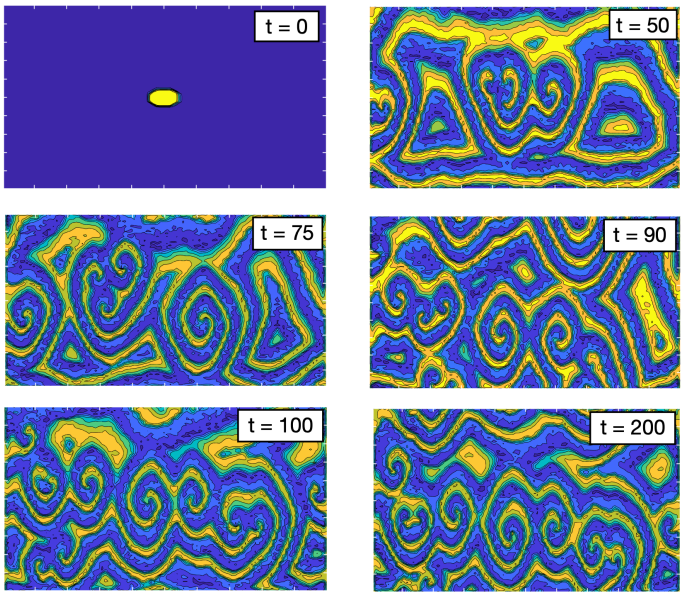

Figure 33: The panels show the development of spiral wave pattern of Ca^{2+} at different instants induced by IP_3 under the effect of the degree of cell stimulation γ, with $\epsilon = 0.2$, $\beta_1 = \beta_2 = 0.8$ and $\gamma = 0.794$.

$\gamma = 0.794$, which leads to the patterns of Fig. 33, where the emergence of spiral waves takes place much earlier than in the case of Fig. 32. Moreover, the oscillating patterns are supported by multi-armed spiral waves, which show the importance of a suitable balance between the cell stimulus and the IP_3 degradation parameter. It can be concluded that the emergence of spiral waves mainly depends on the stimulus, even though intercellular communication in the whole network relies on coupling strength. Nevertheless, the reader should remember that an irregular spatial distribution of patterns was obtained for the above-used values of the coupling strengths. Therefore, the coupling intensity and the degree of cell stimulation become essential to fill the extracellular environment with spiral waves in the network.

III.2 Bifurcation of Synchronized nonlinear intercellular Ca^{2+} oscillation

We study the intercellular complex Ca^{2+} wave in paracrine coupled cell. we begin to the impact of coupling strength for dynamic of Ca^{2+} wave, the bifurcation values, the distribution of synchronization are study and the results.

III.2.1 Impact of coupling strength for modulated dynamic

In order to efficiently predict possible dynamical regimes of calcium waves in the studied model, different indicators can be used. The bifurcation of calcium waves refers to a phenomenon in which the dynamics of calcium signaling changes from one stable state to multiple possible states or patterns, resulting in different types of calcium wave behavior. In the context of calcium waves, bifurcation typically occurs when a certain parameter or condition in the cell or its microenvironment is altered, causing a transition from one type of calcium wave pattern to another. This can have important implications for cellular function and signaling dynamics. This is pointed out in the studied system, where one pays attention to how paracrine signalling contributes to changing oscillatory behaviors of Ca^{2+} patterning as time increases. This is, for example, the case of Fig. 34(a), where the bifurcation diagram shows how the system dynamics changes with time as β increases. One can identify three regions, where specific intervals inform on eventual dynamical signatures of Ca^{2+} mediated by IP_3 oscillations. Suitably, bifurcation in calcium waves can result from changes in key parameters such as intracellular calcium concentration, the activity of ion channels or receptors, or extracellular factors that influence calcium signaling. For instance, over time, the progression of the bifurcation diagram in Fig. 34(a) shows traveling bands for $\beta \leq \beta_{cr}^{(1)}$, while erratic areas appear in the interval $\beta_{cr}^{(1)} \leq \beta \leq \beta_{cr}^{(2)}$, where the dynamics of the Ca^{2+} concentration is expected to be chaotic. Finally, beyond $\beta_{cr}^{(2)}$, quasi-periodic bands govern the bifurcation features.

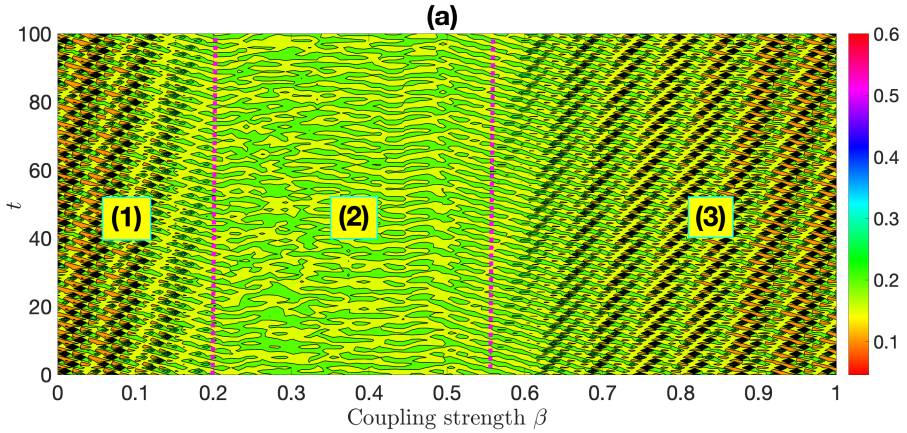

Figure 34: Evolution of the bifurcation diagram versus the paracrine coupling strength β and time, where the three regions (1), (2) and (3) correspond to specific intervals of dynamical signatures of Ca^{2+} mediated by IP_3 oscillations correspond, respectively, to $\beta = 0.1$, $\beta = 0.3$, and $\beta = 0.6$, picked Fig.3.20(a). The other parameters are given by: $v_0 = 2.0\mu\text{Mmin}^{-1}$, $v_1 = 2.0\mu\text{Mmin}^{-1}$, $V_{m2} = 6.0\mu\text{Mmin}^{-1}$, $V_{m3} = 20.0\mu\text{Mmin}^{-1}$, $k_2 = 0.1\mu\text{M}$, $k_y = 0.2\mu\text{M}$, $k_z = 0.5\mu\text{M}$, $k_x = 0.2\mu\text{M}$, $k_f = 1.6$ min^{-1}, $v_{4n} = 2.0\mu\text{M}$, $V_{m5} = 2.0\mu\text{Mmin}^{-1}$, $k_5 = 1\mu\text{M}$, $k_d = 0.4\mu\text{M}$, and $k = 10.0\mu\text{M}$.

The above predictions are confirmed by Figs. 35(b1)-(b3) and (c1)-(c3), where the time series of the cytosolic Ca^{2+} and their corresponding phase plots are respectively displayed. According

to Figs. 35(b1) and (b3), the dynamics of Ca^{2+} at cell $n = 50$ is governed by simple quasi-periodic oscillations as predicted in areas (1) and (3) of the bifurcation diagram, with $\beta = 0.1$ and $\beta = 0.6$, respectively. Here, the dynamics is manifested by rhythmic and repeated oscillations in the concentration of Ca^{2+} within a cell and may be extended to the lattice under paracrine coupling for the intrinsic control of various cellular activities. Moreover, quasi-periodic Ca^{2+} oscillations can facilitate communication between neighboring cells, coordinating activities within tissues and organs, under the strong effect of second messengers like Ca^{2+} itself and IP_3 whose effect is considered here. Remarkably, for $\beta = 0.3$, which falls into the chaotic zone of the bifurcation diagram, one obtains chaotic patterns as depicted in Fig. 35(b2). Here, one notices complex and irregular patterns of Ca^{2+} fluctuations within the cell $n = 50$, which is also evident in the phase plot of Fig. 35(c2).

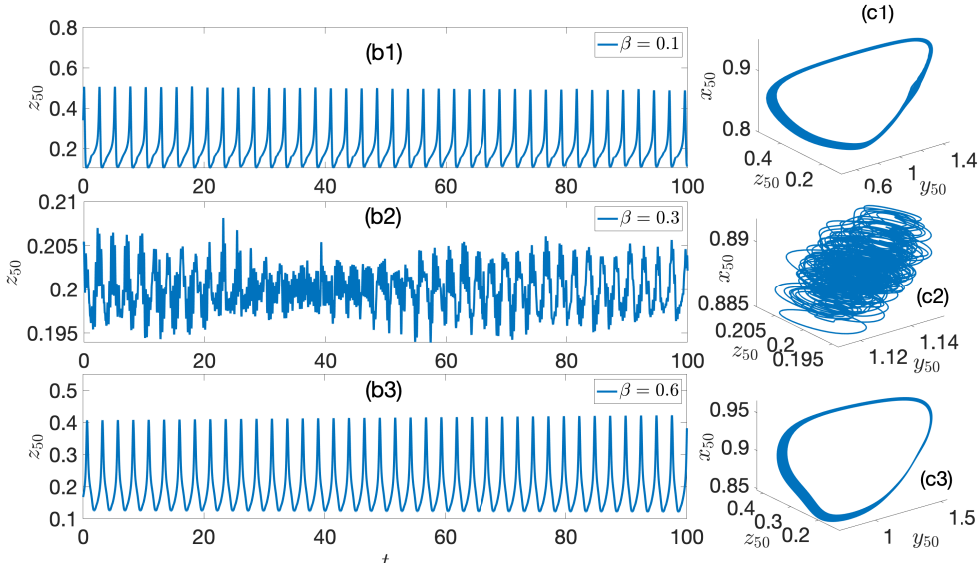

Figure 35: $(bj)_{j=1,,2,3}$ Time evolution of the cytosolic Ca^{2+} concentration $z_n(t)$ in cell $n = 50$ and $(cj)_{j=1,,2,3}$ their corresponding global phase-plot diagrams. From top to bottom, panels $(bj)_{j=1,,2,3}$ and $(cj)_{j=1,,2,3}$ correspond, respectively, to $\beta = 0.1$, $\beta = 0.3$, and $\beta = 0.6$, picked Fig.3.20(a). The other parameters are given by: $v_0 = 2.0\mu\text{Mmin}^{-1}$, $v_1 = 2.0\mu\text{Mmin}^{-1}$, $V_{m2} = 6.0\mu\text{Mmin}^{-1}$, $V_{m3} = 20.0\mu\text{Mmin}^{-1}$, $k_2 = 0.1\mu\text{M}$, $k_y = 0.2\mu\text{M}$, $k_z = 0.5\mu\text{M}$, $k_x = 0.2\mu\text{M}$, $k_f = 1.6$ min^{-1}, $v_{4n} = 2.0\mu\text{M}$, $V_{m5} = 2.0\mu\text{Mmin}^{-1}$, $k_5 = 1\mu\text{M}$, $k_d = 0.4\mu\text{M}$, and $k = 10.0\mu\text{M}$.

III.2.2 Impact of coupling strength for the global network

The same distribution of cytosolic Ca^{2+} is of great importance in preventing some diseases like diabetes since in the pancreatic diabetic β cells, we observe the local aggregate of Ca^{2+} with make the disfunctions of them in insulin secretion. In this subsection, we study the global distribution of Ca^{2+} and the bifurcation point to control the complex wave. The global space-time-concentration in Fig. 37 shows the emergence of complex Ca^{2+} waves like burst and chaos, confirm by phase attractor of the third parameters of the network. We observed semi-periodic

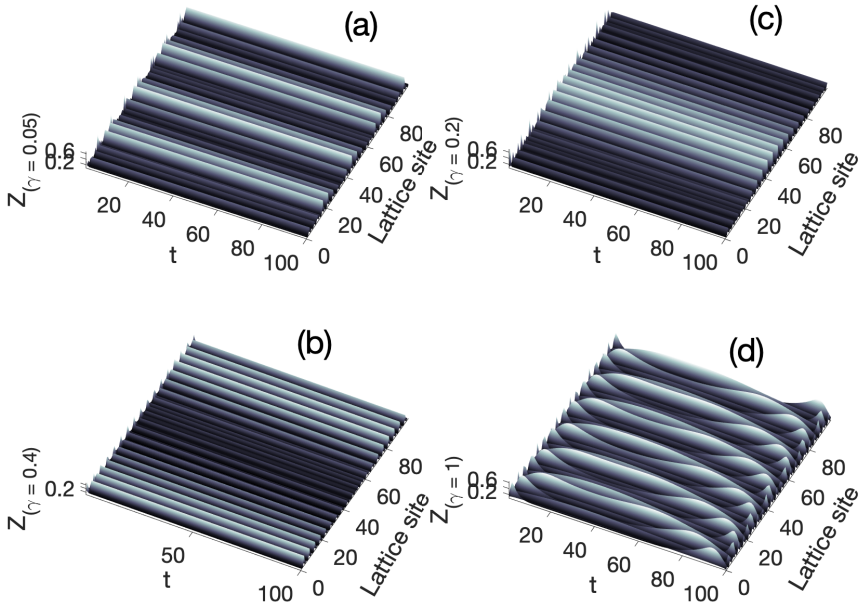

Figure 36: The travelling wave of the stimulation degree γ in coupled model.

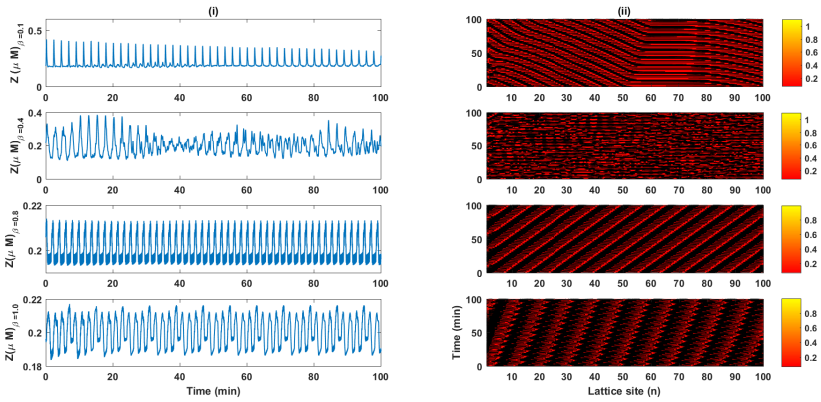

Figure 37: The global space-time-concentration of cytosolic Ca^{2+} concentration Z between coupling strengh. To high for bow the different values of paracrine strength , in first line $\beta = 0.05$ and second $\beta = 0.05$, $\beta = 0.4$, $\beta = 0.8$ and $\beta = 1.0$.

regime to same value $\beta = 0.08$, the emergence of chaos regime when $\beta = 0.4$, burst regime at $\beta = 0.8$, and quasi-periodic regime at $\beta = 1.0$. Paracrine coupling can control the emergence of complex wave in the network, the is same solution to auto-modulate of cytosolic calcium wave.

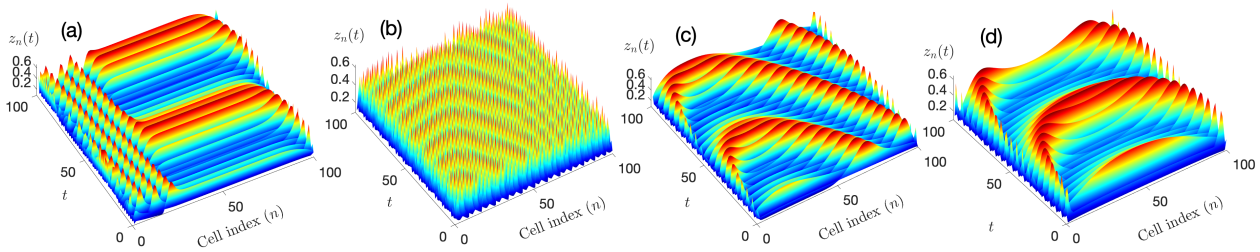

Figure 38: Spatiotemporal evolution of the cytosolic Ca^{2+} concentration $z_n(t)$ under different values of the paracrine coupling strength, as per predictions from the bifurcation diagram Fig.1(a). From panels (a) to (d), β takes the respective values $\beta = 0.1$, 0.3, 0.6 and 0.8, with $\gamma = 0.4$ and the other parameter values being: $v_0 = 2.0\mu\text{Mmin}^{-1}$, $v_1 = 2.0\mu\text{Mmin}^{-1}$, $V_{m2} = 6.0\mu\text{Mmin}^{-1}$, $V_{m3} = 20.0\mu\text{Mmin}^{-1}$, $k_2 = 0.1\mu\text{M}$, $k_y = 0.2\mu\text{M}$, $k_z = 0.5\mu\text{M}$, $k_x = 0.2\mu\text{M}$, $k_f = 1.6$ min^{-1}, $v_{4n} = 2.0\mu\text{M}$, $V_{m5} = 2.0\mu\text{Mmin}^{-1}$, $k_5 = 1\mu\text{M}$, $k_d = 0.4\mu\text{M}$, and $k = 10.0\mu\text{M}$. As the paracrine coupling coefficient increases, one notices a transition between quasiperiodic bands and spatiotemporal erratic patterns.

Fig. 38 displays the spatiotemporal behaviors of the cytosolic Ca^{2+} with values of the paracrine coupling strength obtained from Fig. 34(a). For $\beta = 0.1$, the patterns of Fig. 38(a) are obtained where after a transient oscillatory regime of Ca^{2+}, one notices the appearance of bands that support quasiperiodic oscillations. For $\beta = 0.3$, spatiotemporal erratic patterns take over the dynamics, where one can notice a mix-up of several frequencies, both spatially and temporally. For the rest of the values of the paracrine coupling strength, when $\beta \geq \beta_{cr}^{(2)}$, coherent structures appear, and their spatial distribution depends on the value of the paracrine coupling. As it is well known, dysregulation of periodic Ca^{2+} waves can be associated with various diseases, such as cardiac arrhythmias, neurodegenerative disorders, and certain cancers [105, 106, 107]. Therapeutic interventions sometimes aim to restore or control Ca^{2+} oscillations to treat these conditions. Therefore, understanding the mechanisms behind periodic calcium waves is crucial for gaining insights into normal cell function and the pathophysiology of diseases, which encourages to include more factors in the modeling of such oscillations and how they are transmitted from one cell to another. Interestingly, according to the above results, the frequency and amplitude of periodic calcium waves can be tightly regulated. Various cellular processes and external factors can influence the characteristics of these oscillations, enabling cells to adapt to changing demands.

We have seen previously that the coupling mode chosen has a considerable impact on our study model, but not in a uniform way. We will take it as a control parameter and see its impact on the oscillatory mode. So than we represent the bifurcation diagram. Fig. 39 presents the impact of the paracrine coupling term. In Fig. 39(a) we have a diagram of the bifurcation of Z as a function of time (t) and of the coupling force (β), where we can notice a zone of change in the vibratory regime around [0.2;0.6] compared to to the rest of the domain. This is consolidated

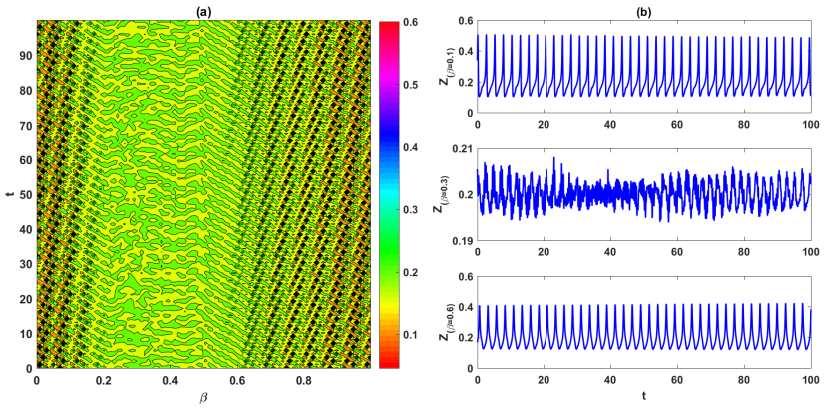

Figure 39: Bifurcation diagram of the cytosolic Ca^{2+} concentration Z in panel (a) and the corresponding time series of the same variable in panels (b) under the variation of the coupling strength β. We see how the coupling strength modify the frequency and amplitude of oscillation of Ca^{2+}-waves. In fact, $\beta = 0.1$ and $\beta = 0.6$ corresponds to spiking regime for different amplitude, and $\beta = 0.3$ corresponds to chaotic regime. The other parameters are given by:k=10,$k_2 = 0.1$,$k_x = 0.2$,$k_d = 0.4$,$k_5 = 1$,$k_f = 1.4$, $k_y = 0.2$,$k_z = 0.5$,$V_0 = 2.0$,$V_1 = 2.0$,$Vm_2 = 6$,$V_{m3} = 20$,$V_4 = 2$,$V_{m5} = 2$

by Fig. 39(b) where the time series are represented for different values of β. We observe the emergence of a chaotic regime between two zones of spikes oscillations.

This prediction behaviors of network can confirm with plotted attractor of phase for interaction between the cytosolic Ca^{2+}, store Ca^{2+} and IP_3 concentrations by Fig. 41.

III.2.3 Synchronized states of IP_3-induced Ca^{2+} oscillations

Synchronized Ca^{2+} waves refer to the coordinated and simultaneous oscillations in intracellular Ca^{2+} concentrations among multiple cells or cellular structures within a tissue, organ, or network [108, 109]. These synchronized Ca^{2+} waves play a crucial role in various physiological processes and are essential for coordinating activities across cell populations [110, 111, 112]. In what follows, synchronized states of Ca^{2+} oscillations are investigated based on the competition between the paracrine signaling strength and other factors such as the stimulation strength and the degradation factor of IP_3.

One should note that the above synchronization factor is calculated numerically using the procedure described so far. When $\mathcal{R} = 1$, perfect synchronization is expected, while non-perfect synchronization is supposed to occur when $\mathcal{R}$ is close to 0. A good illustration of such is delivered by Fig. 42, where $\mathcal{R}$ is plotted against the paracrine coupling strength under increasing values of the degradation factor ϵ of IP_3.

It appears that for $\epsilon = 0.1$, large intervals of β may support synchronization, given that $0 \leq \beta \geq \beta_{cr}$, after which synchronous states are expected to disappear. Under increased values of ϵ, i.e., $\epsilon = 0.2$ and 0.3, synchronization is marginally restricted to weak values of β, which increasing γ contributes to expand as depicted in Fig. 42(c). In that direction, one should remember

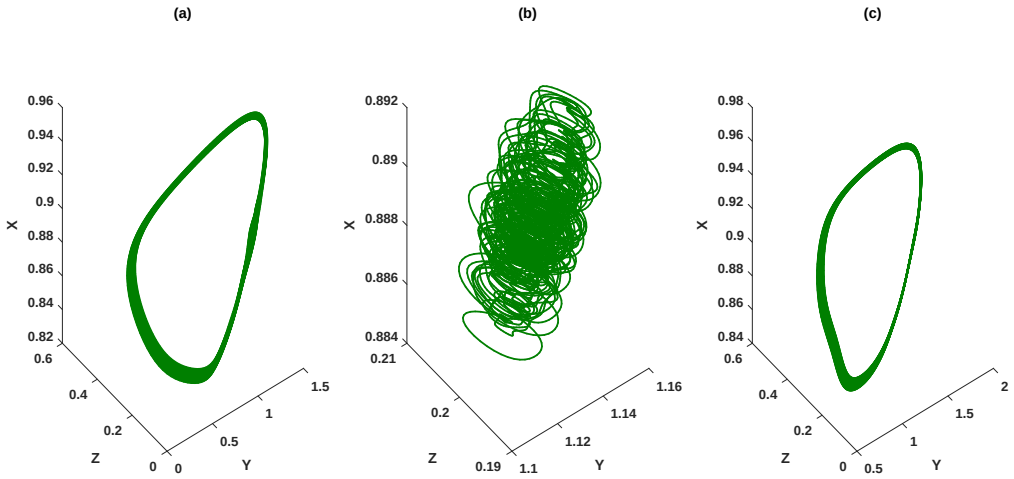

Figure 40: The attractor of phase for interaction between the cytosolic Ca^{2+} concentration Z, store Ca^{2+} concentration Y of CICR and the Ca^{2+}-stimulated degradation of IP_3 concentration X. We set $\beta = 0.1$ for (a), $\beta = 0.3$ for (b) and $\beta = 0.6$ for (c). The other parameters are the same with fig(3.14)

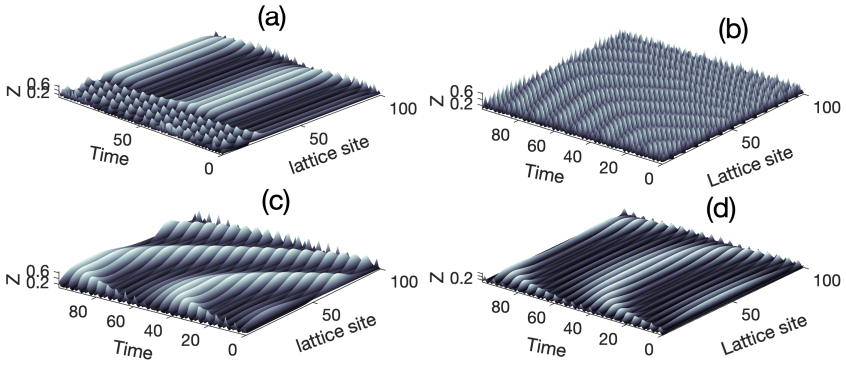

Figure 41: Travelling wave of the cytosolic Ca^{2+} concentration Z vs the variation of the paracrine strength β.

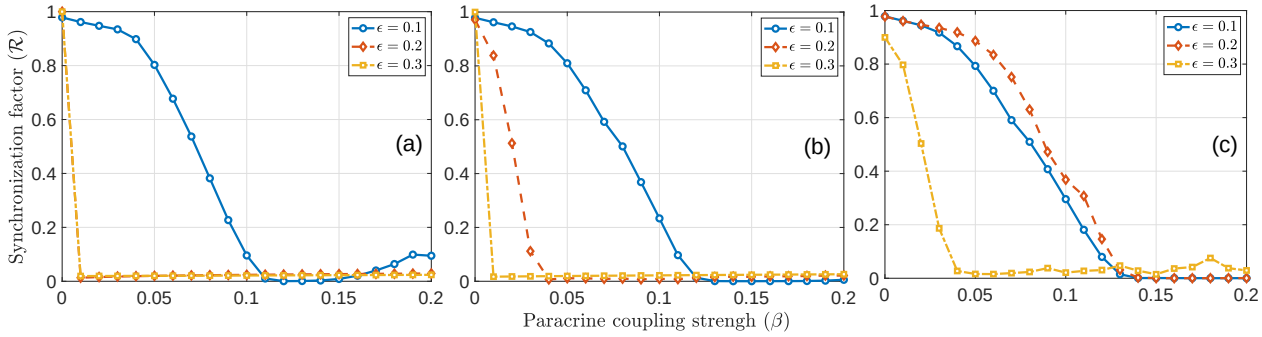

Figure 42: The panels show the factor of synchronization $\mathcal{R}$ versus the paracrine coupling strength β, with the IP_3 degradation factor ϵ taking increasing values in each case. From left to right, the stimulation factor takes the respective values $\gamma = 0.03$, $\gamma = 0.04$, and $\gamma = 0.05$. The other parameter values are: $k = 10$, $k_2 = 0.1$, $k_x = 0.2$, $k_d = 0.4$, $k_f = 1.4$, $k_5 = 1$, $k_y = 0.2$, $k_z = 0.5$, $v_0 = 2.0\mu\text{Mmin}^{-1}$, $v_1 = 2.0\mu\text{Mmin}^{-1}$, $V_{m5} = 2$, $V_{m2} = 6$, $V_{m3} = 20$, and $v_{4n} = 2.5$.

that Figs. 42(a)-(c) correspond, respectively, to $\gamma = 0.03$, 0.04, and 0.05.

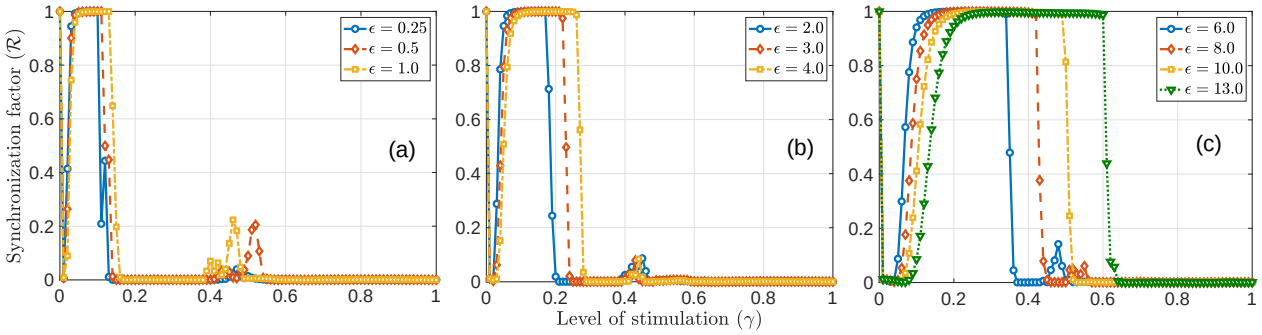

Figure 43: The panels show the factor of synchronization $\mathcal{R}$ versus the stimulation level γ, with the IP_3 degradation factor ϵ taking increasing values in each case. The paracrine coupling strength is fixed as $\beta = 0.02$, while the other parameter values are: $v_0 = 2.0\mu\text{Mmin}^{-1}$, $v_1 = 2.0\mu\text{Mmin}^{-1}$, $V_{m2} = 6.0\mu\text{Mmin}^{-1}$, $V_{m3} = 20.0\mu\text{Mmin}^{-1}$, $k_2 = 0.1\mu\text{M}$, $k_y = 0.2\mu\text{M}$, $k_z = 0.5\mu\text{M}$, $k_x = 0.2\mu\text{M}$, $k_f = 1.6$ min^{-1}, $v_{4n} = 2.0\mu\text{M}$, $V_{m5} = 2.0\mu\text{Mmin}^{-1}$, $k_5 = 1\mu\text{M}$, $k_d = 0.4\mu\text{M}$, and $k = 10.0\mu\text{M}$.

The effect of the latter is particularly assessed in Fig. 43, where the different panels correspond to increasing values of the IP_3 degradation factor ϵ, with $\beta = 0.02$. In Fig. 43(a), where ϵ is given the respective values 0.25, 0.5, and 1, one notices a hump of synchronization that abruptly disappear while desynchronization takes place. As ϵ increases, the domain $\mathcal{R} \simeq 1$ gets expanded, which implies that for a pronounced degradation of IP_3, the stimulation factor gets stronger for synchronization to take place, after which desynchronized states are expected to emerge. This is, for example, the case for Figs. 43(b) and (c), where synchronization is pronounced for $\gamma \leq \gamma_{cr}$.

To investigate of the dynamics parameters who affects the synchronization, we studies vs of degradation factor to specific values of stimulate degree in Fig. 44. This synchronization plot for fixed values of paracrine strength.The features of Fig. 44 confirm the high influence of the

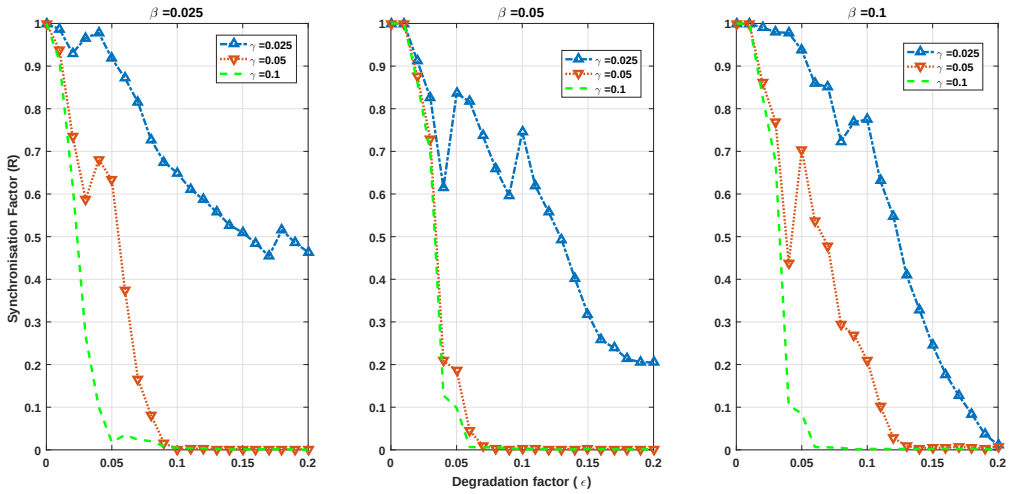

Figure 44: The synchronization factor vs (ϵ) with β increasing from left to rigth, $\beta = 0.025$ in panel (a) $\beta = 0.05$ in panel (b) and $\beta = 0.1$ in panel (c) and in different case we see the impact of stimulate factor γ with increase from $\gamma = 0.025$ (blue line) $\gamma = 0.05$ (red line) and $\gamma = 0.1$ (green line).

paracrine coupling strength on the dynamics of the synchronization factor. Here, panels correspond to the respective values $\beta = 0.025$, 0.05 and 0.1, which γ changes in each panel and $\mathcal{R}$ is shown versus the degradation factor of IP_3. In general, for any value of β, $\mathcal{R}$ is a decreasing function of ϵ, but increasing γ considerably reduces the synchronization interval to weak values of the degradation factor ϵ.

We obtain that the maximum of synchronization distribution occur around $\gamma_s = 0.1$ to many many values of β.

The distribution of Fig. 45 corroborates our previous predictions and shows the strong input from the stimulation factor when $\mathcal{R}$ is considered in the $(\epsilon, \beta)-$plane. Increasing γ contributes to reducing the synchronization band $\epsilon > \epsilon_{cr}$, while the zone for asynchronous states in the $\beta-$direction gets expanded for γ increasing,i.e., when the cells are getting highly excited. This means that the stronger the stimulation degree, the larger the parametric window of chaotic patterns that was already reported in Fig. 45(a). Such a behavior also engages the degradation factor of IP_3 which contributes less to synchronization when γ is high. Instead, it shows selected areas of synchronous states when $\beta < \beta_{cr}^{(1)}$ and $\beta > \beta_{cr}^{(2)}$, as reported in Fig. 45(a).

In Fig. 46, the spatiotemporal dynamics of the cytosolic Ca^{2+} concentration is displayed for increasing values of the paracrine coupling strength. In that context, increasing the latter efficiently maintains synchronous states and equally affects the amplitude of the obtained patterns.

In our study around the parameter γ_s, we analyzed the impact of the degradation factor ϵ on the synchronization distribution while keeping the paracrine strength values fixed. Our findings show that better synchronization can be achieved at $\gamma \leq \gamma_s$, which reduces as we increase γ_s, as depicted in Fig. 47, where the distribution of the synchronization factor is displayed versus the IP_3 degradation factor and the degree of stimulation. When the stimulation level is low,

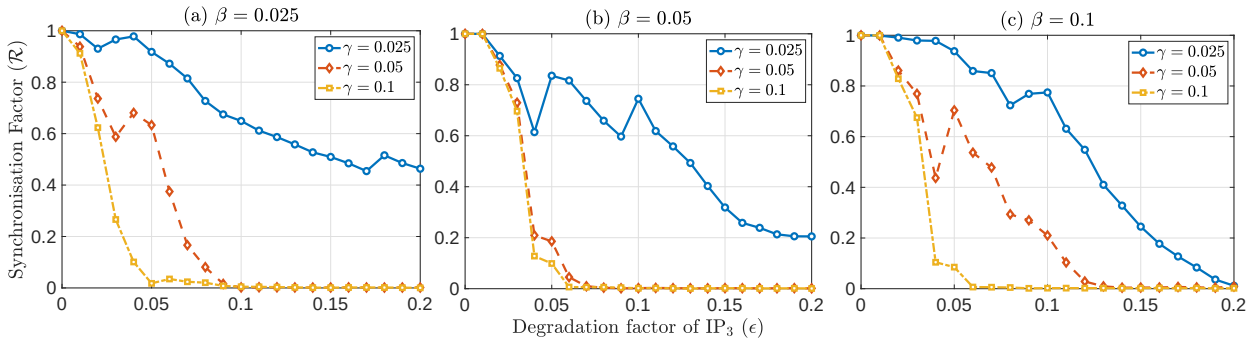

Figure 45: The panels show the factor of synchronization $\mathcal{R}$ versus the IP$_3$ degradation factor ϵ, with stimulation level γ taking increasing values in each case. From left to right, panels correspond to the respective values $\beta = 0.025$, $\beta = 0.05$ and $\beta = 0.1$ of the paracrine coupling strength. The other parameter values are: $v_0 = 2.0\mu$Mmin^{-1}, $v_1 = 2.0\mu$Mmin^{-1}, $V_{m2} = 6.0\mu$Mmin^{-1}, $V_{m3} = 20.0\mu$Mmin^{-1}, $k_2 = 0.1\mu$M, $k_y = 0.2\mu$M, $k_z = 0.5\mu$M, $k_x = 0.2\mu$M, $k_f = 1.6$ min^{-1}, $v_{4n} = 2.0\mu$M, $V_{m5} = 2.0\mu$Mmin^{-1}, $k_5 = 1\mu$M, $k_d = 0.4\mu$M, and $k = 10.0\mu$M. For any value of β, $\mathcal{R}$ is a decreasing function of ϵ, but increasing γ considerably reduces the synchronization interval to weak values of the degradation factor ϵ.

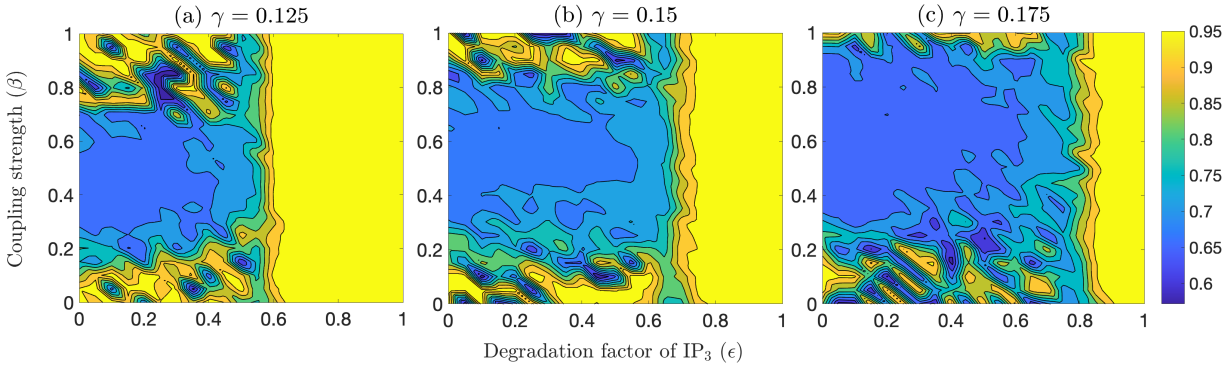

Figure 46: Distribution for synchronization factor in the $(\beta, \epsilon)-$plane with ϵ increasing from left to right and β increasing from bottom to top. The stimulation level changes as $\gamma = 0.125$ in panel (a) $\gamma = 0.15$ in panel (b) and $\gamma = 0.175$ in panel (c). Synchronization is expected in the network when $\mathcal{R} \sim 1$, under parameter values: $v_0 = 2.0\mu$Mmin^{-1}, $v_1 = 2.0\mu$Mmin^{-1}, $V_{m2} = 6.0\mu$Mmin^{-1}, $V_{m3} = 20.0\mu$Mmin^{-1}, $k_2 = 0.1\mu$M, $k_y = 0.2\mu$M, $k_z = 0.5\mu$M, $k_x = 0.2\mu$M, $k_f = 1.6$ min^{-1}, $v_{4n} = 2.0\mu$M, $V_{m5} = 2.0\mu$Mmin^{-1}, $k_5 = 1\mu$M, $k_d = 0.4\mu$M, and $k = 10.0\mu$M. Increasing γ contributes to reducing the synchronization band $\epsilon > \epsilon_{cr}$, while the zone for asynchronous states in the $\beta-$direction gets expanded for γ increasing.

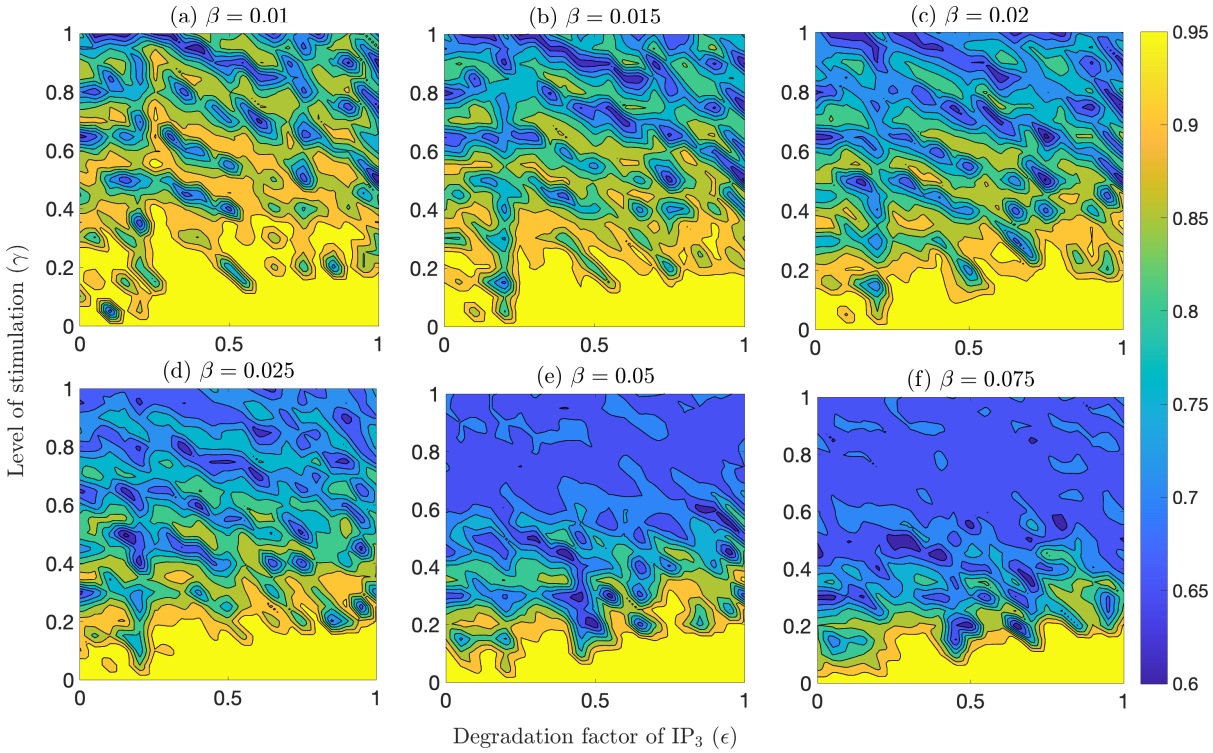

Figure 47: Distribution for synchronization factor in the $(\epsilon, \gamma)-$plane with ϵ increasing from left to right and γ increasing from bottom to top. The paracrine coupling strength changes as $\beta = 0.01$ in panel (a), $\beta = 0.015$ in panel (b), and $\beta = 0.02$ in panel (c). Synchronization is expected in the network when $\mathcal{R} \sim 1$, under the parameter values: $v_0 = 2.0\mu\text{Mmin}^{-1}$, $v_1 = 2.0\mu\text{Mmin}^{-1}$, $V_{m2} = 6.0\mu\text{Mmin}^{-1}$, $V_{m3} = 20.0\mu\text{Mmin}^{-1}$, $k_2 = 0.1\mu\text{M}$, $k_y = 0.2\mu\text{M}$, $k_z = 0.5\mu\text{M}$, $k_x = 0.2\mu\text{M}$, $k_f = 1.6$ min^{-1}, $v_{4n} = 2.0\mu\text{M}$, $V_{m5} = 2.0\mu\text{Mmin}^{-1}$, $k_5 = 1\mu\text{M}$, $k_d = 0.4\mu\text{M}$, and $k = 10.0\mu\text{M}$. A better synchronization can be achieved at $\gamma \leq \gamma_s$, which reduces as we increase γ_s.

there is a critical point where the phosphorylation stimulation strength becomes too strong for synchronous modes to dominate. This is true regardless of the values of β and ϵ. Conversely, if the degree of stimulation is low, synchronous modes are guaranteed, regardless of the strength of stimulation.

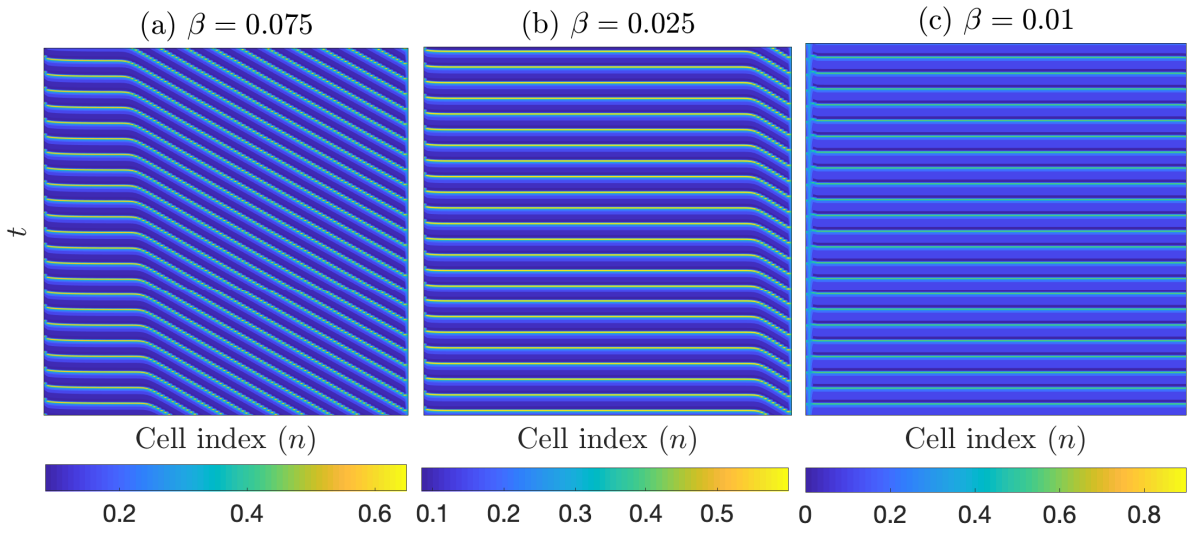

Figure 48: Spatiotemporal evolution of the cytoplasmic concentration of Ca^{2+} with time increasing from bottom to top and space increasing from left to right. Panels from left to right respectively correspond to the paracrine coupling strength $\beta = 0.075$, $\beta = 0.025$, and $\beta = 0.01$. The other parameters are given by: $v_0 = 2.0\mu\text{Mmin}^{-1}$, $v_1 = 2.0\mu\text{Mmin}^{-1}$, $V_{m2} = 6.0\mu\text{Mmin}^{-1}$, $V_{m3} = 20.0\mu\text{Mmin}^{-1}$, $k_2 = 0.1\mu$M, $k_y = 0.2\mu$M, $k_z = 0.5\mu$M, $k_x = 0.2\mu$M, $k_f = 1.6$ min^{-1}, $v_{4n} = 2.0\mu$M, $V_{m5} = 2.0\mu\text{Mmin}^{-1}$, $k_5 = 1\mu$M, $k_d = 0.4\mu$M, and $k = 10.0\mu$M. Increasing the paracrine coupling strength maintains synchronous states and equally affects the amplitude of the obtained patterns.

In Fig. 48, the spatiotemporal dynamics of the cytosolic Ca^{2+} concentration is displayed for increasing values of the paracrine coupling strength. In that context, increasing the latter efficiently maintains synchronous states and equally affects the amplitude of the obtained patterns.

From the weak stimuli, the synchronization distribution is non-zero, which reassures the observation of synchronous modes in the network and the appearance of new vibrational patterns.On the basis of what precedes, the synchronization distribution is a function of the pairs of values of the parameters of the control parameters. Around the γ_s we studies the synchronization distribution vs impact of degradation factor ϵ from the fixed values of paracrine strength. The emerges the same last result add to the fact that we can obtain better synchronization to $\gamma \leq \gamma_s$.

With this prediction, we can plot the timeserie of Ca^{2+} concentration, to observe the type of wave, and the spatiotemporal evolution. To confirm the convergence of wave, we plot the superposition of Ca^{2+} concentration in different space site.

A close illustration of such states is delivered in Fig. 51, where after a transient but short

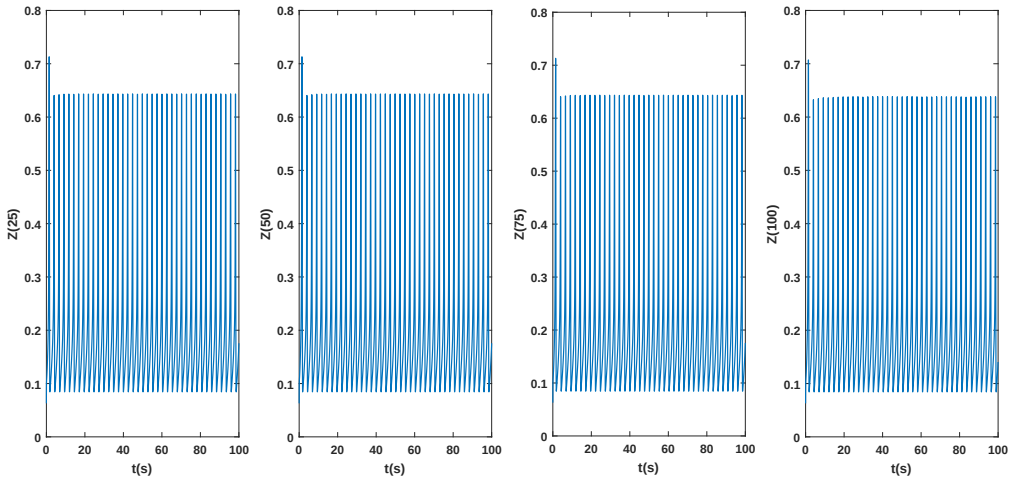

Figure 49: The times series of Ca^{2+} in different time $Z_{25}(t)$,$Z_{50}(t)$,$Z_{75}(t)$ and Z_{100}(t) to illustrate the propagation of Ca^{2+} in network when synchronization factor is high.

period, synchronization is established and remains robust during propagation as per the corresponding synchronization errors. The numerical experiment is repeated and compares the dynamics entertained by the cells $n = 25$, 50, 75 and 100. Moreover, upon examining Fig. 51, we observe identical propagation modes with the same vibrational frequency and zero synchronization error throughout the cell network at the chosen cell indices. The calculations are repeated for $\beta = 0.075$, corresponding to Fig. 50(a), and synchronous states persist.

We have considered $\epsilon = 0.5$ and generated the phase plots of Fig. 52, where panels (a1)-(a2) correspond to the cells of Fig. 51. Increasing ϵ leads to the behaviors of Figs. 52(b1)-(b2), where $\epsilon = 1.5$ for cells 25 and 75. Even in this case, synchronization is ensured, except that the number of scrolls along $x_n(t)$ decreases under ϵ, leading to a drop in the frequency of IP_3 concentration. However, the limit cycle in the $(y_n(t), z_n(t))-$plane remains, showing intrinsic oscillations of Ca^{2+} concentrations between the cytosol and the internal store.

The corresponding point falls well inside the instability region of the diagrams depicted in Fig.51. In what follows, the membrane potentials of the two networks will be recorded and synchronization among some of their nodes will be investigated through the inter-network synchronization error

$$e_n(t) = \left(x_n^{(1)}(t) - x_n^{(2)}(t)\right). \tag{39}$$

It is significant to know that the two NNs display a synchronization state if the following condition is verified

where the same mode of propagation is observed in our cellular network with the same vibrational frequency and zero error. Which for of them we can obtain the condition of better synchronization in the coupled network from the news values of parameters.

In order to further confirm predictions from Fig. 46, we have recorded, for $\gamma = 0.175$, the

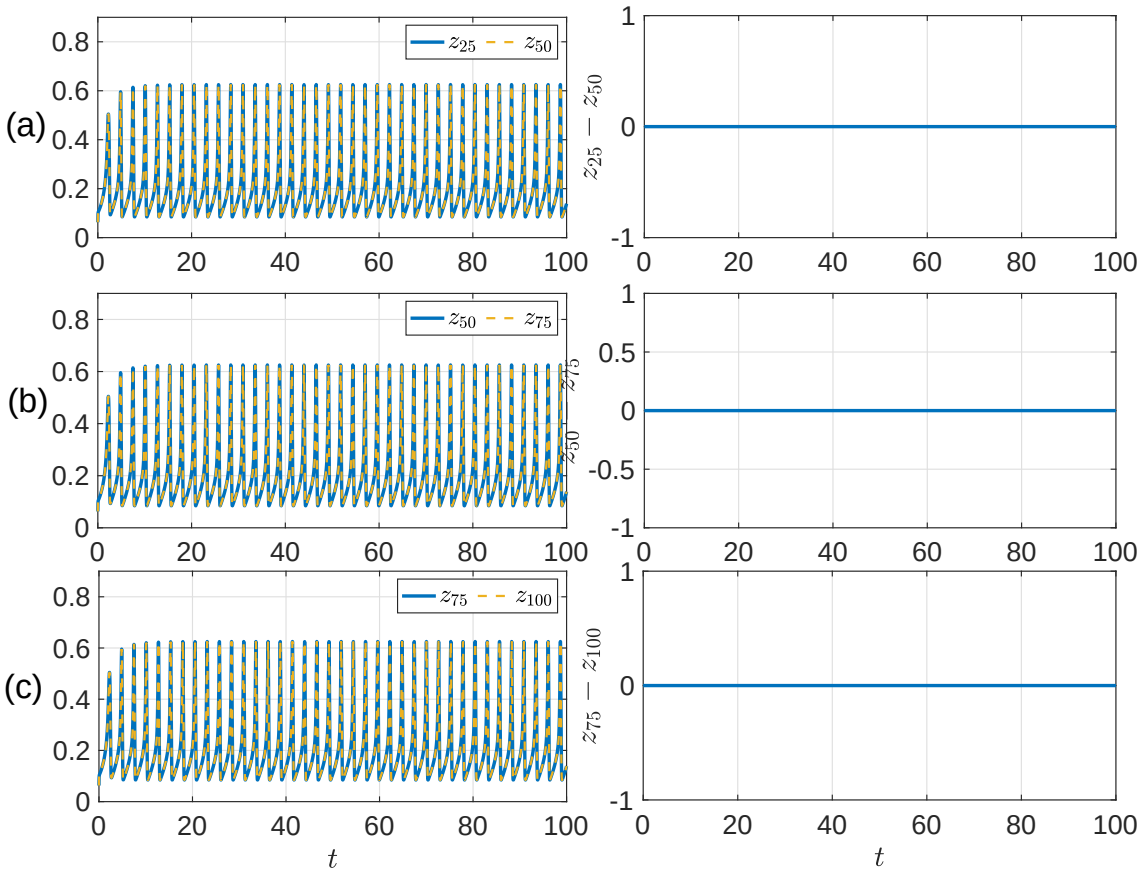

Figure 50: The left column compares times series of cytosolic Ca^{2+} to illustrate synchronous behavior in the network, and the right column shows the corresponding synchronization error for $\beta = 0.01$. The other parameter values are: $v_0 = 2.0\mu\text{Mmin}^{-1}$, $v_1 = 2.0\mu\text{Mmin}^{-1}$, $V_{m2} = 6.0\mu\text{Mmin}^{-1}$, $V_{m3} = 20.0\mu\text{Mmin}^{-1}$, $k_2 = 0.1\mu\text{M}$, $k_y = 0.2\mu\text{M}$, $k_z = 0.5\mu\text{M}$, $k_x = 0.2\mu\text{M}$, $k_f = 1.6$ min^{-1}, $v_{4n} = 2.0\mu\text{M}$, $V_{m5} = 2.0\mu\text{Mmin}^{-1}$, $k_5 = 1\mu\text{M}$, $k_d = 0.4\mu\text{M}$, and $k = 10.0\mu\text{M}$. After a transient but short period, synchronization is established and remains robust during propagation as per the corresponding synchronization errors.

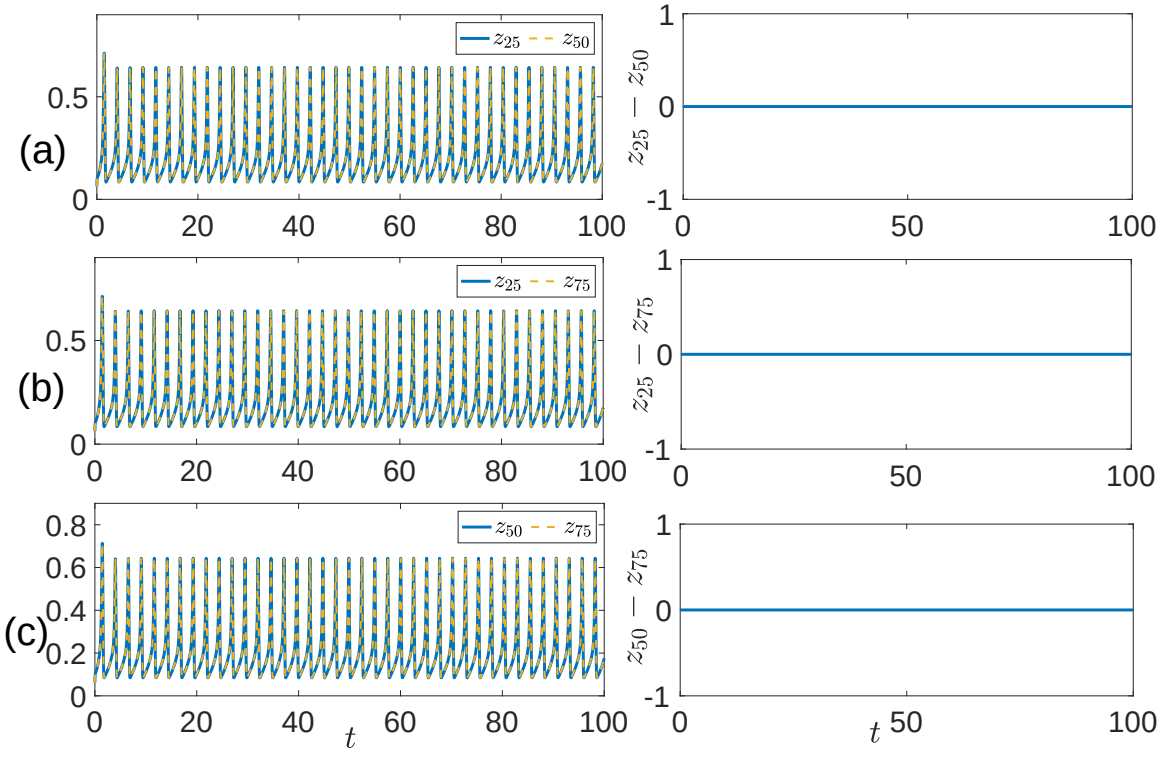

Figure 51: The left column compares times series of cytosolic Ca^{2+} to illustrate synchronous behavior in the network, and the right column shows the corresponding synchronization error for $\beta = 0.075$. The other parameter values are: $v_0 = 2.0\mu\text{Mmin}^{-1}$, $v_1 = 2.0\mu\text{Mmin}^{-1}$, $V_{m2} = 6.0\mu\text{Mmin}^{-1}$, $V_{m3} = 20.0\mu\text{Mmin}^{-1}$, $k_2 = 0.1\mu\text{M}$, $k_y = 0.2\mu\text{M}$, $k_z = 0.5\mu\text{M}$, $k_x = 0.2\mu\text{M}$, $k_f = 1.6$ min^{-1}, $v_{4n} = 2.0\mu\text{M}$, $V_{m5} = 2.0\mu\text{Mmin}^{-1}$, $k_5 = 1\mu\text{M}$, $k_d = 0.4\mu\text{M}$, and $k = 10.0\mu\text{M}$.

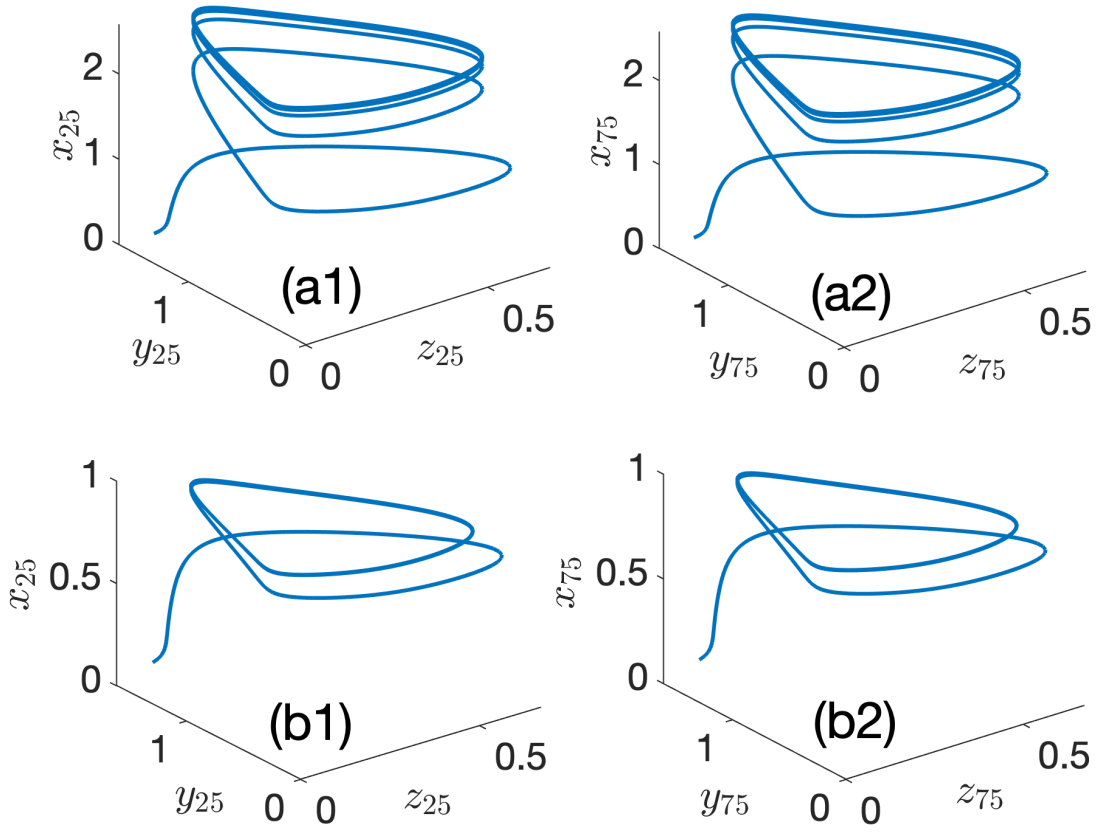

Figure 52: The panels show phase-plots at cell indices $n = 25$ and $n = 75$ for $\beta = 0.075$, with $\epsilon = 0.5$ [(a1) and (a2)], and $\epsilon = 1.5$ [(b1) and (b2)]. In general, the number of scrolls along $x_n(t)$ decreases under ϵ, leading to a drop in the frequency of IP_3 concentration. The limit cycle in the $(y_n(t), z_n(t))-$plane displays intrinsic oscillations of Ca^{2+} concentrations between the cytosol and the internal store when the stimulation level is $\gamma = 0.01$ and the other parameters being: $v_0 = 2.0\mu\text{Mmin}^{-1}$, $v_1 = 2.0\mu\text{Mmin}^{-1}$, $V_{m2} = 6.0\mu\text{Mmin}^{-1}$, $V_{m3} = 20.0\mu\text{Mmin}^{-1}$, $k_2 = 0.1\mu\text{M}$, $k_y = 0.2\mu\text{M}$, $k_z = 0.5\mu\text{M}$, $k_x = 0.2\mu\text{M}$, $k_f = 1.6$ min^{-1}, $v_{4n} = 2.0\mu\text{M}$, $V_{m5} = 2.0\mu\text{Mmin}^{-1}$, $k_5 = 1\mu\text{M}$, $k_d = 0.4\mu\text{M}$, and $k = 10.0\mu\text{M}$.

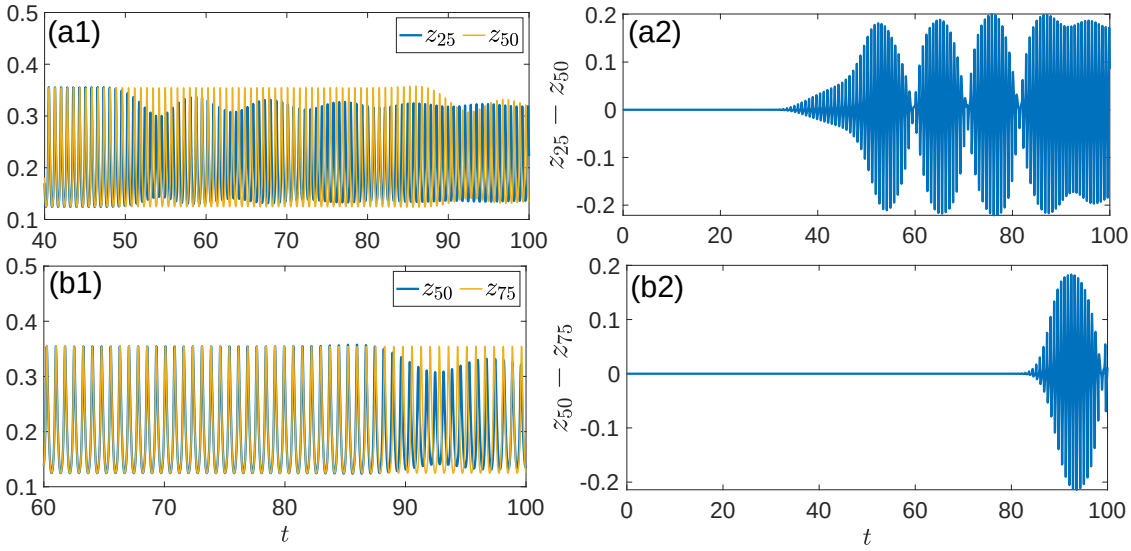

Figure 53: Panel (a1) compares cytosolic Ca^{2+} concentration of cells $n = 25$ and $n = 50$. Panel (b1) compares cytosolic Ca^{2+} concentration of cells $n = 50$ and $n = 75$, while panels (a2) and (b2) show their respective synchronization error. All the calculations have been made for $\gamma = 0.175$ and $\epsilon = 0.2$, with panels (a1)-(a2) corresponding to $\beta = 0.4$ and panels (b1)-(b2) being plotted for $\beta = 0.6$. The other parameter values are: $v_0 = 2.0\mu\text{Mmin}^{-1}$, $v_1 = 2.0\mu\text{Mmin}^{-1}$, $V_{m2} = 6.0\mu\text{Mmin}^{-1}$, $V_{m3} = 20.0\mu\text{Mmin}^{-1}$, $k_2 = 0.1\mu\text{M}$, $k_y = 0.2\mu\text{M}$, $k_z = 0.5\mu\text{M}$, $k_x = 0.2\mu\text{M}$, $k_f = 1.6$ min^{-1}, $v_{4n} = 2.0\mu\text{M}$, $V_{m5} = 2.0\mu\text{Mmin}^{-1}$, $k_5 = 1\mu\text{M}$, $k_d = 0.4\mu\text{M}$, and $k = 10.0\mu\text{M}$.

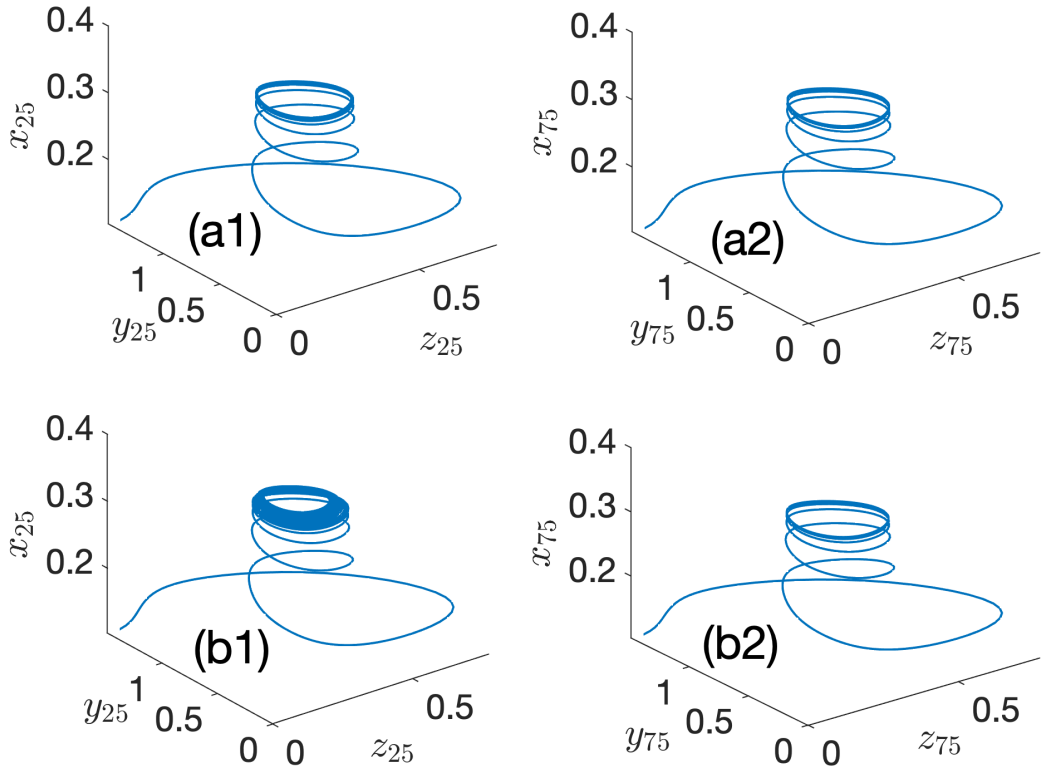

Figure 54: The panels show phase-plots at cell indices $n = 25$ and $n = 75$ for $\gamma = 0.175$ and $\epsilon = 0.2$, with $\beta = 0.4$ [(a1) and (a2)], and $\beta = 0.6$ [(b1) and (b2)]. Desynchronization is manifested in the cytosolic Ca^{2+} oscillations but the activity of IP_3 highly contributes to the process. It is possible to obtain limit cycles in the $(y(t), z(t))-$plane but some of the cells in the network display complex dynamics due to the strong input from the level of stimulation, which indubitably affects oscillations of [IP_3]. The other parameters being: $v_0 = 2.0\mu\text{Mmin}^{-1}$, $v_1 = 2.0\mu\text{Mmin}^{-1}$, $V_{m2} = 6.0\mu\text{Mmin}^{-1}$, $V_{m3} = 20.0\mu\text{Mmin}^{-1}$, $k_2 = 0.1\mu$M, $k_y = 0.2\mu$M, $k_z = 0.5\mu$M, $k_x = 0.2\mu$M, $k_f = 1.6$ min^{-1}, $v_{4n} = 2.0\mu$M, $V_{m5} = 2.0\mu\text{Mmin}^{-1}$, $k_5 = 1\mu$M, $k_d = 0.4\mu$M, and $k = 10.0\mu$M.

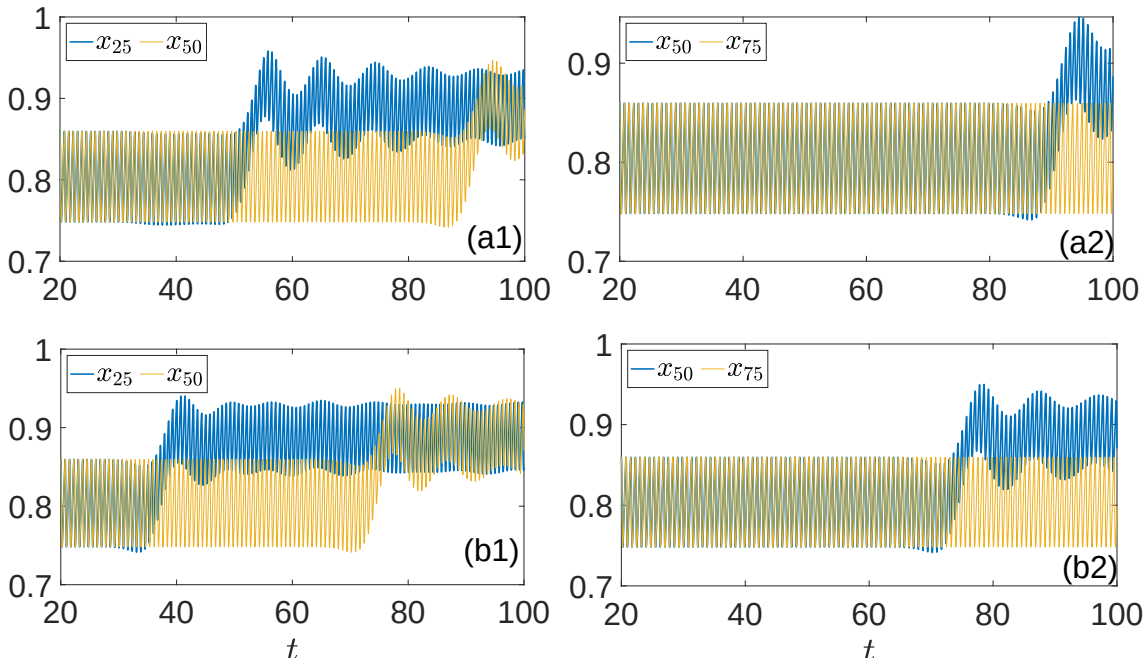

Figure 55: Panels (a1) and (a2) compare IP_3 oscillations in cells $n = 25$ and $n = 50$. Panels (b1) and (b2) compare IP_3 oscillations in cells $n = 50$ and $n = 75$. All the calculations have been made for $\gamma = 0.175$ and $\epsilon = 0.2$, with panels (a1)-(a2) corresponding to $\beta = 0.4$ and panels (b1)-(b2) being plotted for $\beta = 0.6$. The other parameter values are: $v_0 = 2.0\mu\text{Mmin}^{-1}$, $v_1 = 2.0\mu\text{Mmin}^{-1}$, $V_{m2} = 6.0\mu\text{Mmin}^{-1}$, $V_{m3} = 20.0\mu\text{Mmin}^{-1}$, $k_2 = 0.1\mu$M, $k_y = 0.2\mu$M, $k_z = 0.5\mu$M, $k_x = 0.2\mu$M, $k_f = 1.6$ min^{-1}, $v_{4n} = 2.0\mu$M, $V_{m5} = 2.0\mu\text{Mmin}^{-1}$, $k_5 = 1\mu$M, $k_d = 0.4\mu$M, and $k = 10.0\mu$M.

cytosolic calcium dynamics of Fig. 53, where one notices desynchronization at cells $(25, 50)$ [see panels (a1)-(a2)] and $(50, 75)$ [see panels (a1)-(a2)]. The same spectrum of behaviors is also perceptible in the phase plots of Fig. 54 where panels $(aj)_{j=1,2}$ correspond to $\beta = 0.4$ and panels $(bj)_{j=1,2}$ have been recorded for $\beta = 0.6$, values of the paracrine coupling strength falling in the chaotic zone of Fig. 46(c), with $\gamma = 0.175$ and $\epsilon = 0.2$. It is obvious from the above that though desynchronization is manifested in the cytosolic Ca^{2+} oscillations, the activity of IP_3 highly contributes to the process. In that regard, while it is possible to obtain limit cycles in the $(y(t), z(t))-$plane, some of the cells in the network display complex dynamics due to the strong input from the level of stimulation, which indubitably affects oscillations of $[IP_3]$. Such complex dynamics may display chaotic behaviors or simply desynchronized states as delivered by Fig. 54. This will, without any doubt, have strong input into the full cycle of Ca^{2+}, including its propagation, via appropriate messengers, into the extracellular medium. However, at the internal level, i.e., within the cytoplasm and the internal store (ER), the simplified process involves the increase of $[IP_3]$, the release of Ca^{2+} from the ER, which triggers a rapid increase of the cytosolic Ca^{2+} concentration. Remarkably, the process relies on IP_3 that is engaged, once more, when the Ca^{2+} concentration in the mitochondria reaches its maximum level. In the case of desynchronization, cells may display different patterns of $[IP_3]$ as shown in Fig. 55. Interestingly, the paracrine coupling, whose increase enhances earlier desynchronization, also provokes sudden changes in $[IP_3]$ wave amplitude. This once more corroborates the dynamics of the synchronization factor $\mathcal{R}$. Dysregulation of synchronized calcium waves can lead to diseases and disorders. For example, arrhythmias in the heart can result from disturbances in synchronized calcium signaling [113, 114]. Also, understanding the mechanisms that underlie synchronized calcium waves is of great interest in basic research and clinical applications. Researchers are exploring how to modulate these waves for therapeutic purposes, such as in cardiac rhythm control or treating neurological disorders [115, 116].

Now we can apply to the deterministic model if we have synchronization in the network.

III.2.4 Study of synchronization phenomenon in case of bursting oscillation

Contrary to the spike waves, the complex Ca^{2+} waves or the dynamics or emergency condition are sweets know. But if we have the condition of emergency and propagation between coupled network, we can have the possibility to create and control them in case of dysfunction occur in some cell. We consider some determinist model who give the burst Ca^{2+} wave define by Houart et al which applied the condition a paracrine coupled strength and the condition of synchronization in coupled network of 100 cells. Firth we obtain one wave and studies the impact of degradation factor ϵ, the spatial dynamic which third times parameters of model increase network,in end we studies the dynamics of two principal actor of the model, cytosolic Ca^{2+} and cytosolic IP_3.

Study of synchronization of burst cytosolic Ca^{2+}

The amplitude of cytosolic Ca^{2+} are increase with the stimulus degree and lattice but stay constant for constant value of ϵ in increase lattice. In for of that we explore by cycle diagram if the interaction with different variables of our system are affect. The third next figures shows the same aspect of cycle diagram for different values of stimulate degree ϵ.

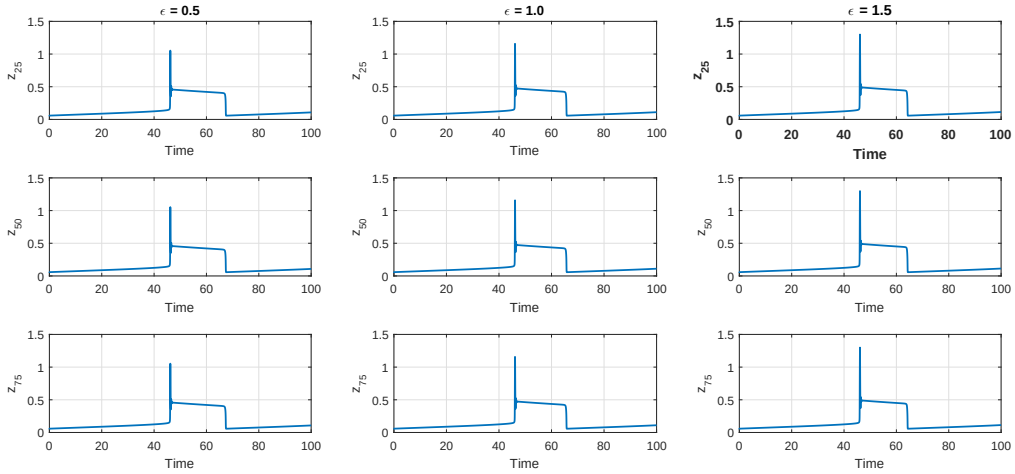

Figure 56: The time series of cytosolic Ca^{2+} site for different stimulate degree ϵ with $Z_{25}(t)$ first line, $Z_{50}(t)$ second line and $Z_{75}(t)$ in third line.

Before the amplitude modulation of cytosolic Ca^{2+}, we obtain the same interaction for the third parameters when the network go to simple from multiplied for third. For verified the stability of emerge and synchronization network, we plot the superposition and error of synchronization.

We represent the cycle diagram to synchrony domain and asynchrony domain which present some chaos attractor. All of this confirm the precedent result obtained in case of news parameters.

we can obtain the parameters condition with make the emergency of synchrony mode of complex Ca^{2+} wave and the FM and AM codage of Ca^{2+}.

III.2.5 Study the impact of passive linear leak to a dynamics of Ca^{2+} and IP_3 propagation

The Ca^{2+} liberated through IP_3R stimulate the synthesis of 3-kinase with induce the dephosphorylation with give IP_3. The passive diffusion coefficient can impact the dynamic of ours network. From this subsection, we study the dynamics of Ca^{2+} and IP_3 to different values of k_f.

Form fourth laster figures 59-62 we see that, when k_f increase from $[0.01; 1.0]$, the frequency and amplitude modulations of cytosolic Ca^{2+} and IP_3 concentrations which confirm to different phase portraits (X,Z). This results attest that form emergency of burst Ca^{2+} wave we obtain

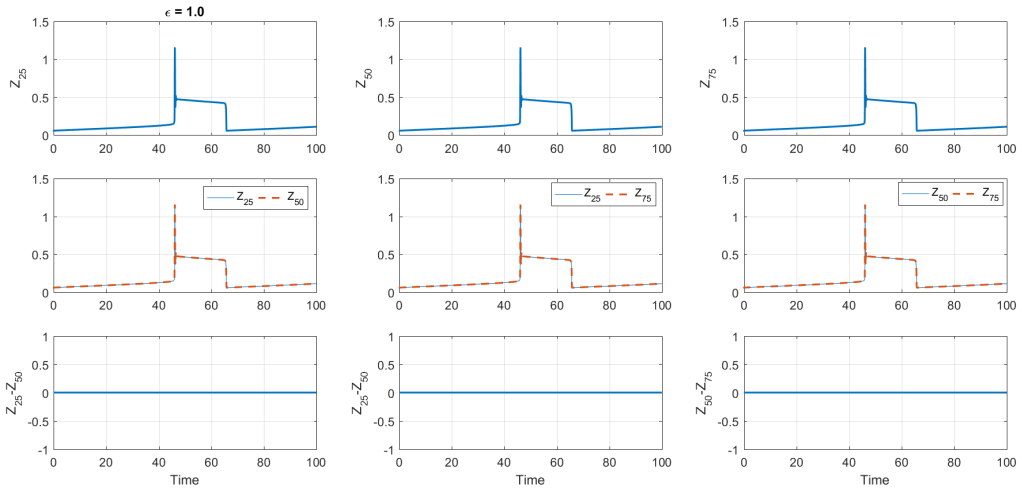

Figure 57: For $\epsilon = 1.0$, the cytosolic Ca^{2+} concentration $Z_i(t)$, in first line we have $Z_{25}(t)$,$Z_{50}(t)$ and $Z_{75}(t)$; to second line, the superposition of two series, $Z_{25}(t)$ and $Z_{50}(t)$, $Z_{25}(t)$ and $Z_{75}(t)$, $Z_{50}(t)$ and $Z_{75}(t)$ to illustrate synchronous behavior of the bursting modes.

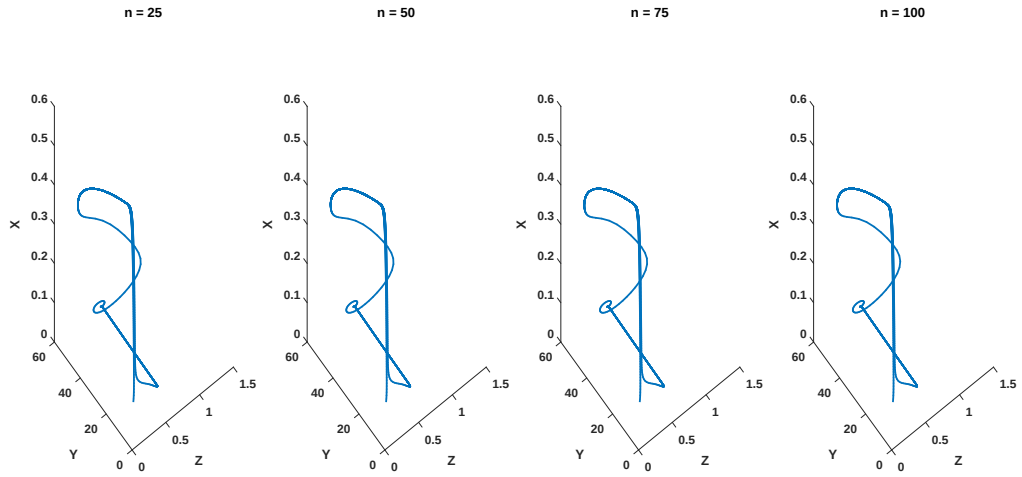

Figure 58: Cycle diagram of three equation parameter of the cytosolic Ca^{2+} concentration Z, store Ca^{2+} concentration Y and cytosolic IP_3 concentration X. We set $\epsilon = 1.5$.

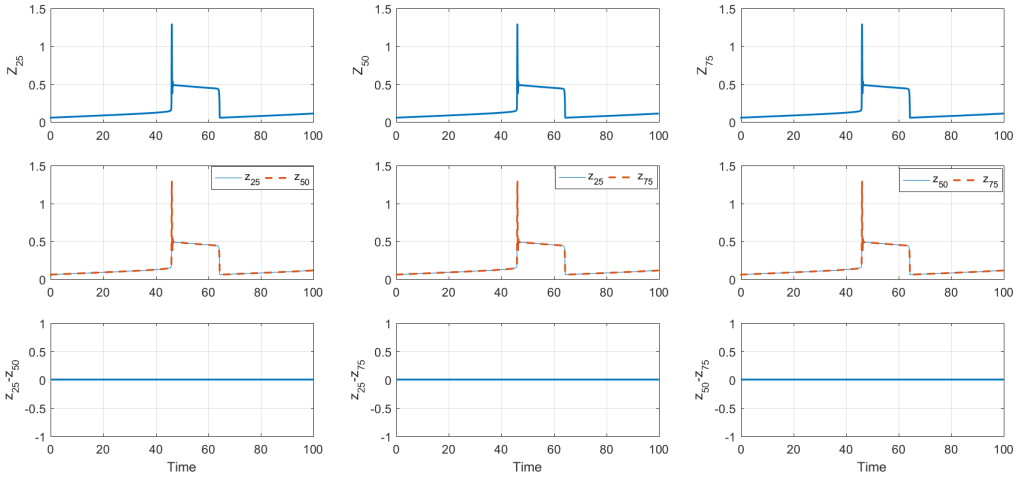

Figure 59: For $k_f = 0.05$, the cytosolic Ca^{2+} concentration $Z_i(t)$, in first line we have $Z_{25}(t)$,$Z_{50}(t)$ and $Z_{75}(t)$; to second line, the superposition of two series, $Z_{25}(t)$ and $Z_{50}(t)$, $Z_{25}(t)$ and $Z_{75}(t)$, $Z_{50}(t)$ and $Z_{75}(t)$ to illustrate synchronous behavior of the bursting modes.

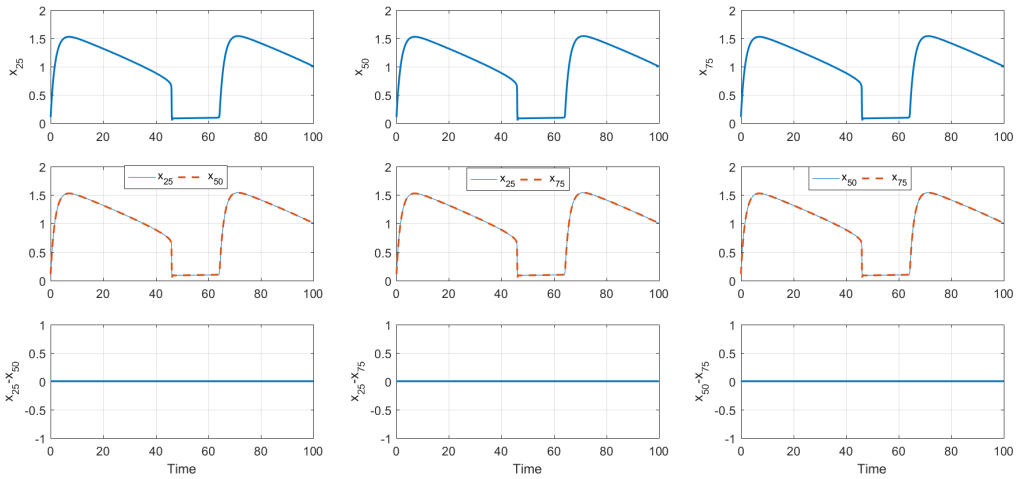

Figure 60: For $k_f = 0.05$, the cytosolic IP_3 concentration $X_i(t)$, in first line we have $X_{25}(t)$,$X_{50}(t)$ and $X_{75}(t)$; to second line, the superposition of two series, $X_{25}(t)$ and $X_{50}(t)$, $X_{25}(t)$ and $X_{75}(t)$, $X_{50}(t)$ and $X_{75}(t)$ to illustrate synchronous behavior of the bursting modes.

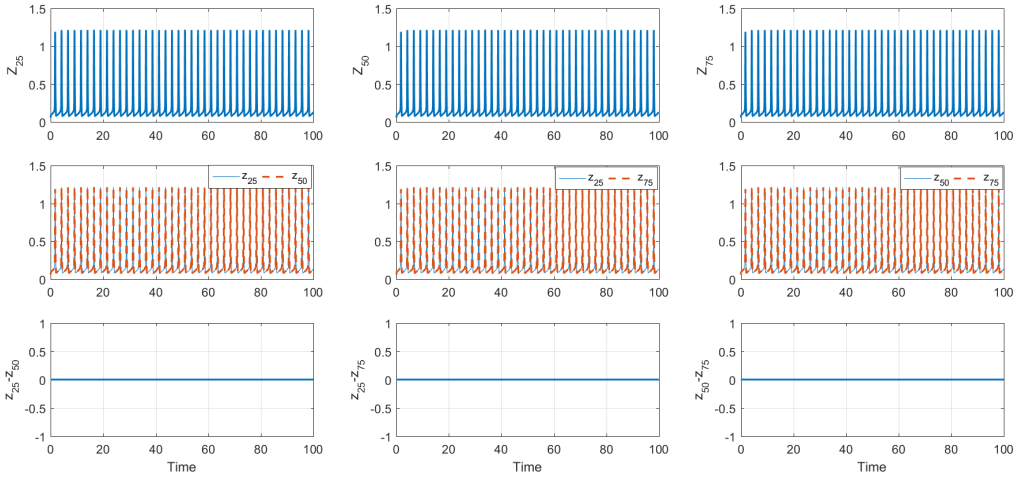

Figure 61: For $k_f = 1.0$,the cytosolic Ca^{2+} concentration $Z_i(t)$, in first line we have $Z_{25}(t)$,$Z_{50}(t)$ and $Z_{75}(t)$; to second line, the superposition of two series, $Z_{25}(t)$ and $Z_{50}(t)$, $Z_{25}(t)$ and $Z_{75}(t)$, $Z_{50}(t)$ and $Z_{75}(t)$ to illustrate synchronous behavior of the bursting modes.

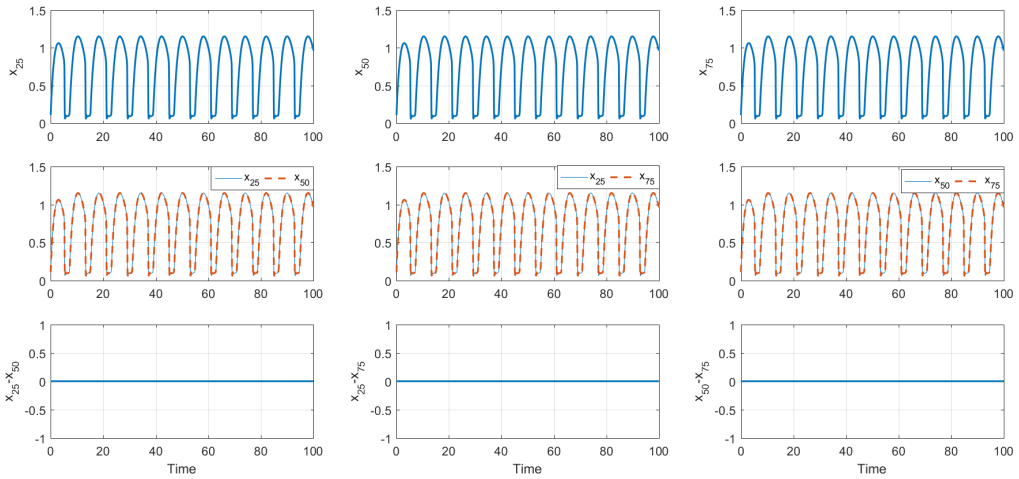

Figure 62: For $k_f = 1.0$, the cytosolic IP_3 concentration $X_i(t)$, in first line we have $X_{25}(t)$,$X_{50}(t)$ and $X_{75}(t)$; to second line, the superposition of two series, $X_{25}(t)$ and $X_{50}(t)$, $X_{25}(t)$ and $X_{75}(t)$, $X_{50}(t)$ and $X_{75}(t)$ to illustrate synchronous behavior of the bursting modes.

amplitude and frequency modulation, which attest the important of study of dynamic of Ca^{2+} to elucidate the dynamics of emergency and auto-modulation of complex Ca^{2+} wave in coupled network cells. The value of the passive flux k_f is linked to the distribution and activation of IP3R receptors on the pools. Its regulation enables Ca^{2+} dynamics to be controlled and regulated, thereby combating certain abnormalities insofar as a causal link has been established between the distribution of receptors, the oscillatory Ca^{2+} regime and the emergence of spiral waves leading to cardiac arrhythmias. Paracrine coupling thus makes it possible to control and maintain cytosolic IP_3-Ca^{2+} interactions and modulate Ca^{2+} wave frequencies when physiological conditions show an irregular distribution of membrane receptors.

Ours study shown that the degree of IP_3 phosphorylation, converge with increase of amplitude of Ca^{2+} in the network and from constant value of phosphorylation degree, the Ca^{2+} waves can propagation in same amplitude and frequency from cell network. This result suggest than, from some decease like cancer, we can initiate a propagation of constant Ca^{2+} wave before specific cell, and induce the apoptose of them. Before the interdependency before Ca^{2+} and IP_3 oscillators, we investigate the dynamic of them.

General Conclusion and Perspectives

In this thesis, we have studied the dynamic of Ca^{2+} patterns waves emergency and their biological implications. Using the continuous version of third equation HD models of complex Ca^{2+} wave, we have developed two discrete models that contribute to collective dynamic of Ca^{2+} in cells network. Our numerical investigations are conducted from a better understanding of main properties of the complex Ca^{2+} wave.

To achieve our mains goal,this thesis has been subdivided into three chapters. In the first, we have presented the general reviews and some basic ideas for our current understanding of the phenomena of calcium. Thereafter, we presents the generalities on the biology of the structural and physiological function of calcium wave. At the end of the chapter, we carried out the principals mathematical models of these systems.

Secondly, we have presented the two improved HD mathematical models which have been developed along with both numerical methods. The first model is the Intercellular paracrine coupled cells, to investigate the effects of paracrine diffusive coupling strength, synchronous structures and modulated of Ca^{2+} wave. The second is the two-dimensional HD where effect of paracrine coupling strength, phosphorylation degree and stimulation degree are study to nonlinear dynamics of IP_3 from emergency of Ca^{2+} patterns. The statistical synchronization have been use to numerical investigation. The RK4 method with periodic boundary conditions has been used in the numerical simulations for integrating of original models.

In the third chapter, we presented the main results. The propagation of Ca^{2+} nonlinear waves in a two-dimensional network of cells linked via bidirectional paracrine signaling has been investigated. The proposed discrete model, which includes the IP_3, has been solved numerically, and the different oscillation modes have been predicted using the synchronization factor (R). Mainly, it was argued that for values of R approaching 1, the dynamics was likely to be governed by synchronous states, while values close to zero were characterizing other modes such as target and spiral waves. The predictions have been confirmed via extensive numerical simulations. The behaviors of target and spiral waves have been discussed. Such patterns have been found to be very sensitive to the change in the paracrine coupling parameter. Under strong values of the latter, target and spiral states get disintegrated, leading to the propagation of turbulent patterns. Several proteins are very responsive to frequency-modulated oscillations of Ca^{2+} levels. Most of them display rich activities for faster frequencies under the so-called high-pass activation. On the contrary, the transcription factor NFAT is optimally triggered at a specific frequency, a behavior we call band-pass activation [117]. Along the same line, Ca^{2+} oscillations in vivo display some intrinsic modulations due to their frequency and amplitude variation, which implies a powerful

modulating effect on cortical oscillation frequencies of established spiral waves. Moreover, the major frequency modes during spiral waves are similar in different animals, and intrinsic frequency selection is inherent to spiral waves in the cortex, with a strong impact on their rotation angular velocity.

The means studied a 1D cell network bidirectionally coupled via paracrine signaling and comprising IP_3 degradation by $3-kinase$. Using direct numerical experiments on the proposed discrete model, the bifurcation of the cytosolic Ca^{2+} waves was first addressed using the paracrine coupling strength as the control parameter. Regions of quasi-periodic oscillations and chaotic patterns have been explored using time series and phase plots. Confirmation has been obtained via the appearance of spatiotemporal patterns. Synchronized states have also been studied. First predicted using the statistical factor of synchronization, different synchronization scenarios were unveiled under suitable effects from the paracrine coupling, level of stimulation and degradation factor of IP_3. Strong values of the paracrine coupling strength have been found to enhance synchronization only under weak values of the stimulation level, with considerable input from the IP_3 degradation factor. Interestingly, the termination of Ca^{2+} waves and the reduction of elevated cytoplasmic Ca^{2+} levels depend on the degradation of IP_3. As it is well known, IP_3 is enzymatically dephosphorylated to inositol, a process that is catalyzed by inositol 1,4,5-triphosphate 5-phosphatases (IP_5Ps) and other enzymes. The degradation of IP_3 reduces the binding to IP_3 receptors, thereby reducing Ca^{2+} release from intracellular stores, a process that is beneficial in recruiting neighbouring cells into signalling. From suitable intervals, values of the paracrine coupling strength, even under appropriate values of the IP_3 degradation factor, were found to promote desynchronization, as well illustrated by the cytosolic Ca^{2+} patterns and the IP_3 oscillations. Indubitably, one can notice the effect of a perturbed CICR process, whereby the messenger released in the extracellular medium does not reach a threshold concentration capable of exciting adjacent cells. However, other formulations of the proposed discrete model might provide efficient ways of achieving exclusive synchronization among the cells. In a forthcoming contribution, we suggest long-range paracrine coupling as a probable mechanism to achieve that. In such a process, the extracellular messenger can travel via the extracellular fluid and connect contacting as well as neighboring non-contacting cells [118, 119]. In that context, synchronized calcium waves that propagate over long distances can coordinate cellular responses and synchronize the activity of cells within a tissue or organ. This coordination is essential for proper functioning and can be observed in processes such as wound healing and tissue regeneration [120, 121].

Future orientations

The work of this thesis has contributed to the improvement of mathematical HD models to better understand the nonlinear dynamics of IP_3 induced Ca^{2+} patterns. Most of the investigations carried out aimed at studying the phenomena of wave propagation and Ca^{2+} as a function of certain parameters, the number of which is not exhaustive. That is why we are prospecting other

research directions that include:

- Thermal effects on Nonlinear dynamics of inositol 1,4,5-trisphosphate-induced Ca^{2+} patterns in two-dimensional cell networks with paracrine signaling interaction, temperature appears to play a crucial role in generation and conduction of the cardiac impulse.
- The electromagnetic effects on Nonlinear dynamics of inositol 1,4,5-trisphosphate-induced Ca^{2+} patterns in two-dimensional cell networks with paracrine signaling interaction.
- The long-rage interaction of nonlinear dynamics of IP_3 wave induced Ca^{2+} patterns.
- Although many contributions have been devoted to a better understanding of the frequency implication and spatiotemporal features of such waves in information processing in cell networks, the question of their origin, especially when other factors such as IP_3 are involved, remains unmasked and deserves to be considered carefully. Calculations in that direction are ongoing.
- Experimental findings to improve this numerical results.

Bibliography

[1] Berridge, M. J, Biochimi. Biophys. Acta **1793**, 933 (2009).

[2] Mikoshiba K, J. Neurochem. **102**, 1426 (2007).

[3] Berridge, M. J., Bootman, M. D., Roderick, H.L., Nature Rev. Mol. Cell Biol. **4**, M517 (2003).

[4] Clapham, D.: Calcium signaling. Cell **131**, 1047 (2007).

[5] Cui, C., Merritt, R., Fu, L., Pan, Z., Acta Pharm. Sin. B **7**, 3 (2017).

[6] Chang, Y., Funk, M., Roy, S., Stephenson, E., et al., Int. J. Mol. Sci. **23**, 1763 (2022).

[7] M. Falcke, Adv. Phys. **53**, 255 (2004).

[8] Berridge, M. J., Nature **361**, 315 (1993).

[9] Rey, O., Young, S.H., Jacamo, R., Moyer, M.P., Rozengurt E., J. Cell Physiol. **225**, 73 (2010).

[10] Ridgway, E. B., Gilkey, J. C., Jaffe, L. F., Adv. Physiol. **74**, 623 (1977).

[11] Lipp, P., Niggli, E., Biophys. J. **65**, 2272 (1993).

[12] Sanderson, M. J., Charles, A. C., Boitano, S., Dirksen, E. R., Mol. Cell. Endocrinol. **98**, 173 (1994).

[13] Robb-Gaspers, L. D., Thomas, A.P., J. Biol. Chem. **270**, 8102 (1995).

[14] Thomas, A. P., Robb-Gaspers, L. D., Rooney, T. A., Hajnoczky, G., Renard- Rooney, D. C., Lin, C., Biochem. Soc. Trans. **23**, 642 (1995).

[15] Harris-White, M. E., Zanotti, S. A., Frautschy, S. A., Charles, A. C., J. Neurophysiol. **79**, 1045 (1998).

[16] Putney, J., Bird, G., Endocr. Rev. **14**, 610 (1993)

[17] Cornell-Bell, A. H., Finkbeiner, S. M., Cooper, M. S., Smith, S. J., Science **247**, 470 (1990).

[18] Charles, A. C., Merrill, J. E., Dirksen, E. R., Sanderson, M. J., Neuron. **6**, 983 (1991).

[19] Charles, A., Glia **24**, 39 (1998).

[20] Venance, L., Piomelli, D., Glowinski, J., Giaume, C., Nature **376**, 590 (1995).

[21] Giaume, C., Venance, L., Glia **24**, 50 (1998).

[22] Fields, R. D., Stevens-Graham, B.,Science **298**, 556 (2002).

[23] Allen, N. J., Barres, B. A., Nature **457**, 675 (2009).

[24] Hashimura, H., Morimoto, Y. V., Hirayama, Y., Ueda, M., Sci. Rep. **12**, 12428 (2022).

[25] Newman, E. A., J. Neurosci. **21**, 2215 (2001).

[26] Newman, E. A., Zahs, K. R., Science **275**, 844 (1997).

[27] Scemes, E., Suadicani, S. O., Spray, D. C., J. Neurosci. **20**, 1435 (2000).

[28] K. Kaouri, K., Maini, P. K., Skourides, P. A., Christodoulou, N., Chapman, S. J., J. Math. Biol. **78**, 2059 (2019).

[29] Katerina Kaouri, K., Méndez, P. E., Ruiz-Baier, R., Viet. J. Math. (2022), https://doi.org/10.1007/s10013-022-00579-y.

[30] Dupont G., Tordjmann T., Clair C., Swillens S., Claret M., Combettes L., FASEB J. **14**, 279 (2000).

[31] Höfer, Th., Biophys. J. **77**, 1244 (1999).

[32] Höfer, Th., Politi, A., Heinrich, R., Biophys. J. **80**, 75 (2001).

[33] Manhas, N., Anbazhagan, N., Chaos Solit. Fract. **145**, 110741 (2021).

[34] Agarwal, R., Kritika, Purohit, S. D., Chaos Solit. Fract. **143**, 110610 (2021).

[35] Gracheva, M. E., Toral, R., Gunton, J. D., J. Theor. Biol. **212**, 111 (2001).

[36] Friedhoff, V. N., Ramlow, L., Lindner, B., Falcke, M., Eur. Phys. J. Spec. Top. **230**, 2911 (2021).

[37] Bär, M., Falcke, M., Levine, H., Tsimring, L. S. X., Phys. Rev. Lett. **84**, 5664 (2000).

[38] Falcke, M., Tsimring, L., Levine, H., Phys. Rev. E **62**, 2636 (2000).

[39] Hassinger, T. D., Guthrie, P. B., Atkinson, P. B., Bennett, M. V., Kater, S. B., Proc. Natl. Acad. Sci. U.S.A. **93**, 13268 (1996).

[40] Höfer, A. M., Curci, S., Doble, M. A., Brown, M. E., Soybel, D. I., Nat. Cell Biol. **2**, 392 (2000).

[41] Kepseu, W. D., Woafo, P., Phys. Rev. E **76**, 041912 (2006).

[42] Goldbeter, A., Dupont, G., Berridge, M. J., Proc. Natl. Acad. Sci. U.S.A. **87**, 1461 (1990).

[43] Kepseu, W. D., Woafo, P.: Long-range interaction effects on calcium-wave propagation. Phys. Rev. E **78**, 011922 (2008).

[44] Tabi, C. B., Maïna, I., Mohamadou, A., Ekobena Fouda, H. P., Kofané, T. C., Europhys. Lett. **106**, 18005 (2014).

[45] Tabi, C. B., Maïna, I., Mohamadou, A., Ekobena Fouda, H. P., Kofané, T. C., Physica A **435**, 1 (2015).

[46] Tabi, C. B., Etémé, A. S., Mohamadou, A., Kofané, T. C., Waves Rand. Complex Media **31**, 1028 (2021).

[47] Borghans, J. A. M., Dupont, G., Goldbeter, A.,Biophy. Chem. **66**, 25-41 (1997).

[48] Houart, G., Dupont, G., Goldbeter, A., Bull. Math. Biol. **61**, 507 (1999).

[49] N. Singh and N. Adlakha, RSC Adv. **9**, 42459 (2019).

[50] A. Pawar and K. R. Pardasani, Phys. Scr. **99**, 015025 (2024).

[51] A. Pawar and K. R. Pardasani, Cogn. Neurodyn. **17**, 239 (2023).

[52] G. Dupont, A. Goldbeter, and M. J. Berridge, Cell Regul. **1**, 853 (1990).

[53] Dupont, G., Falcke, M., Kirk, V., Sneyd, J., Interdisciplinary Applied Mathematics. **43**, (2016).

[54] Tacail, T.,NNT. LYSEN071 (2017).

[55] Gyorgy Baffy., Digestive Diseases and Sciences **12** (2018).

[56] Sutanto. H., Heijman. J., Front. Young Minds **65** 1-7, (2019).

[57] Tayeb, K, S., Lemaigre, F, P. and Duncan, S, A.: j.devcel **011** 01-015, (2010).

[58] Rodrigue, F, F., and Marcelo A.S., Fractal Fract **7**, 592 (2023).

[59] Wang, R., Wang, M., He, S., Sun, G. and Sun, X.: fphar. **11**, 872 (2020).

[60] https://my.clevelandclinic.org/health/diseases/22953-coronary-artery-calcification 05 september (2022).

[61] Dupont. G., Combettes. L., F1000Research. **5**, (2016).

[62] Bootman. M. D., Bultynck. Geert., Cold Spring Harb Perspect Biol: a038802. **12**, (2020).

[63] Berridge, M,J., The Journal of Experimental Biology (JEB0597) **200** , 315-319 (1997).

[64] Berridge, M,J., Neuron, Vol. **21**, 13-26, July (1998).

[65] Dupont. G., Falcke. M., Kirk. V., Sneyd. J., Springer International Publishing Switzerland **43** (2016).

[66] A. S. Etémé, C. B. Tabi, A. Mohamadou and T. C. Kofané: Physica A **533**, 122037 (2019).

[67] Modelling Synchronised Calcium Oscillations in the Liver Complex MRes Case Essay Tom Sumner 12th April 2006

[68] T. Tordjmann, B. Berthon, M. Claret and L. Combettes.,The EMBO J. **16** 5398-5407 (1997).

[69] L.D.Gaspers and A.P.Thomas, J. Biol. Chem. **270** 8102-8107 (1995).

[70] C. Clair, C. Chalumeau, T. Tordjmann, J. Poggioli, C. Erneux, G. Dupont and L. Combettes , J. Cell Sci. **114** 1999-2007 (2001).

[71] M.J. Sanderson, News Physiological Sci. **11** 262-269 (1996).

[72] Giaume, C., Venance, L., Glia **24**, 50 (1998).

[73] Cherry, E. M., and Fenton, F. H.: New Journal of Physics **10** 125016 (2008).

[74] Sandstede, B., and Scheel, A.: arXiv: [nlin.PS] 2002.10352v3 (2021).

[75] Markus, B., and Lutz, B.: New. J. Phys **6** 5 (2004).

[76] Shanna, H., Roland, V., Andriy, B., Dmitry, T.: European Journal of Physiology **473** 377-387 (2021).

[77] Dupont, G., Jos, P., and Albert, G.: Am. J. Physiol **271** C1390-C1399 (1996).

[78] Rozi. A. Jia. Y.: Biophysical Chemistry **106**, 193-202, (2003).

[79] Lavrentovich. M., Hemkin. S.: Journal of Theoretical Biology **251**, 553-560, (2008).

[80] Hongkun. Z., and Min. Y.: Front. Phys. **8**, 8:258 fphy.(2020).

[81] Quanbao. J., and Min. Y.: Hindawi Complexity Volume **2021**, Article ID 8861465, 7 (2021).

[82] Ma. J. et *al*.: Int. J. Bif and Chaos, **21**, No. 2 587-601, (2011).

[83] Indrajit. B. S.: J Chem Biol, **5**, 27-34 (2012).

[84] Malik et *al*.: J. Nanosci. Nanotechnol, **12**, No. 11 (2012).

[85] 1998 Dupont, G.: Am. J.Physiol, **275**, C317-C322, (1998).

[86] Sabir, Z.: Int. J. Biomath. **15**, 2250005 (2022).

[87] Sabir, Z.: Eur. Phys. J. Plus **137**, 638 (2022).

[88] Sabir, Z., Baleanu, D., Ali, M. R., Sadat R.: Int. J. Comput. Math. **99**, 2091 (2022).

[89] Sabir, Z., Ali, M. R., Sadat, R.: J. Amb. Intel. Human. Comput. **Doi: doi.org/10.1007/s12652-021-03638-3**.

[90] Sabir, Z., Raja, M. A. Z, Sánchez, Y. G.: J. Health. Eng. **2022**, 3774123 (2022).

[91] Francois, C.: L.A.G.A., http://www.math.univ-paris13.fr/∼cuvelier.

[92] Wang, Q., Duan, Z., Perc, M., Chen, G.: Europhys. Lett. **83**, 50008 (2008).

[93] Wang, Q., Perc, M., Duan, Z., Chen, G.: Phys. Rev. E **80**, 026206 (2009).

[94] Ma, J., Tang, J., Zhang, A., Jia, Y.: Sci. China Phys. Mech. Astron. **53**, 672 (2010).

[95] Shafiei, M., Parastesh, F., Jalili, M., Jafari, S., Perc, M., Slavinec, M.: Eur. Phys. J. B **92**, 36 (2019).

[96] Majhi, S., Perc, M., Ghosh, D.: Chaos **27**, 073109 (2017).

[97] Majhi, S., Perc, M., Ghosh, D.: Sci. Rep. **6**, 39033 (2016).

[98] Ma, J., Xu, Y., Wang, C., Jin, W.: Physica A **461**, 586 (2016).

[99] Gray. R. A.,Arkady. M. P., and Jalife. J.: Nature **392**, 75-78, (1998).

[100] Fan-Yi. L., Jessica. F., Kristina. W., Carly. L.: fasebj, **20**, 5, (2006).

[101] Fenton. F. H., and Cherry. E. M.: Chaos, **12**, No.3, 852-892, (2002).

[102] Wang, C., Lv, M., Alsaedi, A., Ma, J.: Chaos **27**, 113108 (2017)

[103] Ma, J., Tang, J., Wang, C.-N., and Jia, Y.: Int. J. Bifurc. Chaos **21**, 587 (2011).

[104] Busa, W. B., Ferguson, J. E., Joseph, S. K., Williamson, J. R., Nuccitelli, R.: J. Cell Biol. **101**, 677 (1985).

[105] M. Perc, M. Gosak, and M. Marhl, Chem. Phys. Lett. **437**, 143 (2007).

[106] M. A. Savi, J. Braz. Soc. Mech. Sci. Eng. **27**, 157 (2005).

[107] D. A. Eisner, J. L. Caldwell, K. Kistamás, and A. W. Trafford, Circ. Res. **121**, 181 (2017).

[108] J. Dawitz, T. Kroon, J. J. J. Hjorth, and R. M. Meredith, J. Vis. Exp. **56**, 3550 (2011).

[109] H. Sakaguchi, Y. Ozaki, T. Ashida, T. Matsubara, N. Oishi, S. Kihara, and J. Takahashi, Stem Cell Rep. **13(3)**, 458 (2019).

[110] S. Pirnat, M. Božić, D. Dolanc, A. Horvat, P. Tavčar, N. Vardjan, A. Verkhratsky, R. Zorec, and M. Stenovec, Glia **69(12)**, 2899 (2021).

[111] R. Bychkov, M. Juhaszova, K. Tsutsui, C. Coletta, M. D. Stern, V. A. Maltsev, and E. G. Lakatta, JACC: Clin. Electrophys. **6(8)**, 907 (2020).

[112] D. A. Terrar, Cell Calcium **104**, 102565 (2022)

[113] F. Hohendanner, S. Walther, J. T. Maxwell, S. Kettlewell, S. Awad, G. L. Smith, V. A. Lonchyna, L. A. and Blatter, J. Physiol. **593**, 1459 (2015).

[114] D. A. Terrar, Phil. Trans. R. Soc. B **378**, 20220170 (2023).

[115] N. Kuga, T. Sasaki, Y. Takahara, N. Matsuki, and Y. Ikegaya, J. Neurosci. **31(7)**, 2607 (2011).

[116] I. Nitsan, S. Drori, Y. E. Lewis, S. Cohen, and S. Tzlil, Nature Phys. **12**, 472 (2016).

[117] Schoch, A., Pahle, J.: Biophys. Chem. **245**, 41 (2019) .

[118] V. L. Cressman, E. Lazarowski, L. Homolya, R. C. Boucher, B. H. Koller, and B. R. Grubb, J. Biol. Chem. **274**, 26461 (1999).

[119] K. Enomoto, K. Furaya, S. Yamagashi, and T. Maeno, Cell Calcium **13(8)**, 501 (1992).

[120] W. Wood, Curr. Biol. **22**, R14 (2012).

[121] T. Subramaniam, M. B. Fauzi, Y. Lokanathan, and J. X. Law, Int. J. Mol. Sci. **22(12)**, 6486 (2021).

List of Publications

1- **T. Kenne Tiayo**, A.S. Etémé, C.B. Tabi, H.P. Ekobena Fouda, T.C. Kofane, *Nonlinear dynamics of inositol 1,4,5-trisphosphate-induced Ca^{2+} patterns in two-dimensional cell networks with paracrine signaling interaction*, Nonlinear Dyn. 111(2023) 12593 .
2- C.B. Tabi,**T. Kenne Tiayo**, A.S. Etémé, H.P. Ekobena Fouda, T.C. Kofane, *Bifurcation of synchronized nonlinear intercellular Ca^{2+} oscillations induced by bi-directional paracrine signalling and IP_3-cytosolic Ca^{2+} interaction*, Phys. Lett A **498**, (2024) 129332.